NATIONAL TECHNICAL UNIVERSITY OF ATHENS

SCHOOL OF MINING AND METALLURGICAL ENGINEERING

DEPARTMENT OF METALLURGY AND MATERIALS TECHNOLOGY

LEACHING WITH IONIC LIQUIDS FOR RECOVERY OF REACTIVE METALS (TI, SC, REES)

DOCTORAL THESIS OF

CHIARA BONOMI

Graduate of Chemistry, University of Rome "La Sapienza", MSc

Athens 2020

ΕΘΝΙΚΟ ΜΕΤΣΟΒΙΟ ΠΟΛΥΤΕΧΝΕΙΟ

ΣΧΟΛΗ ΜΗΧΑΝΙΚΩΝ ΜΕΤΑΛΛΕΙΩΝ ΜΕΤΑΛΛΟΥΡΓΩΝ

ΤΟΜΕΑΣ ΜΕΤΑΛΛΟΥΡΓΙΑΣ ΚΑΙ ΤΕΧΝΟΛΟΓΙΑΣ ΥΛΙΚΩΝ

ΕΚΧΥΛΙΣΗ ΜΕ ΙΟΝΤΙΚΑ ΥΓΡΑ ΓΙΑ ΑΝΑΚΤΗΣΗ ΔΡΑΣΤΙΚΩΝ ΜΕΤΑΛΛΩΝ (Ti, Sc, REE)

ΔΙΔΑΚΤΟΡΙΚΗ ΔΙΑΤΡΙΒΗ

CHIARA BONOMI

ΠΤΥΧΙΟΥΧΟΣ ΤΜΗΜΑΤΟΣ ΧΗΜΕΙΑΣ,
ΠΑΝΕΠΙΣΤΗΜΙΟΥ ΡΩΜΗΣ "La Sapienza", MSc

Αθήνα 2020

NATIONAL TECHNICAL UNIVERSITY OF ATHENS

SCHOOL OF MINING AND METALLURGICAL ENGINEERING

DEPARTMENT OF METALLURGY AND MATERIALS TECHNOLOGY

LEACHING WITH IONIC LIQUIDS FOR RECOVERY OF REACTIVE METALS (TI, SC, REES)

DOCTORAL THESIS OF

CHIARA BONOMI

Graduate of Chemistry, University of Rome "La Sapienza", MSc

Advisory Committee:

Dimitrios Panias, Professor, NTUA (Supervisor)

Ioannis Paspaliaris, Professor, NTUA

Maria Taxiarhou, Assistant Professor, NTUA

Examination Committee:

Dimitrios Panias, Professor, NTUA

Ioannis Paspaliaris, Professor, NTUA

Maria Taxiarhou, Assist. Professor, NTUA

Anthimos Xenidis, Professor, NTUA

Anastasia Detsi, Assist. Professor, NTUA

Kostantinos Komnitsas, Professor, Technical University of Crete

Yiannis Pontikes, Assoc. Professor, KU Leuven

Athens 2020

ΕΘΝΙΚΟ ΜΕΤΣΟΒΙΟ ΠΟΛΥΤΕΧΝΕΙΟ

ΣΧΟΛΗ ΜΗΧΑΝΙΚΩΝ ΜΕΤΑΛΛΕΙΩΝ ΜΕΤΑΛΛΟΥΡΓΩΝ

ΤΟΜΕΑΣ ΜΕΤΑΛΛΟΥΡΓΙΑΣ ΚΑΙ ΤΕΧΝΟΛΟΓΙΑΣ ΥΛΙΚΩΝ

ΕΚΧΥΛΙΣΗ ΜΕ ΙΟΝΤΙΚΑ ΥΓΡΑ ΓΙΑ ΑΝΑΚΤΗΣΗ ΔΡΑΣΤΙΚΩΝ ΜΕΤΑΛΛΩΝ (Ti, Sc)

ΔΙΔΑΚΤΟΡΙΚΗ ΔΙΑΤΡΙΒΗ

CHIARA BONOMI

Πτυχιουχος Τμηματος Χημειας, Πανεπιστημιου Ρωμης "La Sapienza", MSc

Συμβουλευτική Επιτροπή:

Πάνιας Δημήτριος, Καθηγητής ΕΜΠ (Επιβλέπων)

Πασπαλιάρης Ιωάννης, Καθηγητής ΕΜΠ

Ταξιάρχου Μαρία, Επίκουρη Καθηγήτρια ΕΜΠ

Εξεταστική Επιτροπή:

Πάνιας Δημήτριος, Καθηγητής ΕΜΠ

Πασπαλιάρης Ιωάννης, Καθηγητής ΕΜΠ

Ταξιάρχου Μαρία, Επίκουρη Καθηγήτρια ΕΜΠ

Ξενίδης Ανθιμος, Καθηγητής ΕΜΠ

Δέτση Αναστασία, Επίκουρη Καθηγήτρια ΕΜΠ

Κομνίτσας Κωνσταντίνος, Καθηγητής Πολυτεχνείου Κρήτης

Ποντίκης Ιωάννης, Αναπληρωτής Καθηγητής Καθολικού Πανεπιστημίου Λουβαίνης

Αθήνα 2020

Approved by the seven-member examination committee:

Dimitrios Panias
Professor, NTUA

Ioannis Paspaliaris
Professor, NTUA

Maria Taxiarhou
Assist. Professor, NTUA

Anthimos Xenidis
Professor, NTUA

Anastasia Detsi
Assist. Professor, NTUA

Kostantinos Komnitsas
Professor, Technical University of Crete

Yiannis Pontikes
Assoc. Professor, KU Leuven

"Approval of this doctoral thesis by the School of Mining and Metallurgical Engineering of the National Technical University of Athens (NTUA) does not constitute in any way an acceptance of the views of the author contained herein by the said academic organisation."
(L. 5343/1932, art. 202).

«Η έγκριση της διδακτορικής διατριβής από τη Σχολή Μηχανικών Μεταλλείων–Μεταλλουργών του ΕΜΠ δεν υποδηλώνει την αποδοχή των γνωμών του συγγραφέα.»

(Ν.5343/1932 άρθρο 202)

Dedicated to Marco

Acknowledgements

First, I would like to warmly thank Professor Dimitrios Panias for his excellent scientific supervision and invaluable support in all stages of my PhD.

The PhD was held at NTUA in the laboratory of Metallurgy and I would like to express my gratitude to those who contributed to its fulfilment. More specifically, I received technical, scientific and academic support by Ioanna Giannopoulou, Panagiotis Davris, Alexandra Alexandri, Vangelis Bourbos, Apostolos Kourtis, Paschalis Oustadakis, Petros Tsakiridis, Katerina Vaxevanidou, Antonis Peppas and all other researchers working at NTUA whom I am grateful to have worked with. I would like to thank Irini Christodoulou and Asimina Katsiapi for their administrative support and Kostantinos Sakkas for his help in the first stage of my "Greek life".

All the researchers and supervisors from other universities and institutions I cooperated with are deeply thanked, Bengi Yagmurlu from MEAB, Dzenita Kasapovic and Mercedes Regadio from KU Leuven, Wenzhong Zhang from University of Helsinki and Angeliki Panagiotopoulou from Demokritos.

I am very thankful for the great experience I had the opportunity to have with the other PhD candidates, supervisors and supporting staff of the MSCA-ETN REDMUD Project.

I owe a warm thank to my colleague and friend Chiara Cardenia for deeply sharing this path with me and for all the support she gave me.

I would like to thank my NTUA-REDMUD colleagues and friends Johannes Vind and Priiti Tam for the fruitful cooperation and the scientific discussions we had during the PhD period and for their help and support.

I would like to express my gratitude to Marco, my parents and my sister who always believe in me and endorse me and push me towards new experiences.

The research leading to these results has received funding from the European Community's Horizon 2020 Programme (H2020/2014–2019) under Grant Agreement no. 636876 (MSCA-ETN REDMUD). This publication reflects only the authors' views, exempting the Community from any liability. Project website: http://www.etn.redmud.org.

Abstract

Bauxite residue, also known as red mud, is the major solid waste generated during primary alumina production with the Bayer process. For each ton of alumina produced, 1 - 1.5 tons of bauxite residue is generated [1–3], leading to over 150 million tons per year of bauxite residue generated globally [2,4]. Management of bauxite residue is the major issue for alumina industry because of its high volume and alkalinity. However, bauxite residue is a polymetallic matrix, containing valuable metals like scandium, titanium, iron, aluminum and rare earth a comprehensive strategy is needed for recovering metals from bauxite residue and utilize the left-over residue in applications like cementitious industry or building materials. This “zero-waste” approach could contribute in finding a way to solve major issues for the management of bauxite residue and furthermore could help to tackle the raw material dependency of Europe.

In this perspective, the main aim of this PhD thesis was to study a process for recovering valuable metals from bauxite residue, with the main objective being recovering valuable metals, such as titanium and scandium. A conceptual flowsheet was presented and two main parts can be outlined.

The first part involved the dissolution of metals from bauxite residue through an innovative ionometallurgical approach. In particular, the direct leaching of bauxite residue by using the Brønsted acidic ionic liquid 1-ethyl-3-methylimidazolium hydrogen sulfate for recovering scandium and titanium at high recovery yields was investigated.

To optimize the process, parameters like stirring rate, time, temperature and pulp density were evaluated. Their optimized combination has shown high recovery yields of scandium, nearly 80 %, and titanium (90 %), almost total dissolution of iron, while aluminum and sodium were partially

extracted in the range of 30 – 40 %. Silicon and rare earth element dissolutions were found to be negligible, whereas calcium was dissolved and reprecipitated as calcium sulfate anhydrate, consuming about the 2 wt.% of the ionic liquid.

Moreover, the left-over solid residue was fully characterized, providing explanations for the destiny of rare earths that remain undissolved during the leaching process. The solid residue produced after dissolution can be further treated to extract rare earths or employed in cement industry or for building materials.

The second part of the conceptual flowsheet involved solvent extraction process for extracting metals from the pregnant liquid solution. Preliminary tests with four major extractants, three organophosphorus acids (D2EHPA, Cyanex 272 and Ionquest 801) and a neutral extractant (Cyanex 923), were tested in a comparative manner to understand the extraction behavior directly from ionic liquid leachates.

Phase separation time, organic to ionic liquid ratio and extractant concentration were studied as variable parameters and kinetic studies were performed to understand metals extraction behavior over time. From the experiments performed, the acidic extractant D2EHPA at 20 % v/v and 1:1 O:IL gave the best results in terms of extracting metals, as almost the total amount of iron, aluminum, titanium and scandium were recovered from the pregnant liquid solution after fifteen minutes. On the other hand, scandium selectivity was achieved using the neutral extractant Cyanex 923.

In this perspective, a multi-stage solvent extraction process for selectively recovering metals from pregnant liquid solution was proposed. In the first two stages Cyanex 923 was employed for recovering almost the total amount of scandium and aluminum, while iron and titanium were moderately extracted. After stripping and purification, aluminum and scandium could be employed in Al-Sc alloys industry. The third stage involved the use of the acidic extractant Cyanex 272 for extracting iron and titanium that can be further stripped and purified.

Finally, the resulting ionic liquid phase could be regenerated and further used again in leaching process.

Περίληψη

Τα κατάλοιπα βωξίτη, επίσης γνωστά ως ερυθρά ιλύς, είναι τα κύρια στερεά απόβλητα που προκύπτουν κατά την παραγωγή αλουμίνας με τη μέθοδο Bayer. Για κάθε τόνο παραγόμενης αλουμίνας, παράγονται 1 - 1,5 τόνοι καταλοίπων βωξίτη [1-3], οδηγώντας παγκοσμίως σε παραγωγή περισσότερων από 150 εκατομμύρια τόνων καταλοίπων βωξίτη ετησίως [2,4]. Η διαχείριση των καταλοίπων βωξίτη είναι το σημαντικότερο ζήτημα για τη βιομηχανία αλουμίνας λόγω του μεγάλου όγκου και της αλκαλικότητάς τους. Τα κατάλοιπα βωξίτη περιέχουν σημαντικές ποσότητες μετάλλων όπως σκάνδιο, τιτάνιο, σίδηρο, αργίλιο και σπάνιες γαίες και γιαυτό το λόγο απαιτείται μια ολοκληρωμένη στρατηγική διαχείρισής τους με στόχο την ανάκτηση μετάλλων από αυτά και τη χρήση του δευτερογενούς καταλοίπου στην τσιμεντοβιομηχανία ή/και στη βιομηχανία παραγωγής δομικών υλικών. Αυτή η προσέγγιση των «μηδενικών αποβλήτων» συμβάλει στην βιώσιμη επίλυση του προβλήματος της διαχείρισης των καταλοίπων βωξίτη καθώς επίσης και στην μείωση της εξάρτησης της Ευρώπης από τις εισαγόμενες πρώτες ύλες.

Έχοντας κατά νου αυτή την προοπτική, κύριος στόχος αυτής της διδακτορικής διατριβής είναι να μελετήσει μια διεργασία ανάκτησης μετάλλων, κυρίως τιτανίου και σκανδίου, από τα κατάλοιπα βωξίτη. Στα πλαίσια της διατριβής αυτής αναπτύχθηκε ένα σύνθετο διάγραμμα ροής που μπορεί να περιγραφεί από δύο κύρια στάδια.

Το πρώτο στάδιο αφορά την ανάπτυξη μιας ιονομεταλλουργικής διεργασίας εκχύλισης των καταλοίπων βωξίτη. Συγκεκριμένα, μελετήθηκε η άμεση εκχύλιση των καταλοίπων βωξίτη

χρησιμοποιώντας το όξινο κατά Brønsted-Lowry ιοντικό υγρό EMIMHSO$_4$ (‘Οξινο Θειικό 1-αίθυλο-3-μεθυλο-ιμιδαζολίο) για την ανάκτηση σκανδίου και τιτανίου με υψηλές αποδόσεις.

Για τη βελτιστοποίηση της διεργασίας, μελετήθηκαν παράμετροι όπως ο ρυθμός ανάδευσης, ο χρόνος παραμονής, η θερμοκρασία και η πυκνότητα πολτού. Υπό τις βέλτιστες συνθήκες επιτεύχθηκαν υψηλές ανακτήσεις σκανδίου (80%) και τιτανίου (90%), σχεδόν ολική διάλυση σιδήρου, ενώ το αργίλιο και το νάτριο ανακτήθηκαν μερικώς (30-40%). Στοιχεία όπως το πυρίτιο και οι σπάνιες γαίες παρουσίασαν αμελητέες ανακτήσεις, ενώ το ασβέστιο αρχικά διαλύθηκε και εν συνεχεία καταβυθίστηκε ως άνυδρο θειικό ασβέστιο, καταναλώνοντας περίπου το 2% κ.β. του ιοντικού υγρού.

Το εναπομείναν στερεό υπόλειμμα της εκχύλισης χαρακτηρίστηκε διεξοδικά, παρέχοντας σημαντικές εξηγήσεις για τη συμπεριφορά των σπανίων γαιών κατά τη διεργασία της εκχύλισης. Το στερεό αυτό υπόλειμμα μπορεί να υποστεί περαιτέρω υδρομεταλλουργική επεξεργασία για την εξαγωγή των σπανίων γαιών είτε να χρησιμοποιηθεί ως πρώτη ύλη στη βιομηχανία τσιμέντου ή στη βιομηχανία παραγωγής δομικών υλικών.

Το δεύτερο κύριο στάδιο του διαγράμματος ροής περιλαμβάνει τη διεργασία εξαγωγής με οργανικό διαλύτη των μετάλλων από το κυοφορούν διάλυμα της εκχύλισης. Έγιναν συγκριτικές προκαταρκτικές δοκιμές με τέσσερεις οργανικούς διαλύτες (εξαγωγείς), τρία όξινα οργανοφωσφορικά οξέα (D2EHPA, Cyanex 272 και Ionquest 801) και ένα ουδέτερο εξαγωγέα (Cyanex 923), με στόχο τη κατανόηση της διεργασίας της εξαγωγής μετάλλων με οργανικό διαλύτη απευθείας από κυοφορούντα διαλύματα ιοντικών υγρών.

Η χρονική διάρκεια διαχωρισμού φάσεων (οργανική/ιοντικό υγρό), η αναλογία όγκων οργανικής φάσης προς ιοντικό υγρό και η συγκέντρωση του εξαγωγέα στην οργανική φάση (εξαγωγέας/διαλύτης/τροποποιητής) μελετήθηκαν ως μεταβλητές παράμετροι και πραγματοποιήθηκαν κινητικές μελέτες για την κατανόηση της συμπεριφοράς εξαγωγής των μετάλλων με την πάροδο του χρόνου. Από τα πειράματα που πραγματοποιήθηκαν, ο όξινος εξαγωγέας D2EHPA (σε συγκέντρωση 20% v/v στην οργανική φάση και αναλογία O:IL 1:1 v/v) έδωσε τα καλύτερα αποτελέσματα όσον αφορά την εξαγωγή των μετάλλων, καθώς σχεδόν η συνολική ποσότητα σιδήρου, αργιλίου, τιτανίου και σκανδίου ανακτήθηκε από το κυοφορούν διάλυμα μέσα σε χρονικό διάστημα δεκαπέντε λεπτών. Από την άλλη πλευρά, επιλεκτικότητα εξαγωγής σκανδίου επιτεύχθηκε χρησιμοποιώντας τον ουδέτερο εξαγωγέα Cyanex 923.

Βάσει αυτών των αποτελεσμάτων, προτάθηκε μια διεργασία επιλεκτικής εξαγωγής μετάλλων πολλαπλών σταδίων από το κυοφορούν διάλυμα ιοντικού υγρού. Στα δύο πρώτα στάδια, χρησιμοποιήθηκε ο εξαγωγέας Cyanex 923 για την ανάκτηση σχεδόν της συνολικής ποσότητας

σκανδίου και αργιλίου ενώ ο σίδηρος και το τιτάνιο εξήχθησαν σε μέτρια ποσοστά παραμένοντας κυρίως στο κυοφορούν διάλυμα ιοντικού υγρού. Μετά την αναγέννηση και τον καθαρισμό της οργανικής φάσης που μπορεί να ξαναχρησιμοποιηθεί πάλι, το διάλυμα αργιλίου και σκανδίου θα μπορούσε να χρησιμοποιηθεί για παραγωγή κραμάτων Al-Sc. Στο τρίτο στάδιο χρησιμοποιείται ο όξινος εξαγωγέας Cyanex 272 για την ανάκτηση σιδήρου και τιτανίου από το κυοφορούν διάλυμα ιοντικού υγρού που έχει προκύψει μετά τα δύο πρώτα στάδια εξαγωγής. Τελικά, η προκύπτουσα φάση του ιοντικού υγρού αναγεννάται και δύναται να χρησιμοποιηθεί περαιτέρω στη διεργασία εκχύλισης των καταλοίπων βωξίτη.

List of abbreviations

P	Density
°C	Celsius degrees
AAS	Atomic Absorption Spectrometry
A:O	Aqueous to organic phase ratio
AoG	Aluminum of Greece plant
BR	Bauxite residue
CRM	Critical Raw material
D	Distribution ratio
DES	Deep eutectic solvents
EAF	Electric Arc Furnace
ED-XRF	Energy Dispersive X-ray Fluorescence Spectroscopy
EI	Economic Importance
EU	European Union
FT-IR	Fourier Transform Infrared Spectroscopy
H	Hours
HMS	Heavy Media Separation
HREEs	Heavy rare earth elements
HTD	High Temperature Digestion
ICP-MS	Inductively Coupled Plasma Mass Spectrometry
ICP-OES	Inductively Coupled Plasma Optical Emission Spectrometry
ILs	Ionic Liquids
LLE	Liquid-liquid Extraction
LOI	Loss of Ignition
LP	Lower Phase
LREEs	Light rare earth elements
Min	Minutes
NMR	Nuclear Magnetic Resonance
O:IL	Organic to ionic liquid phase ratio
PLS	Pregnant Liquid Solution
Ppm	Parts per million
REO	Rare earth oxides
Rpm	Revolutions per minute

SEM-EDS	Scanning Electron Microscopy coupled with Energy Dispersive Spectroscopy
SF	Separation Factor
S/L	Solid to Liquid ratio
SOFCs	Solid Oxide Fuel Cells
SR	Supply Risk
SX	Solvent Extraction
TEM	Transmission Electron Microscope
TGA-DTA	Thermogravimetric Analysis and Differential Thermal Analysis
TSILs	Task specific ionic liquids
UP	Upper phase
XRD	X-Ray powder Diffraction

Table of contents

List of figures

List of tables

1. Background

Bauxite residue, also known as red mud, is the major by-product of the Bayer process for alumina production, produced by the alkali leaching of bauxite ores. On average, for each metric ton of alumina, 1 – 1.5 metric tons of BR are generated, which leads to a global production of over 150 million metric tons per year. The management of bauxite residue involves stockpiling, storage within settling pond and landfilling. However, these approaches are disadvantageous in terms of potential risk for the environment, such as an accidental dam failure in the case of the Ajka alumina sludge spill in Hungary (2010) as well as the degradation of large areas used for storing huge amounts of bauxite residue. Bauxite residue is a polymetallic matrix, therefore investigating metal recovery methods and the utilization of the left-over residue in other application (i.e. cement, building materials) could contribute to solve issues related to bauxite residue management in view of the zero-waste valorization approach.

Bauxite residue composition can differ depending on the type of bauxite ore from which alumina are produced and Bayer processing techniques. During the Bayer process, valuable base and trace elements like iron, some aluminum, titanium, and rare earth elements remain in the bauxite residue. As a consequence, rare earths are enriched with a factor of about 2 in BR comparing to the initial ore. Particularly interesting is the case of scandium, as its concentration in BR (in Greek BR accounts to 130 ppm on average) is much higher than in the Earth's crust (22 ppm on average); that means a notable enrichment of scandium in bauxite residue. Due to the high market price (Sc_2O_3— 4600 US$/kg, 99.99 % purity, in 2017), scandium may represent 95 % of the economic value of rare earths in BR. It has also been listed as a critical raw material by the European Commission due to its high economic importance and supply risk. In fact, scandium is mainly produced as a byproduct

during the processing of various ores, from titanium and rare earths ores (China), uranium ore (Kazakhstan and Ukraine), and apatite ore (Russia). It can also be recovered from previously processed tailings or residues. For these reasons, bauxite residue can be accounted as a secondary raw material source, and the recovery of scandium could represent a high economic interest.

Bauxite residue can also be considered a secondary source for titanium, which is a photocatalyst and it is applied in the white pigment industry. Since the availabilities and qualities of titanium ores are decreasing, it is important to find methods for extracting Ti from secondary sources.

Many studies, patents, and pilot scale implementations have been carried out for scandium and titanium recovery from BR, mainly by investigating hydrometallurgical or combined pyro-hydrometallurgical processes, but none of them has reached an industrial scale. Nowadays, the impact of the zero-waste valorization policy motivates the research community on finding innovative, greener, and economical viable routes for metal extraction from complex polymetallic matrices, such as the bauxite residue. In this perspective, ionometallurgical approach can be exploited as an alternative to conventional hydrometallurgical processing. The term ionometallurgy indicates the use of ionic liquids as solvents in metals processing. Ionic liquids are liquid at room temperature and consist solely of ions; generally, an organic cation and inorganic/organic anion. ionic liquids have superior properties against conventional organic solvents, such as nonflammability, a wide electrochemical window, high thermal stability, negligible vapor pressure, and low volatility. For these reasons and thanks to the vast number of combinations of the cation and the anion during synthesis, ionic liquids have potential for many applications, such as solvent extraction, catalytic reactions, and electrodeposition of metals. In the past few decades, ionic liquids have been used also as lixiviants for metals dissolution. Applying ionic liquid leaching on secondary raw material resources eventually improves efficiency yields, reduce waste effluent, and increases selectivity.

1.1 Scope of the PhD thesis

In this context, a process for recovering valuable metals from bauxite residue has been studied within the framework of this PhD thesis with the main objective being recovering valuable metals, such as titanium and scandium. A conceptual flowsheet is presented in Figure 1 and two main parts can be outlined.

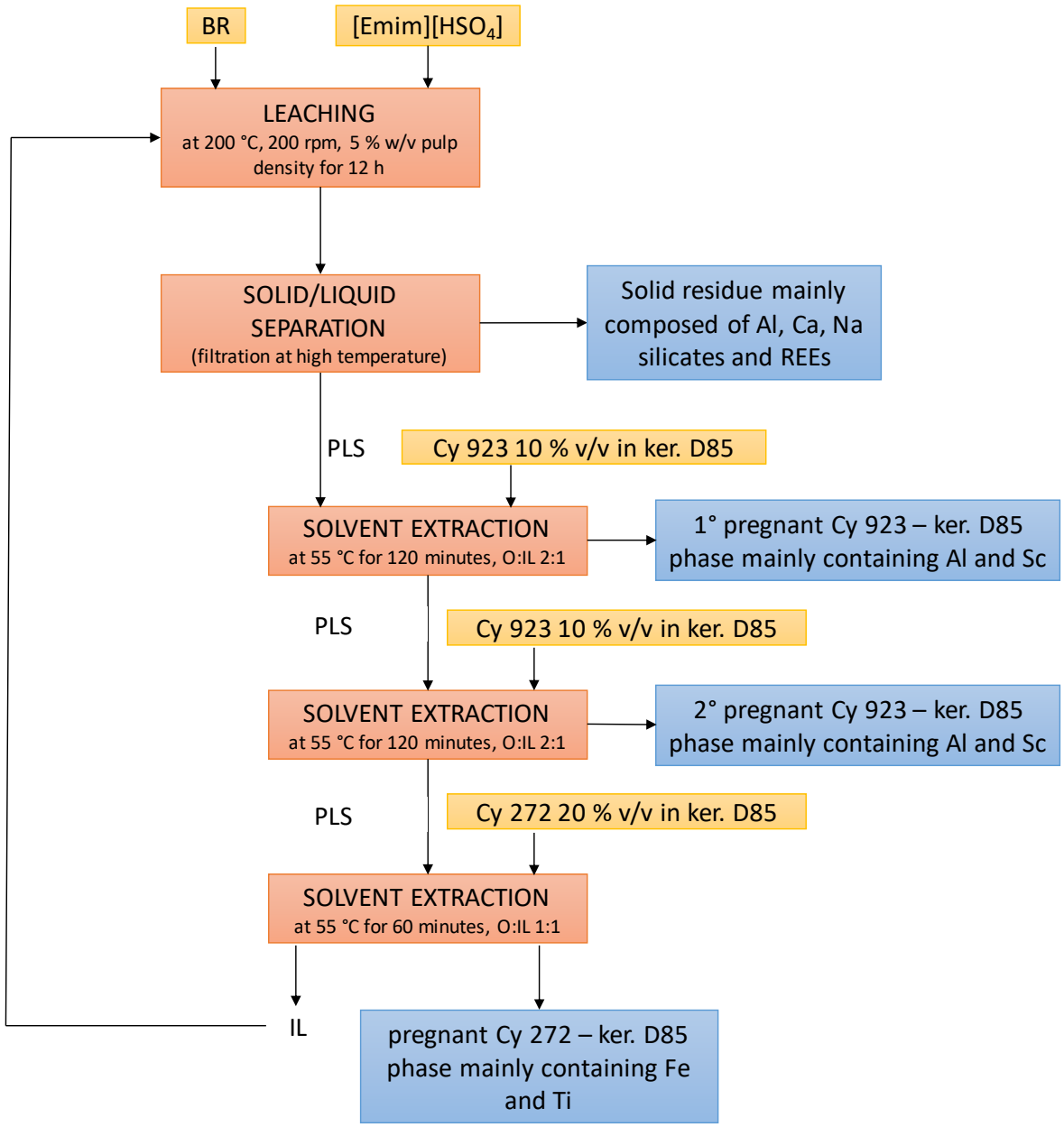

Figure 1 Conceptual flowsheet of the work presented in this PhD thesis focused on the recovery of valuable metals from bauxite residue

(1) Firstly, the direct leaching of bauxite residue by using the Brønsted acidic 1-ethyl-3-methylimidazolium hydrogen sulfate ionic liquid was investigated and high titanium and scandium recovery yields were reached. The process was optimized by evaluating parameters like stirring rate, time, temperature and pulp density. It was found that at the optimum conditions (200 rpm, 200 °C, 12 hours and 5 % w/v pulp density) high recovery yields of scandium (80 %) and titanium (90 %) could be reached. Having high scandium dissolution, led to an almost complete co-extraction of iron, as in bauxite residue, scandium is mainly contained in iron mineralogical phases (75 %). Rare earths were not extracted

with this process and the resulting solid residue was characterized to try to locate them. The matrix was mainly composed of aluminum – calcium – sodium silicates and surrounded phases transitioning from calcite to calcium sulfate anhydrite. Calcium sulfate anhydrite is a new mineralogical phase formed due to the interaction between calcium and the anion of the ionic liquid and it is responsible for a 2 wt. % consumption of the ionic liquid. Heavy rare earths like gadolinium and dysprosium were located in yttrium phosphate particles. This kind of grains were previously located in bauxite residue; therefore, they endure the leaching process. On the other hand, light rare earths, including neodymium, lanthanum and samarium, were identified in small mixed calcium-cerium phosphate particles. This may indicate a partial dissolution of calcium from the mixed Ca – light rare earths phases, leaving behind smaller phosphate particles which are beneficiated in light rare earths. Since rare earths remain in the solid residue, this could be further treated for subsequently extracting them. Moreover, being rich in calcium, aluminum and silicon, the left-over solid residue could be employed in building material or cementitious applications.

(2) Metals recovery from the pregnant liquid solution generated by the leaching process. Preliminary studies on solvent extraction were carried out, by testing different kind of extractants to find the most suitable for extracting metals from the pregnant liquid solutions. For this purpose, three acidic organophosphorus extractants and a neutral mixture of phosphine oxides were tested. It was found that the neutral extractant, the Cyanex 923, was selective for extracting Sc and Al from the leachate. On the other hand, the three acidic extractants, Cyanex 272, D2EHPA and IONQUEST 801 were able to extract all kind of metals. Therefore, a multi-stage solvent extraction process was proposed, by firstly using a dual-stage solvent extraction process with Cyanex 923 for extracting almost the total amount of scandium (99 %) and aluminum (more than 95 %). The second stage of the solvent extraction process involved the acidic extractant Cyanex 272 for recovering nearly the total content of titanium and iron (about 95 %) from the leachate.

After the solvent extraction process, the ionic liquid could be regenerated and subsequentially re-used for a more environmentally friendly process for recovering metals from bauxite residue and a complete valorization in view of a zero-waste approach.

1.2 Outline

This PhD thesis has been divided into nine chapters. The first four chapters refer to the literature review, while from the fifth to the eighth chapter the experimental part is presented. In the ninth

and final chapter conclusions and outlook are given. A more detailed outline of these chapters is given below.

- **Chapter 1** presents the thesis background, scope of this work and the outline of this PhD thesis.
- **Chapter 2** describes the Bayer process in general and more specifically the conditions used in Aluminum of Greece plant. It gives an overview on bauxite residue management, describing its potential applications. Finally, the use of bauxite residue as secondary raw material is reported; particularly an overview of the literature on the scandium and titanium recovery from bauxite residue is given.
- **Chapter 3** specifies ionic liquids definition, characteristics and uses. It describes in detail the ionometallurgy field and specifically the use of the ionic liquids for leaching.
- In **Chapter 4** the solvent extraction technique is described and an overview on extracting metals from leachates with both conventional and non-aqueous solvent extraction processes is given.
- **Chapter 5** discusses the fully characterization of the bauxite residue employed in this work.
- **Chapter 6** is the core of this PhD thesis, as it illustrates the characterization of the ionic liquid 1-ethyl-3-methylimidazolium hydrogen sulfate employed in this work and investigates the mechanisms of the reaction that takes place for dissolving metals from bauxite residue. Moreover, some preliminary tests are shown and finally, the optimization of the leaching process is extensively discussed.
- In **Chapter 7** the characterization of the left-over solid residue after leaching is discussed. REEs in the solid residue were located.
- In **Chapter 8** metal recovery from the leachates is investigated. More in detail, some preliminary tests with several extractants are evaluated and a multi-stage solvent extraction process is proposed.
- **Chapter 9** presents the overall conclusions of the thesis and gives an outlook for further studies that can be performed.

2. Bauxite residue

2.1 From bauxite to alumina: the Bayer Process

The Bayer Process is a cycling method for producing technically pure alumina (>98.3 % Al_2O_3) from bauxite [5–7]. It was developed and patented in 1887 and successively implemented in 1893 by Karl Josef Bayer. Since then, the process has been extensively researched and any technological improvements have been made; however, its basic principles and environmental issues remain unchanged [8]. Today, over 95 % of the alumina produced globally is generated through the Bayer process [9], as it remains the only viable way to produce alumina from bauxite.

On average, 2.65 kg of bauxite ore are required to produce 1 kg of alumina, while the remaining amount of the solid is removed from the process as slurry [10,11], commonly known as red mud. Bauxite is a sedimentary rock principally consisting of a heterogeneous mixture of hydrated aluminum oxides such as gibbsite ($Al(OH)_3$ or $Al_2O_3 \cdot 3H_2O$), boehmite (γ-AlOOH or $Al_2O_3 \cdot H_2O$) and diaspore (α-AlOOH or $Al_2O_3 \cdot H_2O$) with average levels 30 – 65 wt. % (measured as aluminum oxides) [9]. Other constituents are silica (4 – 8 wt. %), iron oxides and hydroxides (10 – 35 wt. %, measured as iron oxides), titanium oxides (2 – 4 wt. %) [12]. Scandium [13], rare earth elements [14] and other trace elements like gallium and vanadium are also present [7].

The Bayer process generally consists of six main units processes (Figure 2, [15]): (I) material preparation (milling and pre-desilication); (II) digestion, (III) clarification, (IV) precipitation, (V) evaporation and (VI) calcination. Each unit process influences the chemical composition of the residues, as well as their physical and mineralogical attributes [5].

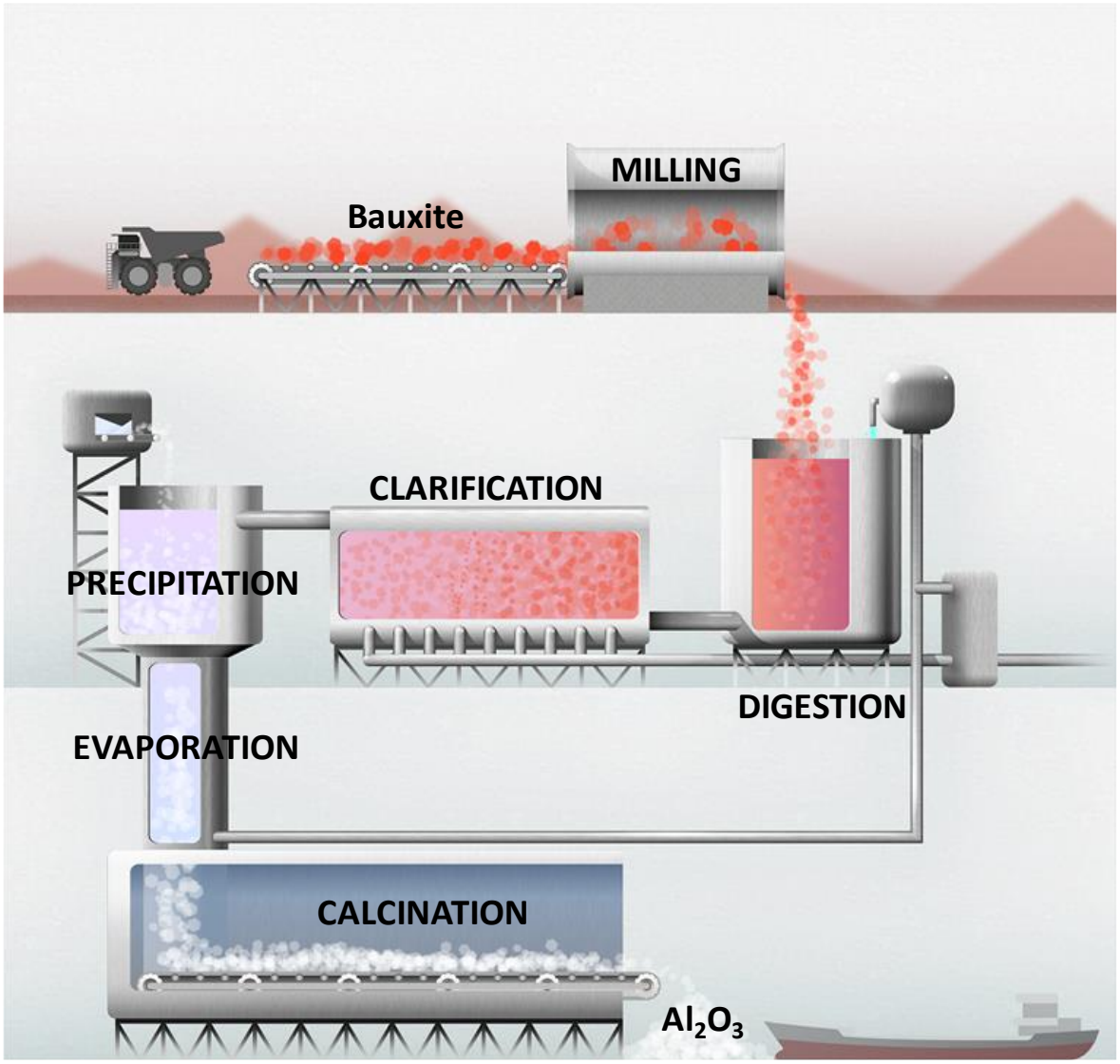

Figure 2 The Bayer Process simplified scheme (source: http://bauxite.world-aluminium.org/index.php?id=208&L=0 [15]).

(I) The first unit process consists of preparing the raw material by crushing and milling bauxite to reduce particle size and increase the surface area for the following stage, which involves desilication, where silica (SiO_2) is removed.

(II) During the next unit process, bauxite is leached with a hot caustic soda (NaOH) solution. At this high pH value and elevated temperature and pressure, aluminum-containing minerals are dissolved selectively, while most of the other compounds remain insoluble and the pregnant liquor is formed ("green liquor"). This is called alkaline digestion and it is based on the solubility of Al^{3+} as aluminate ($Al(OH)_4^-$) relatively to the other constituents of bauxite [12]. The operative conditions of this unit depend on the mineralogy of the processed bauxite. The main aluminum phases in bauxite are

trihydrates like gibbsite (also known as hydrargillite) or monohydrates like boehmite and diaspore. While trihydrates are better soluble at temperatures of about 135 – 150 °C, boehmite is treated at temperatures of 205 – 245 °C and diaspore needs the highest digestion temperatures above 250 °C [16]. Due to its mineral composition, bauxite can be divided into two groups, karst bauxite and lateritic bauxite. Karst bauxite mainly contains boehmite and small amount of diaspore and can be found primarily in Europe. On the other hand, lateritic bauxite is mainly constituted by gibbsite with small amounts of boehmite and are located in tropical deposits [16,17].

The alkaline digestion process is governed by the following reactions [12,17–19]:

Gibbsite: $$Al(OH)_{3(s)} + NaOH \rightarrow Al(OH)^-_{4(aq)} + Na^+_{(aq)} \quad \text{(135-150 °C)} \quad (1)$$

Boehmite: $$\gamma - AlOOH_{(s)} + NaOH + H_2O \rightarrow Al(OH)^-_{4(aq)} + Na^+_{(aq)} \quad \text{(205-245°C)} \quad (2)$$

Diaspore: $$\alpha - AlOOH_{(s)} + NaOH + H_2O \rightarrow Al(OH)^-_{4(aq)} + Na^+_{(aq)} \quad \text{(T>250 °C)} \quad (3)$$

In general, the equilibrium in the above moves to the right with an increase in caustic soda concentration [18].

During this part of the process, iron and titanium containing species remain insoluble, while silica containing species are partly digested according to the following reactions:

$$SiO_{2_{(s)}} + 2NaOH + = Na_2SiO_{3_{(aq)}} + H_2O \quad (4)$$

$$Al_2O_3 \cdot 2SiO_2 \cdot H_2O_{(s)} + 6NaOH = 2NaAlO_{2_{(aq)}} + 2Na_2SiO_{3_{(aq)}} + 5H_2O \quad (5)$$

The soluble products ($NaAlO_2$ and Na_2SiO_3) react to form desilication products (DSP) which are non-soluble aluminosilicate precipitates:

$$2NaAlO_{2_{(aq)}} + 2Na_2SiO_{3_{(aq)}} + 2H_2O = Na_2O \cdot Al_2O_3 \cdot 2SiO_{2_{(s)}} + 4NaOH_{(aq)} \quad (6)$$

Even though the DSP formation process leads to soda and aluminum losses during leaching, its formation is necessary to control the concentration of dissolved silicon. If the bauxite ore does not contain a significant proportion of readily soluble silicon, then the above process cannot take place. In this case, low silicon concentration in the leaching solution, can be achieved by adding an excess of calcium oxide (CaO) in the feed charge. This leads to the formation of cancrinite $Na_6Ca_2Al_6Si_6O_{24}(CO_3)_2$, a slightly soluble phase.

(III) The clarification stage involves multiple steps where flocculants are added to enhance the sedimentation of the solid (red mud) from the sodium aluminate-containing pregnant liquor [12]. The red mud slurry is then washed in counter-current decantation washer to recover NaOH and $Al(OH)_4^-$ for recycling them into the Bayer Process. Depending on the plant requirements, the slurry is undergone to further treatments and stockpiled in the disposal area [5,12].

(IV) In the precipitation stage alumina hydrate ($Al(OH)_3$) is crystallized from the sodium aluminate supersaturated solution:

$$Al(OH)_{4(aq)}^{-} + Na_{(aq)}^{+} \rightarrow Al(OH)_3 + NaOH \quad (7)$$

Precipitation is initiated by the introduction of aluminum hydroxide seed crystals [7].

(V) The spent liquor is then heated for recycling NaOH that is washed and reused into the digestion stage (evaporation).

(VI) $Al(OH)_3$ is then thermally decomposed at T > 1000 °C to produce alumina (Al_2O_3) (calcination) [6,20], which is the final product of the Bayer Process:

$$2Al(OH)_3 \rightarrow Al_2O_3 + 3H_2O \quad (8)$$

The Bayer process is often divided into the “red side” and the “white side”. The “red side” is referred to the units where bauxite and its residue are present, the “white side” denotes the stages after residue removal (clarification) until precipitation, calcination and evaporation stages [5,7,21].

2.1.1 The Aluminum of Greece conditions for the Bayer Process

Bauxite residue employed in this work comes from Aluminum of Greece plant (Metallurgy Business Unit, Mytilineos S.A.; hereafter denoted as AoG). As Vind et al. explain, AoG utilizes mainly two types of bauxite feed: 80 % of the feed is from the locally mined karst (diasporic/boehmitic) bauxite and 20 % is imported lateritic (gibbsitic) bauxite originating from Ghana or Brazil [7,13]. Due to the presence of karst bauxite (boehmitic and diasporic bauxites), AoG uses digestion conditions known as high-temperature digestion (HTD), which implies T > 250 °C and elevated pressure (5.8 – 6.0 MPa) [7,22]. The karst bauxite used originates from Parnassos-Ghiona, which is situated between limestones. For this reason, it is necessary to remove the unwanted limestone from the ore that is inevitably partly mined as a contaminant together with bauxite [7]. As it is possible to observe in Figure 3, prior to the other stages, limestone is removed by heavy media separation (HMS) in ferrosilicon slurry, also referred as “ decalcitation” in literature [7]. AoG also uses an optimization

step (called “sweetening” process), in which lateritic bauxite is digested at a lower temperature after the digestion of karst bauxite. Lateritic bauxite suspension passes through a pre-desilication step to allow the formation of desilication products (sodalite and cancrinite) and avoid the problems of reactive silica (i.e., kaolinite) during digestion. Hence, lateritic bauxite suspension is introduced to the main karst bauxite slurry after the HTD of karst bauxite suspension [7]. It should also be noted that to obtain de-watered bauxite residue (BR), AoG makes use of the plate and frame filter pressing of the initial residue slurry (red mud) after the settling and washing unit [2].

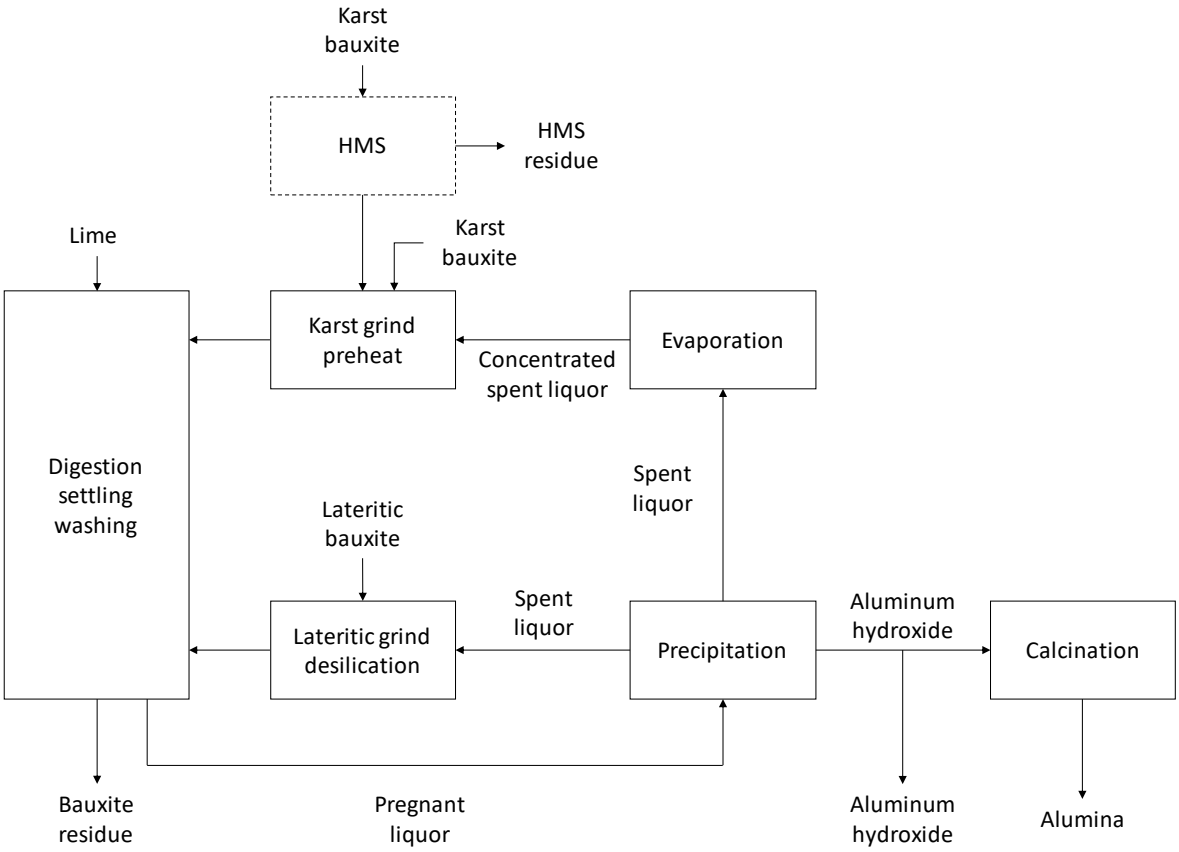

Figure 3 Bayer Process flow diagram described in Vind et al. [7].

2.2 Bauxite residue characteristics

Bauxite usually contains 30 – 60 wt.% of Al_2O_3 [9] and, due to the formation of sodium aluminum silicates, the deposited bauxite residue still contains 10 – 22 wt.% of Al_2O_3 [9,18,23]. Typical bauxite residue composition is reported in Table 1 [9,24].

Table 1 Typical bauxite residue composition [9,24].

Component	Typical range (wt.%)
Fe_2O_3	20-25
Al_2O_3	10-22
TiO_2	4-20
CaO	0-14
SiO_2	5-30
Na_2O	2-8
REEs	0.1-1

BR composition can differ depending on the ore composition, residual alkalinity and other added materials during refining, and Bayer processing techniques [5,10,12,25]. During the Bayer process, base and trace elements (e.g. Fe, Al, Ti and Rare Earth Elements (REEs)) remain undissolved and are concentrated up in BR, representing a significant portion of recoverable and economically valuable metals in terms of volume of waste produced per annum [25].

Many minerals are present in BR, some of them are also present in bauxite itself, while others are produced during the Bayer process. The typical mineralogical composition of BR is shown in Table 2.

Table 2 Typical range of minerals found in bauxite residue [2].

Component	Typical range (wt.%)
Sodalite ($3Na_2O{\cdot}3Al_2O_3{\cdot}6SiO_2{\cdot}Na_2X$) [X=carbonates, chlorides, sulphates, etc.]	4-40
Al-goethite ($(Fe, Al)_2O_3{\cdot}nH_2O$)	1-55
Hematite (Fe_2O_3)	10-30
Magnetite (Fe_3O_4)	0-8
Silica (SiO_2) crystalline and amorphous	3-20
Calcium aluminate ($3CaO{\cdot}Al_2O_3{\cdot}6H_2O$)	2-20
Boehmite (AlOOH)	0-20
Titanium dioxide (TiO_2) anatase and rutile	2-15
Muscovite ($K_2O{\cdot}\ Al_2O_3{\cdot}6SiO_2{\cdot}2H_2O$)	0-15
Calcite ($CaCO_3$)	2-20
Kaolinite ($Al_2O_3{\cdot}2SiO_2{\cdot}2H_2O$)	0-5
Gibbsite ($Al(OH)_3$)	0-5
Perovskite ($CaTiO_3$)	0-12
Cancrinite ($Na_6[Al_6Si_6O_{24}]{\cdot}2CaCO_3$)	0-50
Diaspore (AlOOH)	0-5

Some of the elements are soluble in the Bayer process and either build up in the Bayer liquor or precipitate along with the aluminum hydroxide [2]. Sodium is the only element not found in the bauxite itself and in BR may be present in DSP or a soluble form. In fact, small quantities of soluble sodium compounds resulting from soda used during digestion will remain. The amount of this residual will depend on the de-watering and washing conditions used. These species, a mixture of

sodium aluminate and sodium carbonate are responsible for elevated pH for BR slurries, which are then neutralized by carbon dioxide from the air to form sodium carbonate and other metal carbonate species [2].

Physical characteristics, such as moisture content and particle size are also important when considering BR management or as a raw material. The median particle size is normally in the range of 5 – 10 µm. However, the grains width can spread from 1mm size to sub-micron particles. Also this factor depends from the kind of bauxite used and the parameters employed during the Bayer process by the alumina refinery [2].

2.3 Bauxite residue management and possible applications

The global demand for alumina increases rapidly (Figure 4), in fact, in 2015 over 115 million tons of alumina were produced globally, while in 2018 the production increased of 15 million tons compared to 2015 (for a total of 130 million tons) [26].

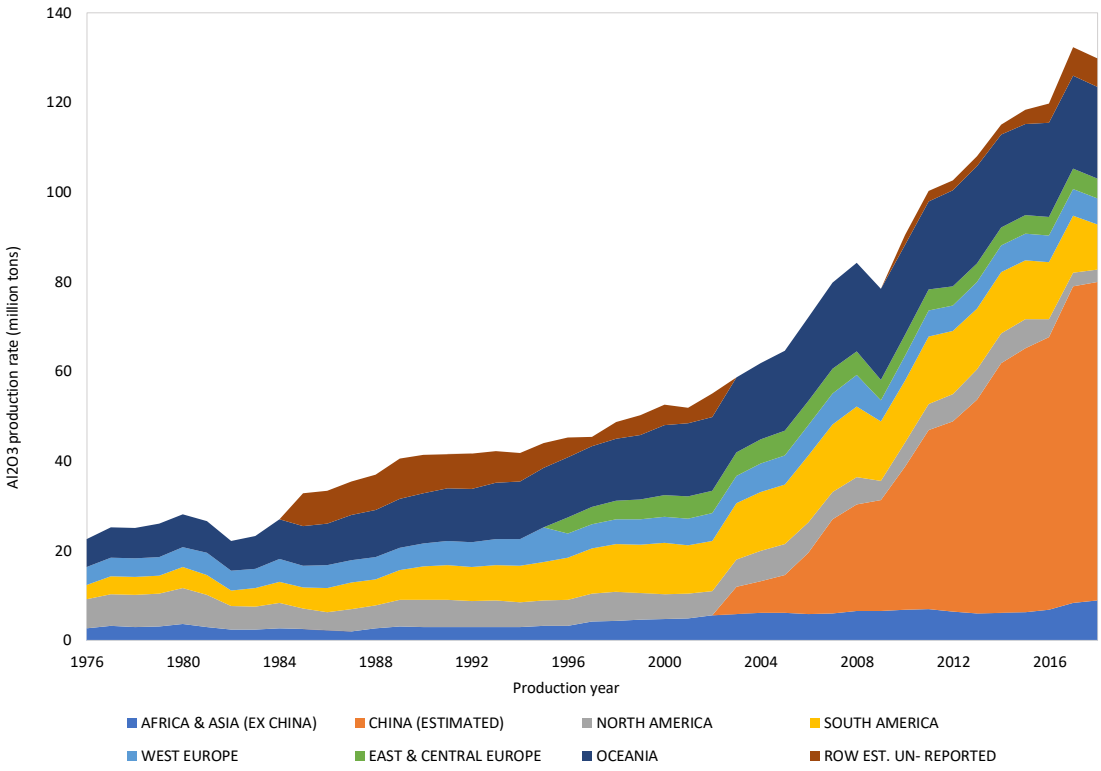

Figure 4 Al_2O_3 global production from 1974 to 2018 (source: http://www.world-aluminium.org/statistics/alumina-production/#histogram [26]).

It is estimated that for each ton of alumina produced, 1 – 1.5 tons of bauxite residue is generated [1–3], leading to over 150 million tons per year of bauxite residue generated globally [2,4]. The amount of bauxite residue generated in a particular refinery is governed by factors like alumina's

extraction efficiency and bauxite characteristics (alumina content, karst or lateritic bauxite employment and silica content) [2]. BR is currently generated at 80 active Bayer plants, while there are at least other 50 closed legacy sites, so the combined stockpile of bauxite residue at the active and legacy sites is estimated at 3 – 4 billion tons [2,9,27].

The management of BR has evolved over the decades and continues to be a global issue [2,9,28]. The way BR is handled and stored depends on factors like age of the plant, land availability, proximity to the sea, climate logistics, nature of the residue and regulations [9]. Historically, in the early Bayer alumina plants, the residue was often just disposed either close to the site or adjoining lands [2,27]. This method had the advantage of filling depressions, valleys and mine workings, but these areas were often not lined, causing high alkaline leaching of the landfill [9].

Another method largely employed between the 1940s and 1960s and definitely phased out in 2015, was marine discharge, where the slurry was directly pumped from the washing circuit to the sea or discharged into the deep ocean [2,5,9]. Prior to 1980, most of the inventory of BR was stored in lagoon-type impoundments and the practice continues at some facilities. Lagooning involves pumping of the bauxite residue slurry with a solid content of 18 – 30 % into land-based ponds. Such ponds may be formed within natural depressions or old mine workings using dams to ensure secure containment [2,5,9]. If the residue material is not neutralized before discharging it into the lagoon, it remains highly alkaline (pH > 12 and soda level excess of 2000 mg/L) for many years after the residue slurry pumping had stopped [2]. For this reason, this approach is disadvantageous in terms of potential risk for the environment, as the dam may fail. If that happens muds and process liquids may flow a considerable distance, as though in the case of the accidental dam failure at Ajka, in Hungary in 2010 [29,30]. Another major disadvantage of this disposal method is the degradation of large areas used for storing huge amounts of BR and the cost of monitoring both leachate, site and surrounding area [9].

Dry stacking was adopted as disposal method where lagooning was not possible due to lack of space and since the 1980s, this method has been increasingly used to reduce the land area required as well as to reduce the risk of a leakage of the caustic liquor [2]. This method involves filtration with drum filters and plate and frame filter presses and helps to maximize the recovery of caustic soda and alumina which are sent back to the Bayer process. This is currently the preferred technology for storing bauxite residue at large alumina refineries; in fact, it provides considerable economic benefits as the solid residue contains less than 28 % moisture and therefore transport issues and costs are dramatically reduced [2]. Aluminum of Greece adopted the frame filter press and dry stacking disposal method. However, in this alumina refinery, the BR disposal takes up to 1 km^2 of land for an annual 0.75 million tons of BR. Because of the big amount of waste generated and huge

areas needed for disposal, many potential options for reusing BR have been considered. Possible applications can be divided into various categories [2]:

- Cement manufacture [31–34];
- Recovery of specific components like iron [10,18,35,36], titanium [36–40], aluminum [37,41], scandium [39,42,43], yttrium [24];
- Building or construction materials [4,44];
- Soil amelioration, landfill capping [4], treatment of acid mine drainage [45], road construction [46];
- Pigments or glass ceramic.

This wide research is also demonstrated by the more than 700 patents since 1964 [47], in Figure 5 the different areas of BR processing are shown [27,47].

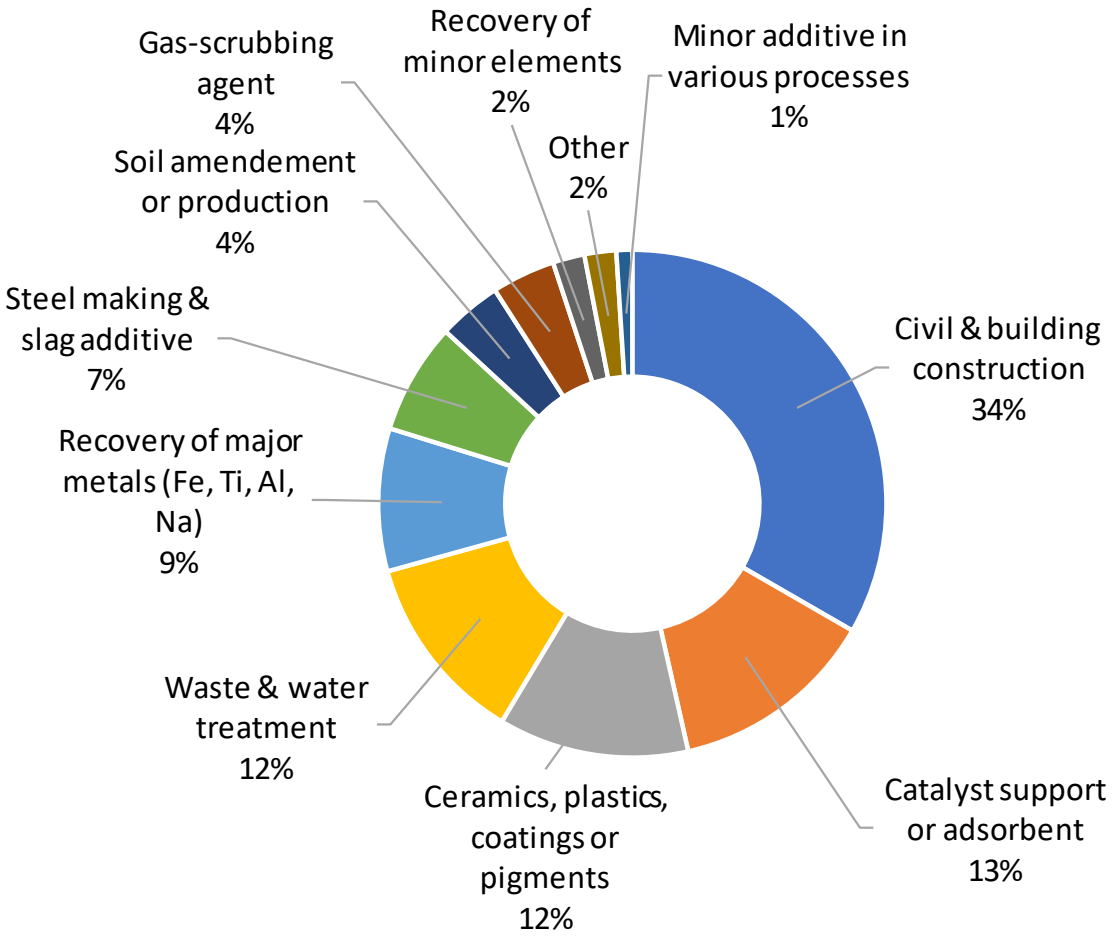

Figure 5 Patents distribution on BR processing (Klauber et al. [47]).

The processing of BR as a raw material has its challenges such as high economic costing for energy requirements in drying BR, acid-consuming nature of BR due to high alkalinity, interfering elements and complex structure of minerals that inhibit the metal extraction process, and restrictions in physical and chemical parameters of extractive agents [5,10,12,25,48]. For these reasons, a number of processes have been proposed, but never implemented, for the simultaneous recovery of the major metals from BR [27]. However, exergy analysis of Bayer process performed by Balomenos et al. [8] reported very low exergy efficiency value 2.94 % indicating that the process is inefficient from the exergetic point of view mainly due to high exergy content of the unexploitable by-products [10,48]. Therefore, to improve the efficiency of the overall Bayer process, there is the need to find possible ways for reusing BR and/or recovering metals from it [8,10].

2.4 Bauxite residue as a secondary raw material

Thanks to its composition, BR can be considered a secondary source of valuable base and trace metals. Many studies, patents and pilot scale implementations have been carried out with the intention of recovering metals from this secondary resource, mainly by investigating hydrometallurgical or combined pyro-hydrometallurgical processes [23–25,35,38,40,42,43,49–57], but none of them has reached an industrial scale. This is due to the fact that BR utilization in a different industry is either technically complicated or financially non-viable [58].

However, the impact of the zero-waste valorization policy motivates the research community on finding innovative, greener and economical viable routes for metal extraction from complex polymetallic matrixes such as BR. In the next section an overview of recovering methods from BR of the two targeted metals (titanium and scandium) is given.

2.4.1 Titanium

Titanium dioxide (TiO_2), better known as titania, has a high refractive index and for this reason is commonly used as white pigment in various fields of industry, such as dyes, plastics and drugs [23,38,59,60]. Thanks to its high strength-to-weight ratio and inertness to many corrosive environments, it is also used in space industry and automotive applications [61].

Since the availabilities and qualities of Ti ores are decreasing [38], it is important to find methods for extracting Ti from secondary sources. In bauxite residue, it is present either in the form of rutile or anatase, or it can coexist with other minerals [25]. BR can be considered a secondary source also for Ti, as its amount can vary between 4 and 20 wt.% (Table 1).

There are different methods to recover titanium from BR, pyrometallurgical and hydrometallurgical processes, or a combination of them. Pyrometallurgy is normally used as a pretreatment method

for recovering iron from BR. Reductive smelting of BR [10] either as it is or after palletization with a carbonaceous reducing agent is the preferred method. Molten iron and slag that contains mainly titanium dioxide, alumina and silica are obtained. After separation of the molten pig iron, the slag is digested to recover aluminum and titanium from solution [25].

There are two main acidic treatments to recover titanium, by hydrochloric or sulfuric acid leaching. Agatzini-Leonardou et al. [40] suggested that through a 6 N H_2SO_4 leaching at 60 °C with a solid-to-liquid ratio of 5 %, Ti recovery can reach up to 64.5 %. Kasliwal and Sai [59] carried out experiments which involved a leaching step of bauxite residue with hydrochloric acid. They found that the titanium dioxide content in the leaching tailings was enriched from 18 % in the raw BR to 36 % under the optimum leaching conditions (90 °C, acid to BR ratio 10.3, acid concentration 5.2 M). In order to enrich more the tailings in TiO_2, they added a second treatment step which was consisting of roasting the leaching tailings with sodium carbonate and subsequently leaching the resulted cinders with water. Under the optimum roasting conditions (1150 °C, Na_2O/Al_2O_3 molar ratio 2.8, retention time 115 min) and followed by water leaching, the resulted tailings had a TiO_2 content of 76 %.

Ghorbani and Fakhariyan [60] made a comparison between a single acid leaching of red mud and a combination of two acids at different ratios. The highest extraction of titanium was 97.7 % and it was obtained with a combination of concentrated sulfuric and hydrochloric acids with 3:1 ratio at 100 °C and 2 hours retention time. Additionally, the co-dissolution of iron and aluminum were 92 % and 91.3 % respectively [60].

Alkan et al. made a comparison by dissolving BR with H_2SO_4, HCl and a combination of them (HCl to H_2SO_4 ratio 1:3). The highest leaching efficiency (above 67 %) was reached with H_2SO_4 after 2 hours. However, 50 % of Fe was also leached [38]. To improve Ti leaching efficiency and suppress the formation of silica gel that inhibits filtration, Alkan et al. also proposed another process that implied the use of 2.5 M H_2SO_4 and 2.5 M H_2O_2. After 30 minutes, at 100 °C and 1:10 solid to liquid ratio, 90 % of Ti was recovered, while Fe leaching was limited to 35 % [42].

2.4.2 Scandium

In 2017, scandium has been listed as a critical raw material (CRM) by the European Commission, as a single element [62] and not included together with REEs as in 2010 [63] (Figure 6). The CRMs list has been assessed combining the criteria of supply risk (SR) and economic importance (EI), with a material defined as critical when exceeding both the thresholds (SR ≥ 1, EI ≥ 2.8); 61 materials were assessed, 26 of which were identified as critical [62]. EI is intended as the impact that the raw material has on the European manufacturing economy in terms of end-use applications and the

value added of the corresponding EU manufacturing sector. Furthermore, the economic importance is corrected by the substitution index (SI_{EI}) related to the technical and cost performance of the substitutes for individual applications [64]. The SR parameter reflects the risk of a disruption in the EU supply of the material and it is assessed considering governance performance and trade aspects of the raw material producing countries, which are classified into two categories: the global suppliers and the countries from which the EU is sourcing the raw materials. SR is measured at the stage of extraction or processing the material, which represents the highest supply risk for the EU. Substitution and recycling are considered risk-reducing measures [64]. In particular, in 2017, the EI and SR factors were assessed to be 3.7 and 2.9 for Sc respectively [65], as reported in Figure 6.

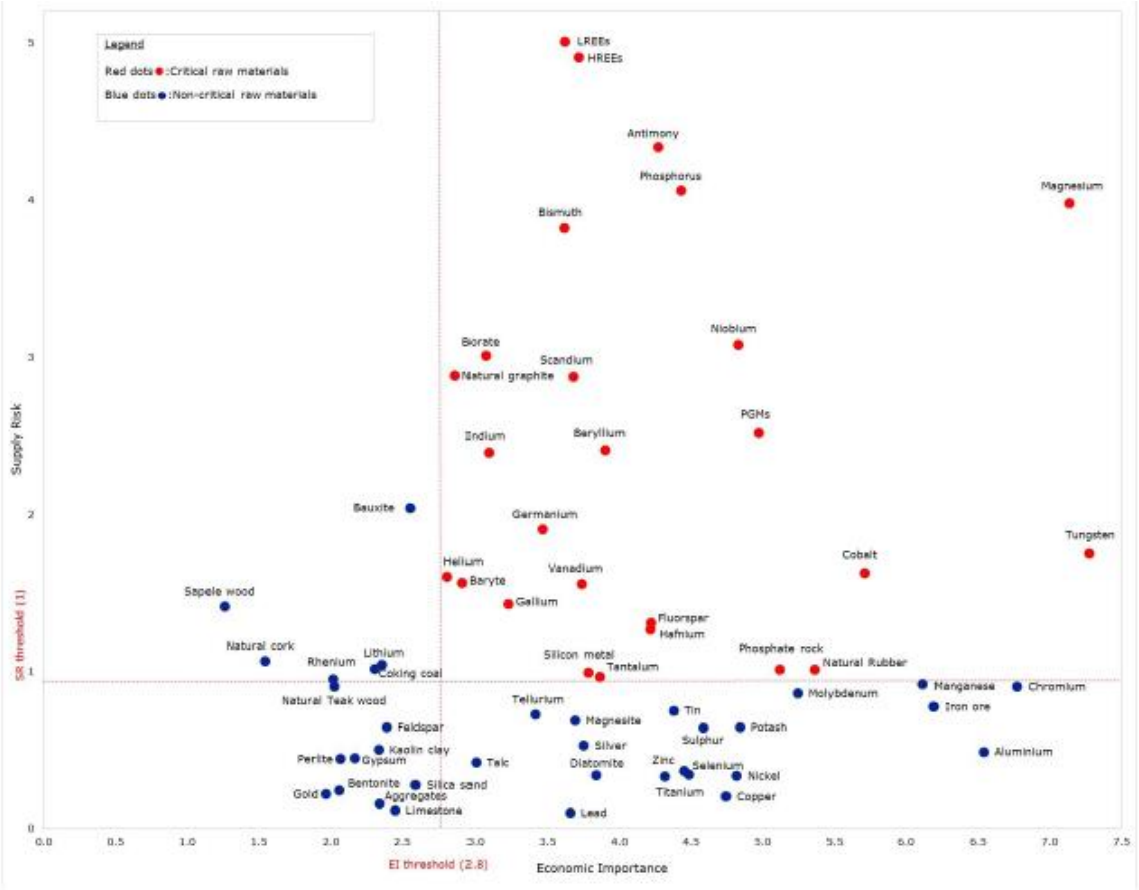

Figure 6 Critical raw materials list, published by the European Commission in 2017 [62].

China is the first producer of scandium in the form of oxide (SC_2O_3) with about 10 tons per year (around 66 wt.%). It comes mainly as a by-product of REEs extraction, but also from the recovery of sulfate wastes from the manufacture of titanium pigments [66,67]. Russia produces 3 to 5 tons per year (33 wt.%), mainly from apatite [67] and uranium ore [66,67]. Kazakhstan is estimated to

produce 100 – 200 kg of Sc_2O_3 annually (about 1 wt.%) from uranium ore [66,67]. There is no Sc extraction in the EU, therefore the EU import reliance for Sc is 100 % [65].

Sc is mainly used (90 % of the total production) as a stabilizing agent for zirconia in advanced Solid Oxide Fuel Cells (SOFCs) and in aluminum-scandium alloys (9 % of the total production) with applications in aerospace industry and automotive transportation [65], as it increases the strength of aluminum alloys [68]. Sc is also used in ceramics, electronics and lightning [69].

As already discussed before, during the Bayer process, Sc along with Fe, Ti, REEs and other undissolved material remain unchanged ending up in BR. Ochsenkühn-Petropoulou et al. investigated REEs concentration in bauxite from Parnassos-Ghiona reserves in Greece and in the resulting solid residue after the Bayer process. The total average concentration in bauxite was 506 ppm, whereas in BR was 1040 ppm [70]. As a consequence, REEs are enriched with a factor of about 2 in BR comparing to the initial ore [7,55,70]. Remarkable is the case of scandium (Sc), as its concentration in BR (in Greek BR it accounts to 130 ppm on average [55]) is much higher than in the Earth's crust (22 ppm on average [71]) and that means a notable enrichment of Sc in BR. Due to the high market price (Sc_2O_3 - 4600 US$/kg, 99.99 % purity, in 2017) [67], Sc may represent the 95 % of the economic value of rare earths in BR [58]. For these reasons, BR can be accounted for a secondary raw material source [55] and the recovery of Sc could represent a high economic interest.

Researchers have employed different approaches for recovering Sc from BR, mainly involving hydrometallurgical processes or a combination of pyrometallurgical and hydrometallurgical processes. Most of them use the pyrometallurgical treatment to recover iron leaving behind Sc (or REEs in general) which are leached by acids.

Ochsenkühn-Petropoulou et al. [72] recovered selectively and almost quantitatively up to 93 % scandium from BR. They dissolved BR in 1.5 M of HCl and the solution was then passed through a chromatographic column containing a cation resin. The metals Fe, Al, Ca, Si, Ti, Na Ni, Mn, Cr were eluted with 1.75 M HCl. REEs were eluted with 6 M HCl. They extracted scandium with di(2-ethylhexyl)phosphoric acid (D2EHPA) in hexane and Sc was back-stripped with 2 M NaOH [72].

In a following work, the same team recovered lanthanides and yttrium from BR by selective leaching using diluted mineral acids and subsequent liquid-liquid extraction. Results showed that diluted HNO_3 could successfully leach Sc (about 80 %) and heavy REEs but not iron at room temperature and pressure. Diluted HCl revealed similar results for the recovery of Sc and REEs, but it is not selective for iron. They have also studied different types of pre-treatment such as the oxidizing roast, the magnetic separation and the size fractionation by sieving analysis. These treatments

showed no significant enrichment of Sc and REEs in any fraction of BR [24]. This work was implemented in a pilot-scale process for recovering Sc from BR [43].

Borra et al. [57] compared six mineral and organic acids (HNO_3, HCl, H_2SO_4, citric acid, acetic acid, and methanesulphonic acid) to leach REEs from BR. They found that REEs dissolution increased with acid concentration. Extraction of Sc was the highest for 6 N HCl leaching (about 70 %) followed unavoidably by high iron dissolution (about 60 %) [57]. In a more recent work, Borra et al. proposed an integrated flowsheet to firstly recover iron from BR in a pyrometallurgical step and secondly to leach REEs. They succeeded in removing the 95 % of iron via pyrometallurgical route and then they treated the slag with HCl and HNO_3 at 90 °C, recovering almost the total amount of Sc [56].

Alkan et al. proposed an approach that suppresses the silica gel that is formed when BR is leached with H_2SO_4. 2.5 M of H_2O_2 is added at 2.5 M H_2SO_4, leaching temperature was set at 90 °C and solid to liquid ratio was 1:10. In this way, 68 % of Sc was recovered together with 91 % of Ti [42]. The same team proposed an integrated process to remove Fe via pyrometallurgical treatment (with an electrical arc furnace), the resulting slag was undergone to dry digestion to recover Sc at high rate (about 80 %) [73].

As Qu and Lian explain, Sc recovery could be achieved through a bio-hydrometallurgical approach. They carried out bioleaching experiments with acid-producing fungi identified as *Penicillinium tricolor* RM-10 directly isolated from BR. They achieved the recovery of about 70 % of Sc (together with other REEs) by incubating the fungus together with the red mud and medium [74].

An innovative method for extracting scandium from BR involves the use of ionic liquids and it will be thoroughly discussed in chapter 3. However, in this section it is important to mention the work of Davris et al., who studied the direct leaching of BR by using ionic liquid and specifically the protonated betaine bis(trifluoromethylsulfonyl)imide ([Hbet][Tf2N]). They recovered 45 % of Sc with good selectivity for iron (Fe dissolution was significantly low, 2.7 %) at 150 °C, 400 rpm, 5 % w/v pulp density for 24 hours [75].

3. Ionic liquids

Ionic liquids (ILs) are liquids that consist entirely of ions [76–78], generally an organic cation and an organic/inorganic anion [79]. This term was coined to distinguish ILs from molten salts, which consist on inorganic cations and anions [80]. Many researchers describe ILs as molten salts that are liquid below 100 °C [79,81,82]. They underline the fact that a lower melting point comparing to common ionic salts, is due to the composition and space arrangement of ILs, resulting in a low lattice energy [79,80]. Their ions, in fact, are large and not symmetric [80] and therefore they are not packed [79]. Another factor that affect the melting point, is the presence of hydrogen bonds in the lattice. ILs with a strong hydrogen bond have a higher melting point than ILs that do not have any hydrogen bond in their lattice [77]. Other researchers consider the threshold 100 °C too restrictive and arbitrary, as there are many ILs with melting point above 100 °C [83].

ILs composition makes them unique materials that are different from both conventional organic solvents, consisting of neutral molecules, and from salts solutions, which are composed of neutral molecules and ions [83]. The most common cations in IL are alkyl-substituted organic molecules such as the heterocyclic ring molecules imidazolium, pyrrolidinium and pyridinium, quaternary ammonium and quaternary phosphonium. Anions can be inorganic, including chloride, bromide, iodide, thiocyanate, tetrafluoroborate, hexafluorophosphate, bis(trifluoromethylsulfonyl)imide hydrogensulfate, or organic, such as acetate or benzoate [80,83]. From the combination of typical cations and anions, a wide range of ILs can be obtained (at least 10^6 simple ILs can be synthetized) (Figure 7) [77].

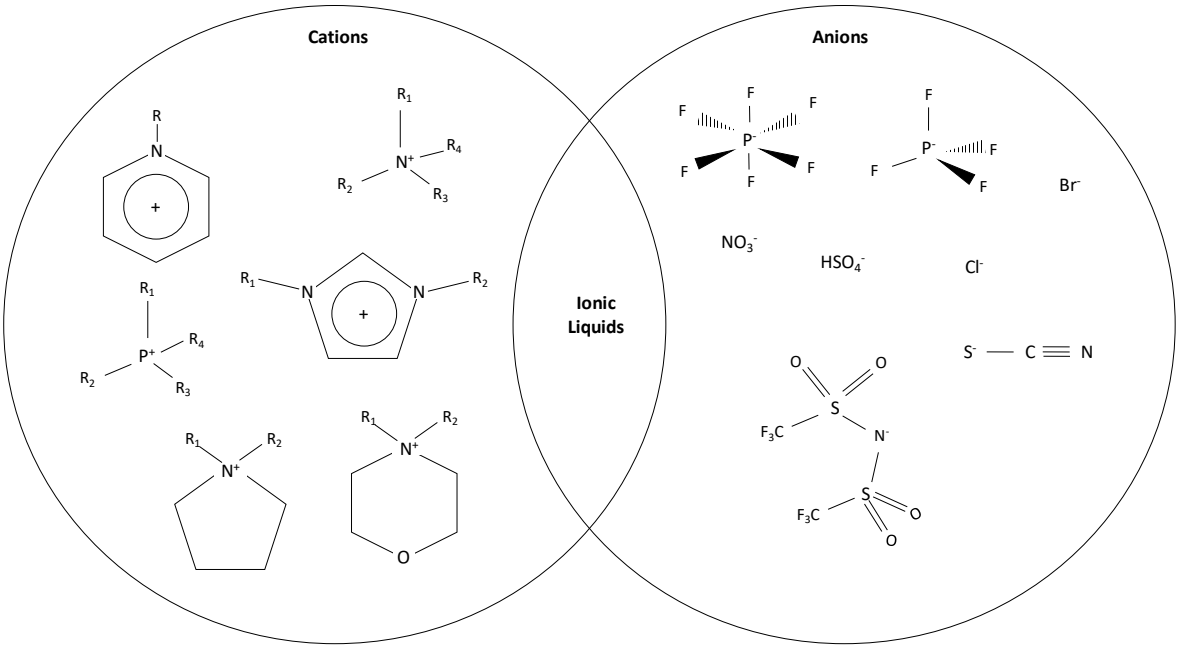

Figure 7 Common cations and anions in ionic liquids (Binnemans et al.).

ILs have superior physiochemical properties compared with classical organic solvents, which can be controlled and determined by the cation/anion combination, anion and cation size, position and length of the alkyl chains [78,79]. In general, the cation is responsible for physical properties like viscosity, density and melting point, whereas the anion controls the chemical properties and reactivity [77,80]. Each IL has different properties tuned by factors already mentioned, nevertheless, some generalizations can be made (Table 3).

First, ILs usually have extremely low vapor pressure, having a negligible loss at room temperature and can be vacuum dried, whereas some ILs can be distilled in high vacuum at high temperatures. Their electrochemical stability and ionic conductivity are also important properties, in fact they have a wide electrochemical window (more than 4 V, in some cases 6 V) and therefore they are electrical conductors. In addition, their ionic conductivity is comparable to sea water as it is about 10 mS/cm. However, their high viscosity inhibits the ionic conductivity, therefore a combination of high conductivity and low viscosity would be preferable for using the IL as electrolyte. ILs have a wide liquid range, it is common to find an IL which is fluid at temperatures above 250 °C. They also have remarkably high thermal stability. However, as already mentioned, ILs are usually much more viscous than a common organic solvent and this can prevent mass transport and slow down the rate of the chemical process. On the other hand, by heating the IL or adding a small amount of an organic solvent, viscosity dramatically decreases [79,83].

Table 3 Ionic liquids properties (Park et al. [79]).

Properties	Values
Melting point	(preferably) < 100°C
Liquidous range	> 200 °C
Thermal stability	High
Viscosity	< 100 cP
Dielectric constant	< 30
Polarity	Moderate
Ionic conductivity	< 10 mS/cm
Molar conductivity	< 10 Scm^2/mol
Electrochemical window	> 4 V
Vapor pressure	Negligible

Another key issue is that usually ILs are very expensive, as they are designer solvents and can be based on ions of a very wide range regarding costs. For example, ionic liquids based on the 1-alkyl-3-methylimidazolium cation can be quite costly, when coupled with the bis(trifluoromethylsulfonyl)imide anion. In general, ILs are 5 – 20 times more expensive than molecular solvents. However, one of the advantages of ILs is that they can be recycled lowering in that way the final cost when comparing with the conventional solvents [77].

ILs have a low-volatility and non-flammability, which make them very attractive for a wide range of industrial applications such as organic synthesis [84,85], fine chemical production [86,87], electrolytes for capacitors [88] and batteries [89]. Other applications of ILs are in extractive metallurgy, since they can be used either as electrolytes for electrodeposition of reactive metals [90], as solvents for liquid-liquid metal extraction or separation [91] as well as lixiviants [75,81–83,92,93]. The term used for describing the use of ILs as solvents in the field of metal processing is ionometallurgy [83].

3.1 Ionometallurgy

Metal oxides have traditionally been processed using hydrometallurgical techniques based upon dissolution in mineral acids and bases. Separation has usually been achieved using solvent extraction with specific chelating agents for given metals [80].

Nevertheless, in the last decades, thanks to the zero-waste valorization policy, more sustainable routes have been investigated. In the applications of metals processing, ionometallurgy can be considered an innovative approach as alternative to conventional methods. In fact, thanks to their negligible vapor pressure, ILs have been reported as green solvents compared to common organic solvents [81]. There are many advantages in using IL in metal processing and this can have a significant impact to waste valorization. In ionometallurgical processes there are no bulk aqueous phases and therefore the consumption of water is extremely limited. This is also true for the acid consumption, which is surely less comparing to the conventional acid leaching. Processes are also intensified as the different unit operations, like leaching and solvent extraction, can be combined, reducing the number of steps. In addition, using ILs for leaching leads to a higher selectivity than leaching with mineral acids. Therefore, both problems related to the co-dissolution of metals from polymetallic matrices and formation of silica gel are reduced. This makes them suitable for processing metals from low-grade ores, mine tailings and industrial process residues [83].

3.1.1 Ionic liquid leaching

As already discussed, ILs have been introduced to metal extraction processes as leaching agents.
The first reported studies of leaching metal oxides in ionic liquids concerned the dissolution of uranium oxide (UO_3) in imidazolium chloroaluminate melt. The solubility of UO_3 was found to be $1.5 – 2.5 \cdot 10^{-2}$ mol/dm^3 and the main species in solution was found to be $[UO_2Cl_4]^{2-}$ [94]. Another example, Nockemann et al. succeeded to leach metal oxides and hydroxides into a number of task specific ionic liquids (TSILs), which are ILs designed for specific purposes [95,96]. The TSIL betaine bis(trifluoromethylsulfonyl)imide ([Hbet][Tf2N]) has been used for the dissolution of rare earth oxides [95]; while oxides like UO_3, lead oxide (PbO), zinc oxide (ZnO), cadmium oxide (CdO), mercury oxide (HgO), copper oxide (CuO), silver oxide (Ag_2O), nickel oxide (NiO), palladium oxide (PdO) as well as several hydroxides where found to be soluble into the TSILs based on imidazolium, pyridinium, pyrrolidinium, piperidinium, morpholinium, and quaternary ammonium bis(trifluoromethylsulfonyl)imide salts [96].

Abbott et al. have extensively studied the dissolution of metals and metal oxides deep eutectic solvents (DES) of choline chloride mixtures with hydrogen bond donors such as carboxylic acids, amines and alcohols [80,81,97–101]. The solubilities of iron oxide (Fe_3O_4) and copper oxide (CuO)

have been tested in three deep eutectic solvents between choline chloride and carboxylic acids at 50 °C. Fe_3O_4 resulted to be more soluble in oxalic acid/choline chloride (ChCl) system (molar ratio 1:1), whereas twenty times less soluble in phenyl propionic acid mixture. CuO showed the opposite behavior, suggesting that deep eutectic solvents can be applied for selectively leaching of metals [98]. In addition, the same team tested the solubility of seventeen metal oxides in the elemental mass series Ti through Zn was reported in three ionic liquids based on choline chloride mixtures with urea, malonic acid, and ethylene glycol.

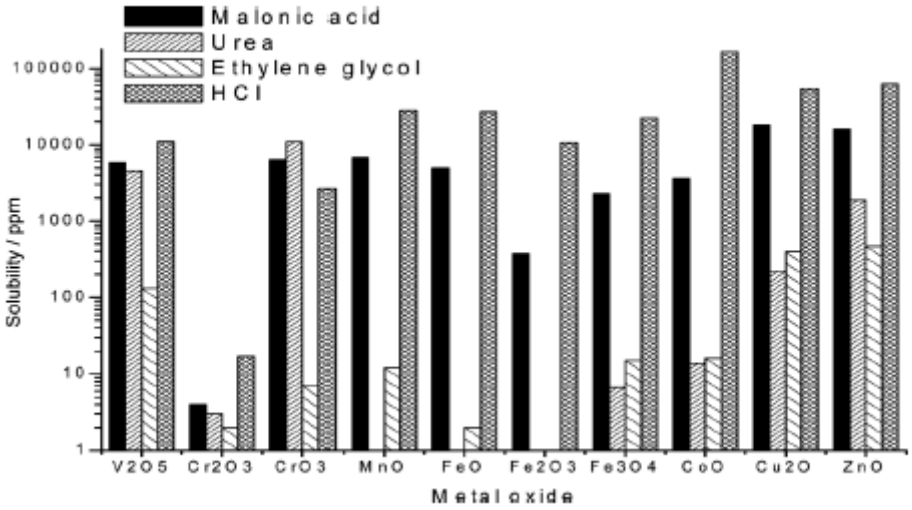

Figure 8 Solubility of metal oxides in a variety of Deep Eutectic Solvents (DESs) and HCl (Abbott et al. [81]).

It has been shown (Figure 8) that these types of ionic liquids can dissolve a range of metal oxides. In general, the malonic-acid-based DESs showed the highest solubility for metal oxides. However, all these liquids are totally miscible with water and cannot be used for biphasic extraction. Selectivity for extracting certain metals from complex matrices can be reach by choosing right hydrogen bond donor [99].

Few studies have been published regarding the ionometallurgical leaching of metal and metal oxides from polymetallic matrixes as alternative to hydrometallurgical leaching.

For example, Abbott et al. selectively dissolved metals by using a eutectic mixture of choline chloride (ChCl) and urea (molar ratio 1:2) at 60 °C for 48 hours, from the polymetallic matrix derived from the Electric Arc Furnace (EAF) dust, which mainly consists of metal oxides. They found that ionic oxides such as zinc oxide (ZnO), lead oxide (PbO) and copper oxide (Cu_2O) exhibit high solubility. On the other hand, aluminum oxide (Al_2O_3) was found to be essentially insoluble. ZnO

was found to have the highest solubility. Zinc, lead and copper can be subsequently recovered by electrodeposition [81,100].

The 1-alkyl-3-methylimidazolium ILs were studied as solvent medium either in neat or in aqueous mixtures for dissolving metals. Whitehead et al. used a leaching system based on ionic liquids for recovering gold, silver and copper from gold-bearing ores [102,103]. The room-temperature ionic liquid 1-butyl-3-methylimidazolium hydrogensulfate [Bmim][HSO_4] in presence of thiourea and iron sulfate ($Fe_2(SO_4)_3$) was used for recovering over 85 % of gold and over 60 % of silver at 50 °C [102]. The remaining metals like zinc, copper, iron and lead have low recovery yields. Whitehead et al. employed [Bmim][HSO_4] in presence of thiourea and Fe (III) as the oxidant for recovering 85 % of copper and about 8 % of iron from chalcopyrite at 60 °C with 20 % w/v of water. When increasing [Bmim][HSO_4] concentration, also copper extraction increased [103]. [Bmim][HSO_4] in water was employed by Dong et al. for leaching chalcopyrite at a temperature range of 50 – 90 °C. By increasing IL concentration from 10 to 100 %, also copper extraction increased from 52 to 88 % [104].

McCluskey et al. used the 1-butyl-3-methylimidazolium tetrafluoroborate ([Bmim][BF_4]) ionic liquid as the solvent with water (volume ratio 1:1) and $Fe(BF_4)_3$ as the oxidant for recovering 90 % of copper from chalcopyrite after 8 hours at 100 °C [105].

[Bmim][HSO_4] was also used, with 30 % of H_2O_2 as oxidant, for leaching almost the total amount of copper contained in waste printed-circuit boards (WPCBs) [106].

[Bmim][HSO_4] was employed for recovering copper and zinc from brass ash, which consists mostly of metal oxides (ZnO, CuO). Zinc was almost completely dissolved after 4 hours at 70 °C in a 50 % v/v [Bmim][HSO_4] solution in water without any oxidant. On the other hand, copper extraction was low, resulting to be about 25 %. To increase the extraction of copper, H_2O_2 was added as oxidizing agent to the IL solution. This led to an 82 % recovery of copper and a faster zinc dissolution [107].

Dupont et al. studied the recovery of REEs from the neodymium–iron–boron (NdFeB) magnets by leaching them with the carboxyl-functionalized ionic liquid betainium bis(trifluoro-methylsulfonyl) imide [Hbet][Tf2N]. This IL has a switching thermo-morphic behavior as upon addition of water is hydrophobic at temperatures below 55 °C, whereas above 55 °C forms an aqueous solution, therefore the mixture resulted homogeneous during leaching at 80 °C (temperature above the cloud point temperature) and biphasic when cooling back down to room temperature. After 48 hours they were able to leach the total amount of REEs, up to 50 % of cobalt and less than 25 % of iron [108]. In a previous work, the same team used [Hbet][Tf2N] for leaching lamp phosphors. They achieved to selectively dissolve up to 100 % of Y_2O_3:Eu^{3+} [109].

As already discussed in chapter 2.4.2, Davris et al. studied the application of [Hbet][Tf2N] ionic liquid for directly leaching metals from bauxite residue. They performed experiments at 150 °C, 400 rpm, 24 hours retention time and 5 % w/v pulp density at 40 % v/v water addition into IL. Selective leaching of REEs (in a range of 60 - 85 %) was achieved against Fe, Ti and Si, whereas no selectivity occurred against Ca, Na and Al. Sc recovery did not exceed 45 % [75]. The same team applied the same ionic liquid to the Rödberg polymetallic matrix, a low-grade REE ore from the Fen carbonatite complex ore deposit located in Norway. They found that [Hbet][Tf2N] resulted to be efficient for recovering both light and heavy REEs. In fact, they achieved to recover 65 – 100 % of light REEs and 40 – 60 % of heavy REEs. Ca and Mg are co-dissolved at a range of about 80 – 90 %, whereas the IL resulted to be selective against Fe and Si [93].

4. Solvent extraction

Solvent extraction (SX) is a particularly important technique in hydrometallurgy for the separation and purification of metals. This term refers to a preferential distribution of a solute between two immiscible liquid phases in contact with each other [110]. The conventional solvent extraction involves an aqueous phase and an organic phase, but SX systems can also consist of (1) two mutually immiscible molten salts, (2) a molten salt and a molten metal, (3) a molten salt and an organic solvent or (4) two mutually immiscible organic solvents. [83,111]. For these reasons it is more correct to use the terms more polar phase and less polar phase. Generally, a pregnant liquid solution (PLS) that contains the dissolved solute, is put into contact with another immiscible phase Figure 9.

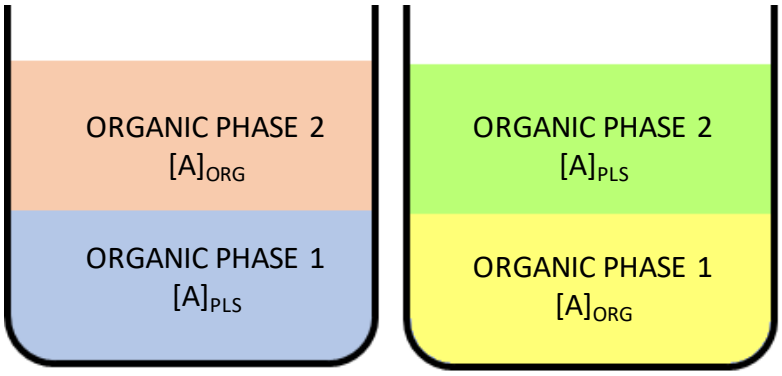

Figure 9 Principles of non-aqueous solvent extraction.

The two phases need to have different polarities and be immiscible with each other, in order to create two distinct phases. Moreover, they need to show a short phase disengagement time after mixing and the extractant has to be soluble in the less-polar phase and insoluble in the more-polar phase [83]. By using the non-aqueous SX is possible to overcome issues that the conventional SX presents. For example, this approach can be applied for separating covalent compounds such as halide complexes of p-block elements and early d-block elements, as well as organometallic compounds which hydrolyze in water. In addition, it is possible to perform separations that are not efficient in aqueous solutions because of the differences in the extraction mechanism [83].

As illustrated in Figure 9, the solute A, which initially is dissolved in only one of the PLS, eventually distributes between the two phases. When this distribution reaches equilibrium, the solute is at concentration $[A]_{ORG}$ in one layer and at concentration $[A]_{PLS}$ in the other layer.

The distribution ratio (D) of the solute is defined as the ratio of "the total analytical concentration of the substance in the organic phase to its total analytical concentration in the aqueous phase, usually measured at equilibrium" [112]. In this case, it is possible to generalize indicating as upper phase (UP) the lighter one and as lower phase (LP) the heavier one. The distribution ratio can be calculated as the following formula:

$$D = \frac{[A]_{UP}}{[A]_{LP}} \tag{9}$$

Extraction efficiency is given by the formula:

$$E\% = \frac{[A]_{ORG}}{[A]_{ORG} + [A]_{PLS}} \cdot 100 \tag{10}$$

where $[A]_{org}$ and $[A]_{PLS}$ are the metal concentrations at equilibrium in the extraction phase and PLS, respectively.

When in a SX system there are two or more solutes, it is possible to evaluate the selectivity of the solvent for a solute (A) against another solute (B). This parameter is defined as the separation factor (SF):

$$\mathrm{SF} = \frac{D_A}{D_B} \tag{11}$$

The separation is possible when SF > 1. The higher is the number, the more the system is selective. If SF $\leq$ 1, then separation is not feasible.

4.1 Metal extraction from leachates

A number of extractants can be employed for extracting metals from leachates with conventional solvent extraction approach [111,113–120]. For instance, Lee et al. investigated the extraction behavior of indium and gallium from mixed sulfuric acid solutions using 0.05 M bis(2-ethylhexyl) phosphoric acid (D2EHPA) in kerosene. They obtained a good separation factor at pH 1.6 [113].

Yoon et al. performed experiments for extracting lanthanides dissolved in nitric acid (HNO_3) at different concentration. They used D2EHPA diluted with several kinds of ILs or hexane. The ILs tested were 1-ethyl-3-methylimidazolium hexa- fluorophosphate ([C2mim][PF_6]), 1-butyl-3-methylimidazolium hexafluorophosphate ([C4mim][PF_6]), and 1-butyl-4-methyl-pyridinium hexafluorophosphate ([C4mpy][PF_6]). It was found that the distribution of lanthanides from an aqueous to an organic phase increased with the temperature and concentration of D2EHPA and decreased as the concentration of HNO_3 increased. The best parameters combination was 0.1 M D2EHPA with a 0.01 M lanthanide mixed solution and a concentration of 0.1 M HNO_3 at 313 K. Moreover, ILs containing imidazolium cation and ethyl group functionalized imidazolium cation showed a higher distribution coefficient than pyridinium cation and butyl group functionalized imidazolium cation containing ILs except for the case of ytterbium (Yb). Yb showed much higher selectivity than other lanthanides, especially the [C4mpy][PF_6] system [114].

Wang et al. investigated the extraction of Sc from sulfuric acid solutions by using several extractants. They achieved an almost complete extraction of scandium by using 0.1 M D2EHPA and 0.05 M tributyl phosphate (TBP) diluted in Shell D70 using an aqueous to organic ratio (A:O) of 5:1 at 40 °C and 0.4 pH. At these conditions they did not co-extracted iron. Afterwards, Sc was precipitated as scandium hydroxide ($Sc(OH)_3$) with the addition of 2 M sodium hydroxide (NaOH) [115].

Anitha et al. investigated the feasibility of using the aromatic analogue of D2EHPA, the di-nonyl phenyl phosphoric acid (DNPPA) for the extraction of rare earths from chloride medium. They achieved to extract almost the total content of REEs by performing experiments in solutions at 0.01 M rare earths and 3 M HCl and using 0.6 M DNPPA at aqueous to organic phase ratio (A:O) of 1:1. Selectivity between REEs was checked, finding high SFs between heavy and light rare earths [116].

Vander Hoogerstraete et al. examined the neodymium extraction by the factionalized IL [Hbet][Tf2N] in combination with betaine as extractant. Neodymium (III) chloride ($NdCl_3$), neodymium (III) nitrate ($Nd(NO_3)_3$), and neodymium (III) bis(trifluoromethylsulfonyl)imide ($Nd(Tf2N)_3$) were tested and results gave almost no differences in extraction between the three different anions. They succeeded in extract almost the total content of Nd [117]. In a following

work, the same team used [Hbet][Tf2N] for selectively extracting scandium from sulfating-roasted leachates of bauxite residue. They performed a pre-treatment with 0.2 M ascorbic acid to reduce Fe (III) to Fe (II) for preventing co-extraction. The pretreated leachates were then contacted with [Hbet][Tf2N] in a 1:5 O:A phase ratio in presence of 0.5 M NaOH for adjusting the pH. At these conditions, they could extract more than 80 % of Sc, while most of the other elements remained in the raffinate [118].

In addition, Wang and Cheng published a review on scandium extraction and purification methods through different kinds of extractants. They reported studies on organophosphorus acidic organophosphorus extractants, basic extractants, chelating extractants, phosphorus-based solvating extractants and neutral phosphorus-based extractants under various conditions [121].

As previously discussed, non-aqueous solvent extraction offers several advantages over conventional aqueous solvent-extraction systems. However, as Binnemans et al. reported in a recent paper, only few studies were published on this technique [83]. They reported that Larsen and Trevorrow tried to separate hafnium from zirconium. With this aim, they investigated the distribution of zirconium chloride ($ZrCl_4$) and hafnium chloride ($HfCl_4$) between acetonitrile and isoamyl ether. However, the separation factors were too small to be of practical use [122]. Several metal salts (chloride, bromide, thiocyanate, and nitrate) were extracted to a diethyl ether phase that was equilibrated with a second immiscible phase, being ethanolamine, formamide, or adiponitrile. These solvents could extract nearly all metal complexes from the ether phase with an extraction efficiency of more than 90 %. Only tin (IV) chloride showed a higher affinity for the ether phase [123]. Thallium (III) was separated from Ga (III), In (III), Fe (III), Sn (II) and Sn (IV) by extracting the elements first from an aqueous 2 M HBr solution with methyl isobutyl ketone (MIBK), followed by stripping of the MIBK layer using a 1.5 M HBr solution in formamide. All the thallium (III) remained in the MIBK layer, while all the other metal ions were transferred to the formamide layer [124].

Foreman described the extraction of rare earths and transition metals from a deep-eutectic solvent (DES) based on choline chloride and lactic acid (molar ratio 1:2) to another organic phase. By using the quaternary ammonium salt Aliquat 336 dissolved in an aromatic diluent and in biodiesel, the transition metals were extracted, while rare earths were extracted using D2EHPA dissolved in aliphatic diluents. The extraction using Aliquat 336 was found to be more sensitive to the water content of the DES than when using D2EHPA [125].

Batchu et al. developed a SX process for rare earths that involved two immiscible organic phases. The more polar organic phase was ethylene glycol, which replaced water, with the dissolved rare

earth nitrate salts. Rare earths are extracted from an ethylene glycol phase, which represents the less polar phase, with dissolved lithium nitrate ($LiNO_3$), by the extractant Cyanex 923 dissolved in n-dodecane. Compared with aqueous feed solutions, the light rare earth elements (LREEs) were less efficiently extracted, and the heavy rare earth elements (HREEs) were more efficiently extracted from an ethylene glycol feed solution, resulting in a better separation of the HREEs from the LREEs. The SFs between neighboring elements were higher for extraction from the ethylene glycol solution than those for extraction from an aqueous solution [111].

5. Bauxite residue characterization

The present work is based on bauxite residue produced by Aluminum of Greece plant, Metallurgy Business Unit, Mytilineos S.A. (AoG). As already discussed in paragraph 2.1.1, BR was collected by AoG in the form of a filtered cake after the dewatering of the washed bauxite residue in the filter presses. They provided a batch of about 58 kg of BR which was dried at 100 °C for 72 hours to eliminate the water content. It was homogenized and split to obtain a representative sample following the scheme represented in Figure 10.

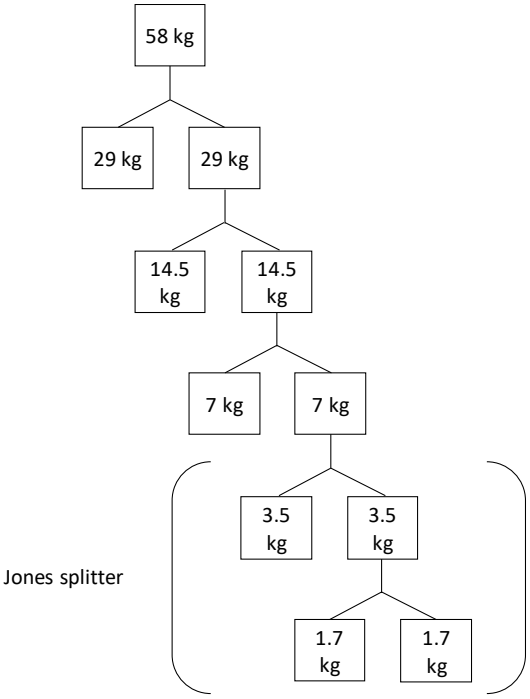

Figure 10 Sample preparation scheme.

When obtained a sample of about 7 kg, a riffle splitter (also called Jones splitter) (Figure 11) was used to guarantee the homogeneity of the sample. The Jones splitter is a mechanical method that is used for sample homogenization or sample size reduction. It has an equal number of sloping chutes with alternate chutes discharging the sample in opposite directions into two collecting bins [126]. The sample was poured through the splitter and after the sample passed through the splitter, one collection pan was replaced with a clean pan. The material in the "replaced pan", which contained about one-half of the original sample, was then passed through the Jones splitter again thereby reducing the volume in the clean pan to one-quarter of its original sample volume [126]. This process of sample reduction was repeated two times and a sample of about 1.7 kg was obtained. The 1.7 kg of BR was then crushed, ground and sieved obtaining a representative sample which was fully characterized.

Figure 11 The Jones riffle splitter present at NTUA laboratory.

Particle size was measured with a Malvern MastersizerTM Laser particle size analyzer and it was found that 50 % of the particles were below 1.87 µm, while 90 % were smaller than 42.87 µm (Figure 12).

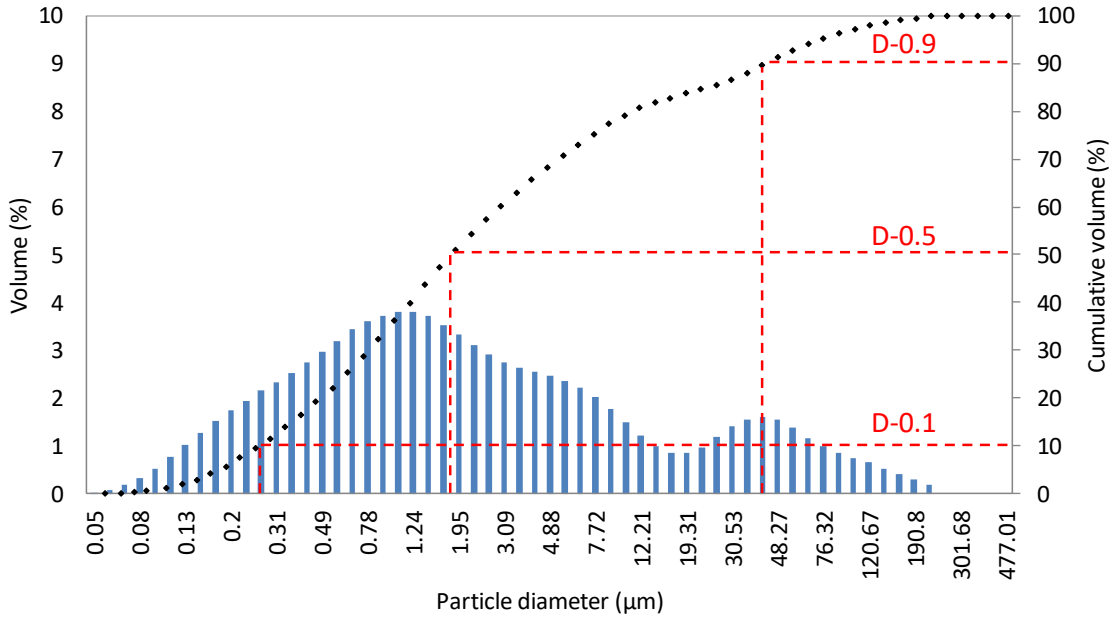

Figure 12 Particle size of BR used for the experiments.

Calcium oxide content was detected in solid samples with a Spectro Xepos Energy Dispersive X-ray fluorescence spectroscopy (ED-XRF). The bulk chemical composition for the other elements was determined after dissolving BR via fusion method: 0.1 g of BR was mixed with 1.5 g of lithium tetraborate ($Li_2B_4O_7$) and 0.1 g of potassium nitrate (KNO_3) and then fused in platinum crucibles at 1000 °C for 1 hour. The obtained sample was then dissolved in 10 % v/v nitric acid (HNO_3).

Main elements were identified by a Perkin Elmer 2100 Atomic Absorption Spectrometer (AAS), while minor elements were analyzed by a Thermo Fisher ScientificTM X-series 2 Inductively Coupled Plasma Mass Spectrometer (ICP-MS) and a Perkin Elmer Optima 8000 Inductively Coupled Plasma Atomic Emission Spectrometer (ICP-OES).

The main component of BR was found to be Fe_2O_3, accounting 42.34 wt.%, followed by Al_2O_3 with 16.25 wt.%, while TiO_2 was 4.27 wt.% and total rare earth oxides (REO) assessed to 0.19 wt.%, as it is shown in Figure 13. In particular, cerium (Ce) was determined to be the main rare earth element in concentration (402.2 ± 0.2 mg/kg), followed by lanthanum (La) (145 ± 12 mg/kg), scandium (Sc) (134 ± 4 mg/kg), neodymium (Nd) (127.1 ± 0.1 mg/kg) and yttrium (Y) (112 ± 2 mg/kg); error was calculated as the standard deviation based on the duplicate measurements.

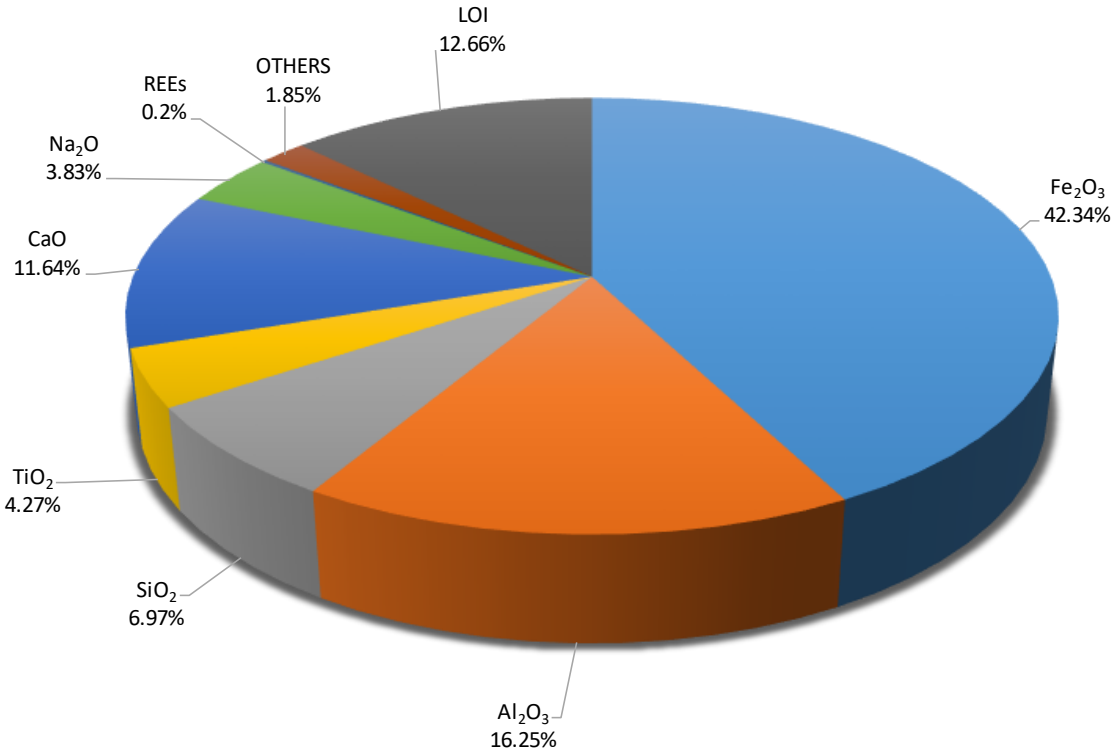

Figure 13 Bauxite residue chemical analysis. Note: REO, rare earth oxides; LOI, loss of ignition.

The loss of ignition (LOI) was 12.66 wt.% (Figure 13 and Figure 14) and it was measured with the thermogravimetric analysis (TGA), by using SETARAM TG Labys-DS-C system in inert atmosphere in the range temperature of 25 – 1000 °C at a 10 °C/min heating rate. The differential thermal analysis (DTA) showed (Figure 14) a strong endothermic peak at 280 °C related to the dehydroxilation of goethite to form hematite. This peak is partially overlapped by the one related to the dehydration of gibbsite ($Al_2O_3 \cdot 3H_2O$). Between 200 and 300 °C dehydration of calcium aluminum iron silicate hydroxide ($Ca_3AlFe(SiO_4)(OH)_8$) is also present. The endothermic peak at 500 °C is correlated to the dehydration of diaspore (α-AlOOH) and overlaps the peak associated to the dehydration of cancrinite $Na_6Ca_2(AlSiO_4)_6(CO_3)_2$ (between 400 and 625 °C); decarbonization of cancrinite occurs at 750 °C [35,127,128].

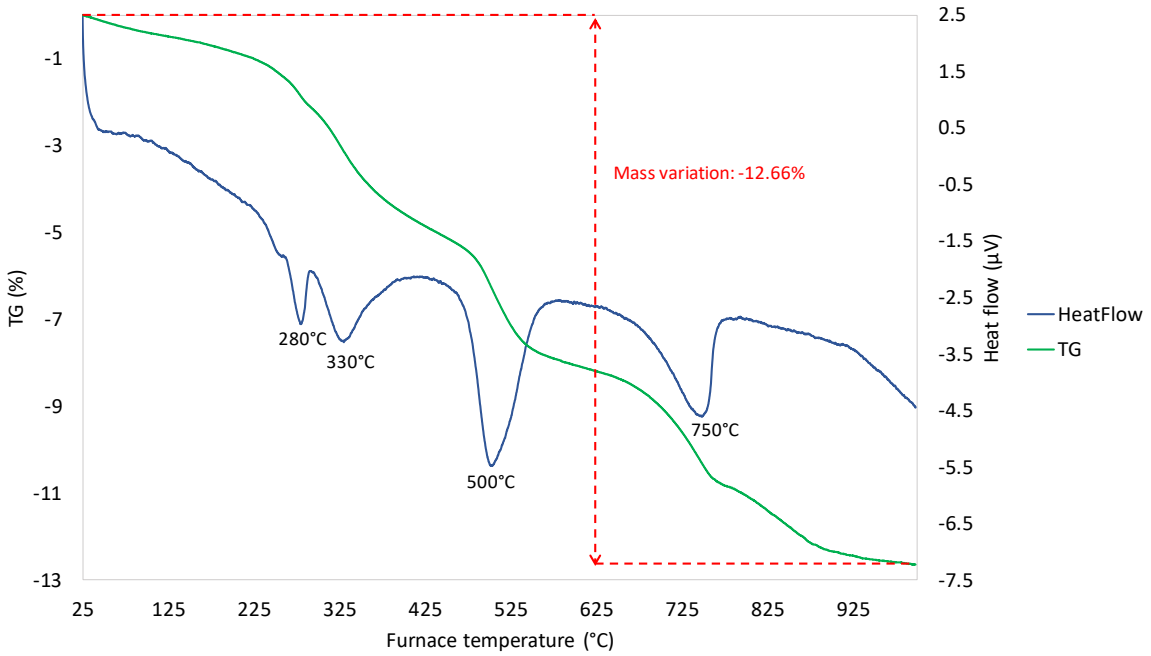

Figure 14 Thermogravimetric and differential thermal analysis (TGA-DTA) of BR.

Mineralogical characterization was performed with a Bruker D8 focus X-ray powder diffractometer (XRD) with nickel-filtered CuKa radiation and quantitative evaluation was done via profile fitting by using XDB Powder Diffraction Phase Analytical System version 3.107 that targets specifically bauxite and bauxite residue [129,130].

Identification (Figure 15) and quantification of mineralogical phases (Table 4) denoted hematite as the main mineral in BR with 30 wt.%, other Fe-containing phases were determined as goethite and calcium aluminum iron silicate hydroxide with a contribution of 9 and 17 wt.% respectively. Diaspore was found to be the main Al-containing mineralogical phase (9 wt.%), followed by chamosite (4 wt.%), boehmite (3 wt.%), gibbsite (2 wt.%) and cancrinite (15 wt.%), while Ti containing phases were perovskite, anatase and rutile with 4.5, 0.5 and 0.5 wt.% respectively.

Table 4 Bauxite residue mineralogical phases and quantification.

Mineralogical phase	**Formula**	**wt.%**
Hematite	Fe_2O_3	30
Calcium aluminum iron silicate hydroxide	$Ca_3AlFe(SiO_4)(OH)_8$	17
Cancrinite	$Na_6Ca_2(AlSiO_4)_6(CO_3)_2$	15
Diaspore	α-AlOOH	9
Goethite	$Fe_2O_3 \cdot H_2O$	9
Perovskite	$CaTiO_3$	4.5
Chamosite	$(Fe^{2+},Mg)_5Al(AlSi_3O_{10})(OH)_8$	4
Calcite	$CaCO_3$	4
Boehmite	γ-AlOOH	3
Gibbsite	$Al_2O_3 \cdot 3H_2O$	2
Rutile	TiO_2	0.5
Anatase	TiO_2	0.5
Sum		98.5

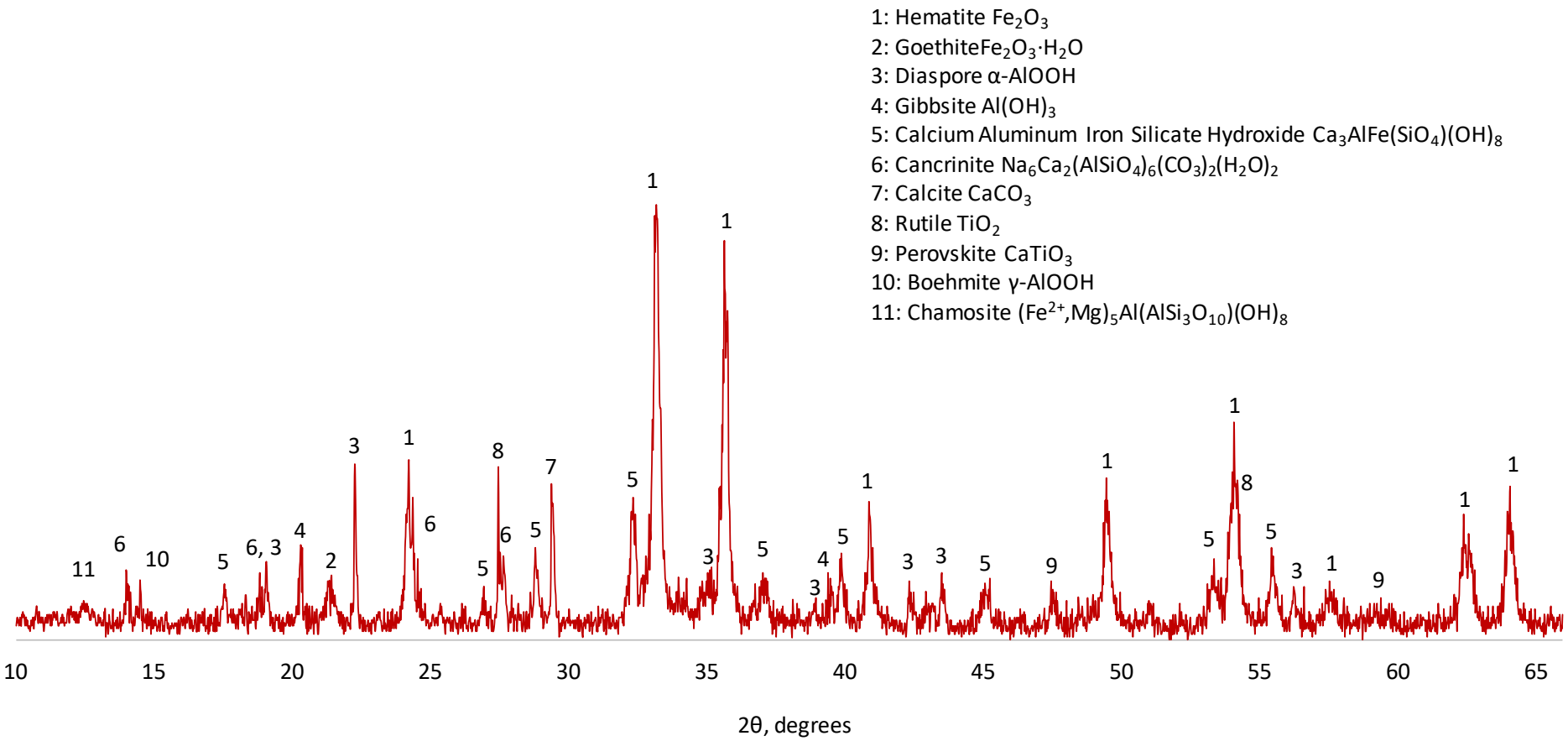

Figure 15 XRD profile of bauxite residue.

6. The Ionic liquid 1-ethyl-3-methylimidazolium hydrogensulfate as the leaching agent

As already discussed in chapter 3.1.1, several IL have been studied as leaching agents for extracting metals and metals oxides from polymetallic matrixes [75,93,100,102–108]. Since BR is mainly constituted by oxides, hydroxides and oxyhydroxides, it was necessary to find an IL with acidic characteristics that would be able to break particles and complex metals. [Emim][HSO_4] was chosen because it provides a good complexation, as it is a Brønsted acidic ionic liquid, it is also a non-fluorinated IL and it is relatively cheap compared to other ILs. On the other hand, it has some drawbacks that need to be managed, as it is hydrophilic and consequently not easily regenerated and presents high viscosity at low temperatures. A way for handling the drawbacks consists in mixing the IL with other solvents or ILs.

6.1 [Emim][HSO_4] characterization

The ionic liquid 1-ethyl-3-methylimidazolium hydrogensulfate ([Emim][HSO_4]) is a Brønsted acidic ionic liquid whose molecular weight is 208.24 g/mol and density (ρ) at room temperature is 1367.9 kg/m^3. It was supplied by Iolitec Ionic Liquids Technologies with > 98 % purity and fully characterized. Its molecular structure is shown in Figure 16.

For evaluating the ionic liquid thermal stability, five samples were prepared and weighed, they were heated in a muffle at different temperatures (25, 250, 300, 350 and 400 °C) and afterward, they were weighed again. The weight change was calculated as a percentage with the following formula:

$$[Weight\ change, \%] = \frac{[sample\ mass, g]_f}{[sample\ mass, g]_i} \cdot 100 \quad (12)$$

Where *f* stands for final and *i* for initial.

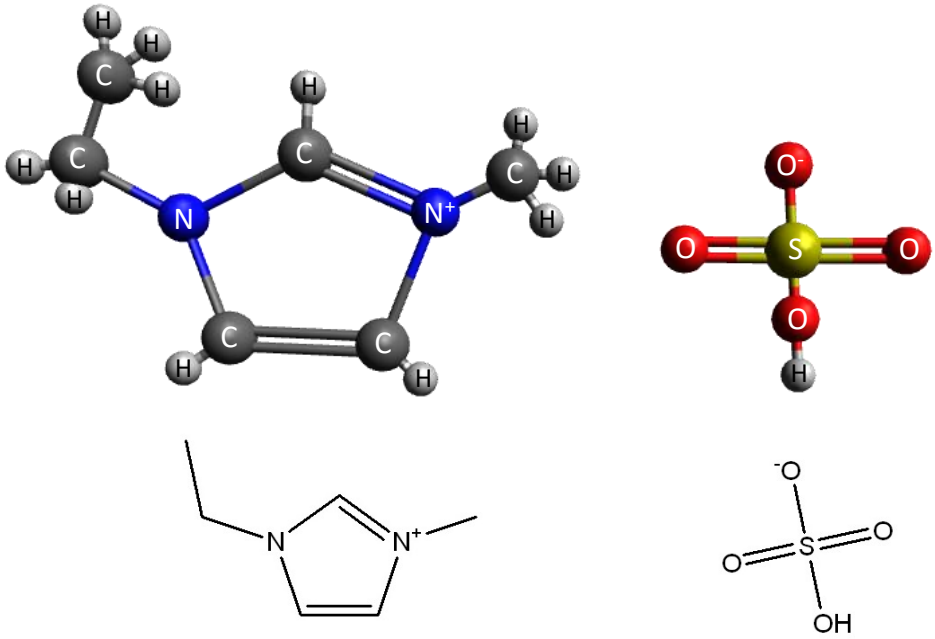

Figure 16 [Emim][HSO_4] molecular structure.

As it is possible to observe in Figure 17, [Emim][HSO_4] has a very high thermal stability, in fact, its decomposition starts at 250 °C.

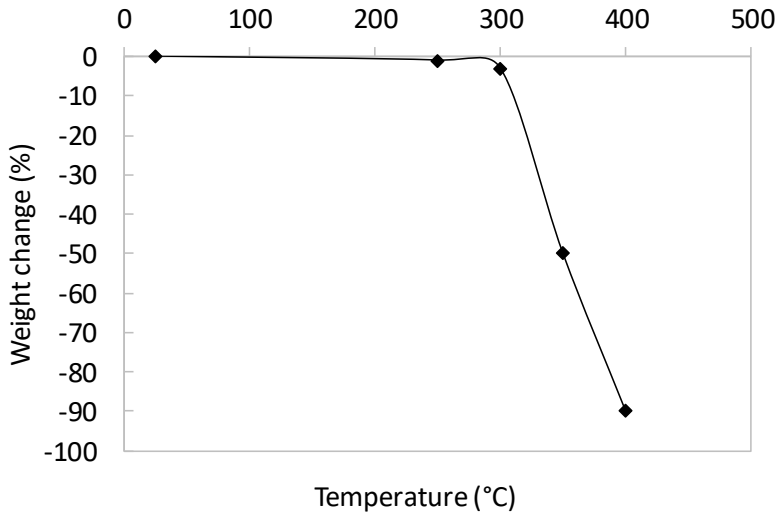

Figure 17 [Emim][HSO_4] thermal stability, measured as weight change (%) versus temperature (°C).

Viscosity analysis was performed with a Brookfield viscometer DV-I + LV supported by a Brookfield Thermosel accessory.

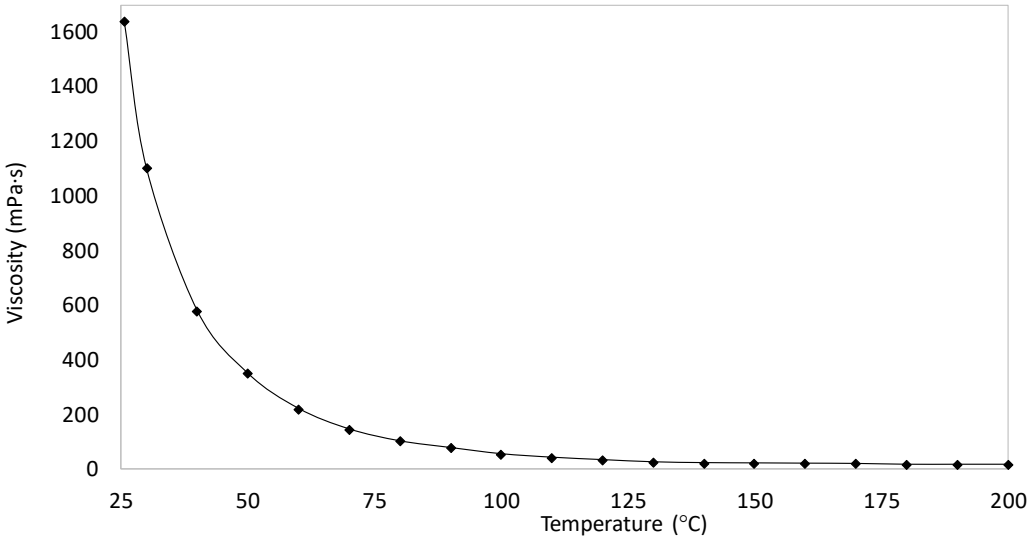

Figure 18 Viscosity of [Emim][HSO_4] versus temperature.

Viscosity measurements (Figure 18) have revealed that even though [Emim][HSO_4] is very viscous at room temperature (1642 mPa·s), by increasing temperature its viscosity dramatically decreases, reaching 221 mPa·s at 60 °C, 33 mPa·s at 120 °C and 15 mPa·s at 200 °C.

Mid-infrared measurements were conducted with a Perkin Elmer FTIR spectrum 100. The spectrum (Figure 19) have shown bands (cm^{-1}) at 3452 (-OH, vibration), 3151 (imidazole C-H, vibration), 3106 (imidazole ring, vibration), 2985 (methyl group C-H, stretching), 2944 (CH), 2881 ($(CH_2)_n$–CH_3, vibration), 2583–2497 (hydrogen bond H-O-S-O•••H-O-S-O), 1636 (-OH, vibration), 1572 (C=C, stretching; C=N, stretching; C–N, bending), 1454 (CH_3, stretching), 1431 ($S=O_2$, anti-symmetric bending), 1389 (CH_3, stretching), 1211 ($S=O_2$, symmetric stretching), 1160 (S–OH, asymmetric bending), 1089 (HSO_4^-, stretching), 1023 (C–N–C, stretching), 960 (O–S–O, stretching), 832 (imidazole ring, bending), 757 (CH of imidazole ring, bending) and 701 (C–H–C, stretching).

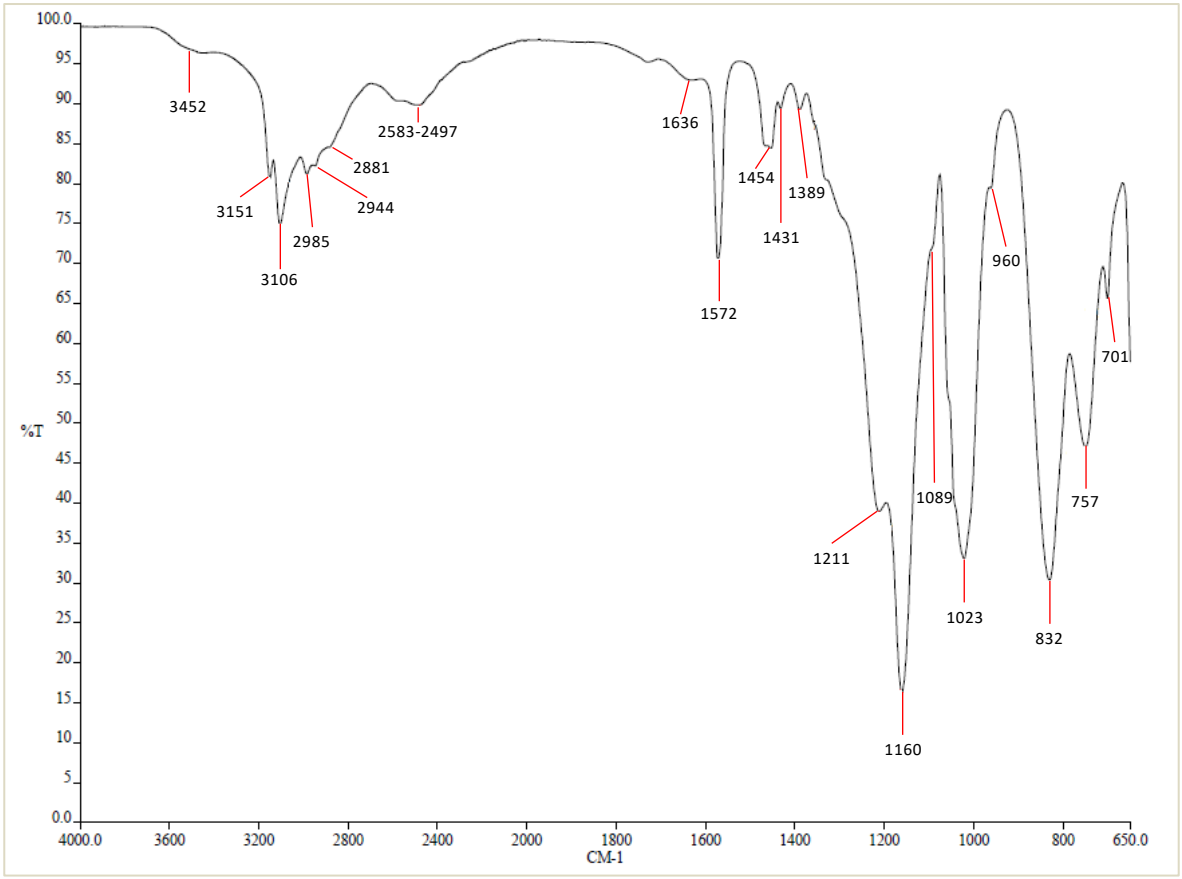

Figure 19 FT-IR spectrum of [Emim][HSO_4]

Nuclear magnetic resonance (NMR) spectra were obtained in DMSO-d6 at 25 °C on a Bruker Avance DRX 500 MHz (^{1}H at 500.13 MHz and ^{13}C at 125.77 MHz) equipped with a 5 mm multi nuclear broad band inverse detection probe. ^{1}H NMR (500 MHz, DMSO) δ (ppm): 1.36 (t, 3H, CH_3), 3.85 (s, 3H, CH_3), 4.19 (q, 2H, CH_2), 7.71 (s, 1H, CH=CH), 7.78 (s, 1H, CH=CH), 9.19 (s, 1H, N-CH-N).

6.1.1 Reaction mechanism

To investigate the mechanism of the reaction that takes place, two monometallic solutions were prepared. Al was chosen as one of the main elements and Sc as one of the minor elements present in BR. Scandium oxide (Sc_2O_3) and aluminum oxide (Al_2O_3) were dissolved in [Emim][HSO_4] ionic liquid and two solutions of 11 g/L of Sc and 11 g/L of Al were obtained.

The two monometallic solutions were then analyzed with ^{1}H and ^{13}C NMR. Assignment of ^{1}H and ^{13}C chemical shifts was based on the combined analyses of a series of ^{1}H - ^{1}H and ^{1}H - ^{13}C correlation experiments recorded using standard pulse sequences from the Bruker library.

From the results (Figure 20 and Figure 21) it could be concluded that there is no significant rearrangement in the carbon chain after the dissolution procedure in all three metal cases.

^{1}H and ^{13}C NMR spectra did not indicate any notable differences in the chemical shifts depending on the leached metal. The similar chemical shifts for the protons and the carbons localized in-between the two nitrogen atoms indicate metal interaction through the anion of the IL.

There is not any steric effect of electron clouds changing of electrostatic interactions between ionic charges.

The results obtained from the NMR analysis of two monometallic leachates have led to the following proposed reaction:

$$Me_2O_n + n[Emim][HSO_4] \leftrightarrow Me_2(SO_4)_n + nOH^- + n[Emim]^+ \quad (13)$$

where Me is the metal and n is the oxidation state of the metal.

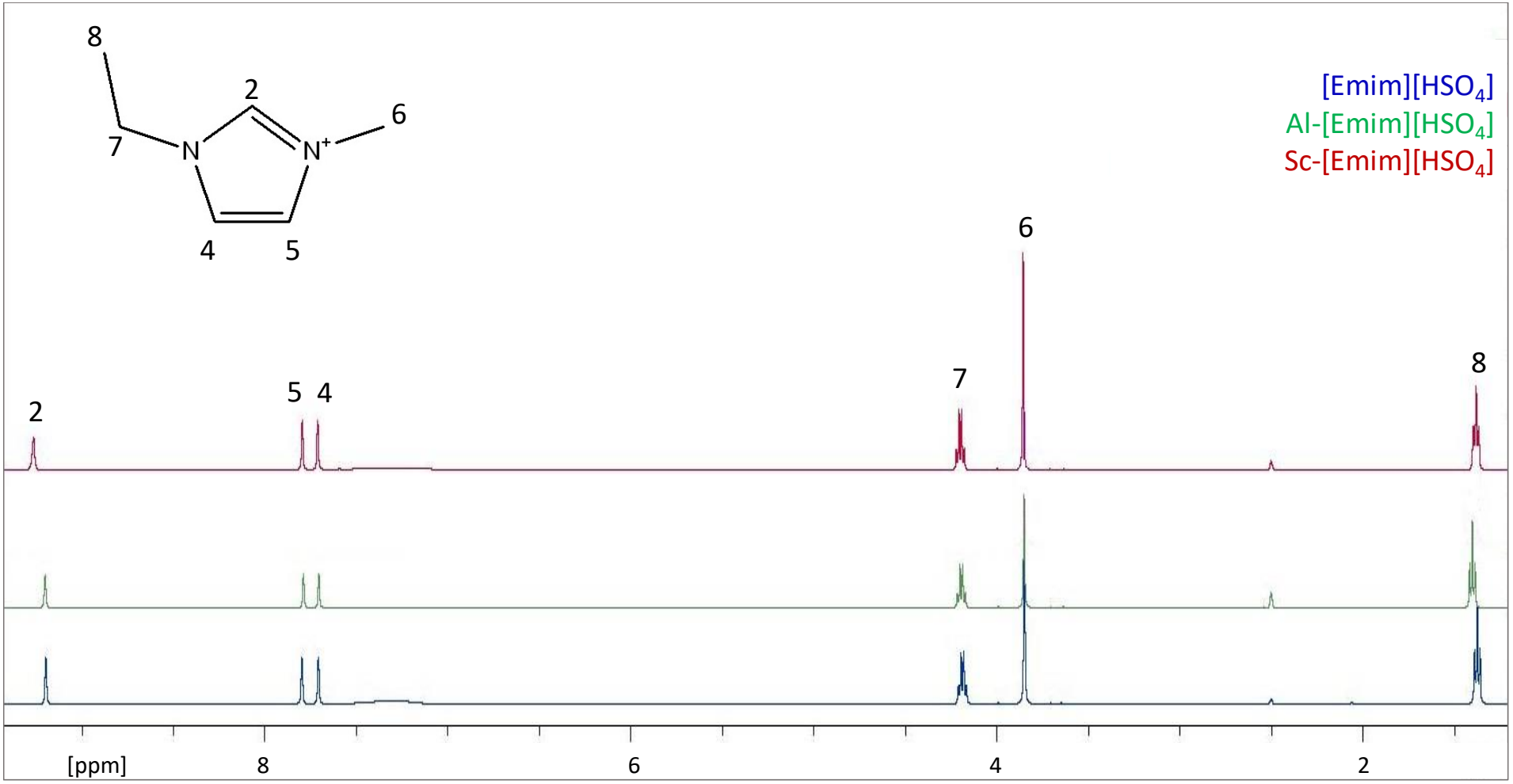

Figure 20 ^{1}H NMR comparison between [Emim][HSO_4] (blue), [Emim][HSO_4] after leaching Al_2O_3 (green), [Emim][HSO_4] after leaching Sc_2O_3 (red).

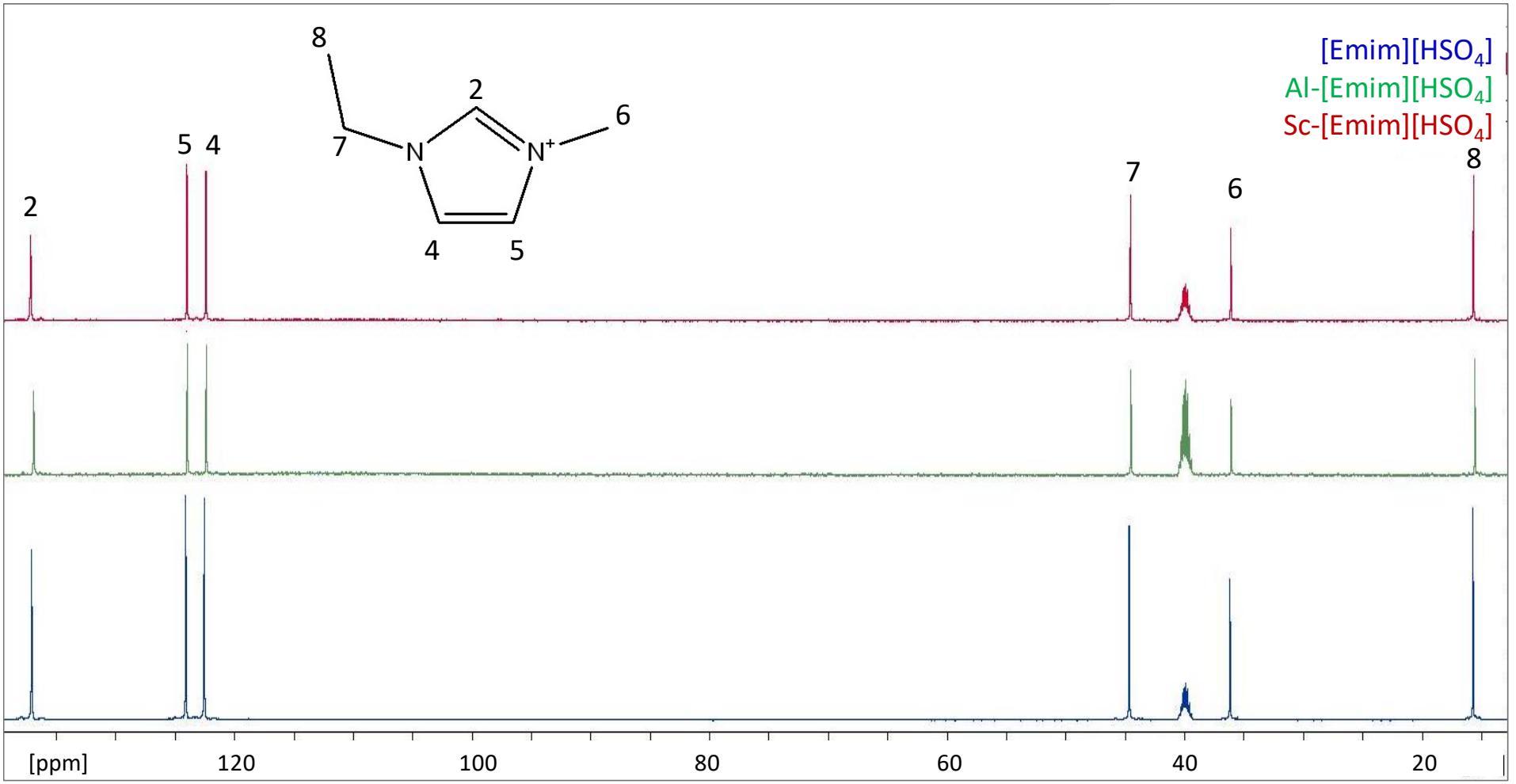

Figure 21 ^{13}C NMR comparison between [Emim][HSO_4] (blue), [Emim][HSO_4] after leaching Al_2O_3 (green), [Emim][HSO_4] after leaching Sc_2O_3 (red).

6.2 Preliminary tests

In order to choose the best system for dissolving metals and for eventually recovering the ionic liquid, some preliminary tests have been carried out and different scenarios were explored:

- [Emim][HSO4] neat;
- [Emim][HSO4] in water;
- [Emim][HSO4] in dimethyl sulfoxide (DMSO);
- [Emim][HSO4] in 1-butyl-1-methylpyrrolidinium bis(trifluoromethylsulfonyl)imide (BMP-TFSI).

Regarding these systems some considerations can be drawn. In fact, by mixing [Emim][HSO_4] with H_2O, the acidity of the system increases and viscosity decreases, but the working temperature has to be lower than 90 °C. Moreover, by adding water, the chemistry of the system changes as the IL is hydrophilic and water reacts with the anion of the IL, producing H_2SO_4. Therefore, a part of the IL would be destroyed and hampering its regeneration.

In the system [Emim][HSO_4] – DMSO, viscosity is reduced but the acidity is lower compared with the neat IL. The working temperature must be minor than 170 °C, as its boiling point is 189 °C.

By mixing [Emim][HSO_4] with BMP-TFSI, viscosity is even lower than the other systems, and the working temperature can reach 250 °C. On the other hand, acidity is low, as it is hydrophobic, but this would allow a higher selectivity.

To have a complete overview of the possible scenarios, experiments with neat [Emim][HSO_4] and sulfuric acid (H_2SO_4) were conducted, as H_2SO_4 is one of the mineral acids used for recovering REEs and Ti from BR [24,40,56,115,131,132].

The preliminary tests were performed in a magnetic stirring plate with a magnetic stirrer to provide vigorous agitation, a condenser to avoid water evaporation and a thermocouple to control the temperature. In every case, the pulp density was 5 % w/v and experiments were carried out for 24 hours, while the temperature was set depending on the kind of ionic liquid. Conditions and parameters chosen for each experiment are shown in Table 5.

Table 5 Parameters and conditions of the preliminary leaching experiments.

Leaching agent	Concentration (M)	Temperature (°C)	Pulp density (% w/v)	Time (hours)
H_2SO_4	1	90		
[Emim][HSO_4] neat	-	180		
[Emim][HSO_4] in H_2O	1	90	5	24
[Emim][HSO_4] in DMSO	1	120		
[Emim][HSO_4] in BMP-TFSI	1	90		

Each test was repeated three times and results are given as the average recovery percentage. Fe, Na, Ca, Al and Si were analyzed by using AAS; Ce, La, Y and Nd with ICP-MS; Ti and Sc with ICP-OES. Results are given in Figure 22.

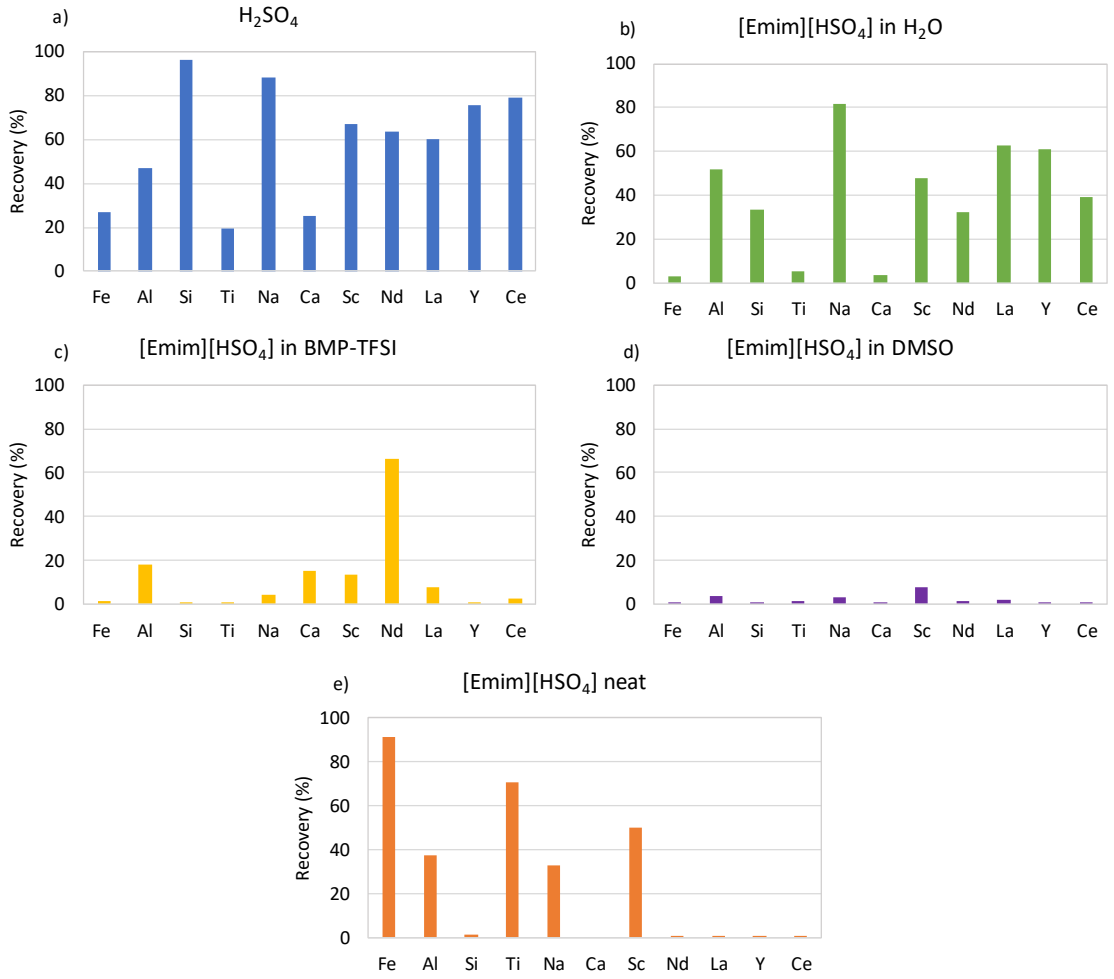

Figure 22 Results of the preliminary tests performed by dissolving BR with a) H_2SO_4; b) [Emim][HSO_4] in H_2O; c) [Emim][HSO_4] in BMP-TFSI; d) [Emim][HSO_4] in DMSO; e) [Emim][HSO_4] neat.

As it is possible to observe in Figure 22a, when BR is leached with H_2SO_4, even though silica gel is not formed due to the low pulp density [42,56], Si is dissolved at a very high rate (96 %) together with Na (88 %). Fe and Al recoveries are limited to 28 % and 47 % respectively, while Ti and Ca are barely dissolved (19 %), as Ca forms $CaSO_4$ precipitate [56]. REEs are leached in a range of 60 – 80 %.

These results are comparable with the results obtained by leaching BR with [Emim][HSO_4] in H_2O (Figure 22b), but in this case, Fe and Ti recoveries are negligible (lower than 5 %) and Si extraction is moderate (34 %). Also in this system, Ca is very low extracted as it forms $CaSO_4$ precipitate. Moreover, REEs recovery yields are moderate, as Sc extraction is 47 %, La and Y are about 60 %, Ce 38 % and Nd 32 %.

In both systems, [Emim][HSO_4] in BMP-TFSI (Figure 22c) and [Emim][HSO_4] in DMSO (Figure 22d), the recovery yields for all the metals were negligible, as consequence neither of them can be employed as leaching agent to dissolve metals from BR.

Neat [Emim][HSO_4] (Figure 22e) resulted to be the best system for extracting Ti (71 %) and also Sc recovery is 50 %. On the other hand, it is not selective for Fe which is almost totally dissolved (92 %). REEs remain in the solid and can be leached afterward. Al and Na recovery yields are moderate (37 and 33 % respectively). Si is not leached, while Ca dissolves and precipitates as $CaSO_4$.

In consideration of the fact that it resulted to be the most efficient system for recovering Ti and Sc, which are the target of this work, neat [Emim][HSO_4] was chosen for extracting metals from BR.

6.3 [Emim][HSO_4] leaching: process optimization

Batch leaching experiments were performed in a 50 mL Trallero and Schlee mini reactor combined with a mechanical stirrer, a vapor condenser and a temperature controller (Figure 23), by adding BR to the IL when the set temperature was reached.

Vacuum filtration was executed by cooling the system at 120 °C and adding a non-viscous/volatile solvent (dimethyl sulfoxide, further denoted as DMSO) to the leachates, to decrease viscosity and ease the process.

After filtration, pregnant leaching solutions (PLS) were digested through acidic treatment (HNO_3 65 % v/v and aqua regia) to oxidize and destroy the organics and then analyzed with AAS, ICP-OES and ICP-MS.

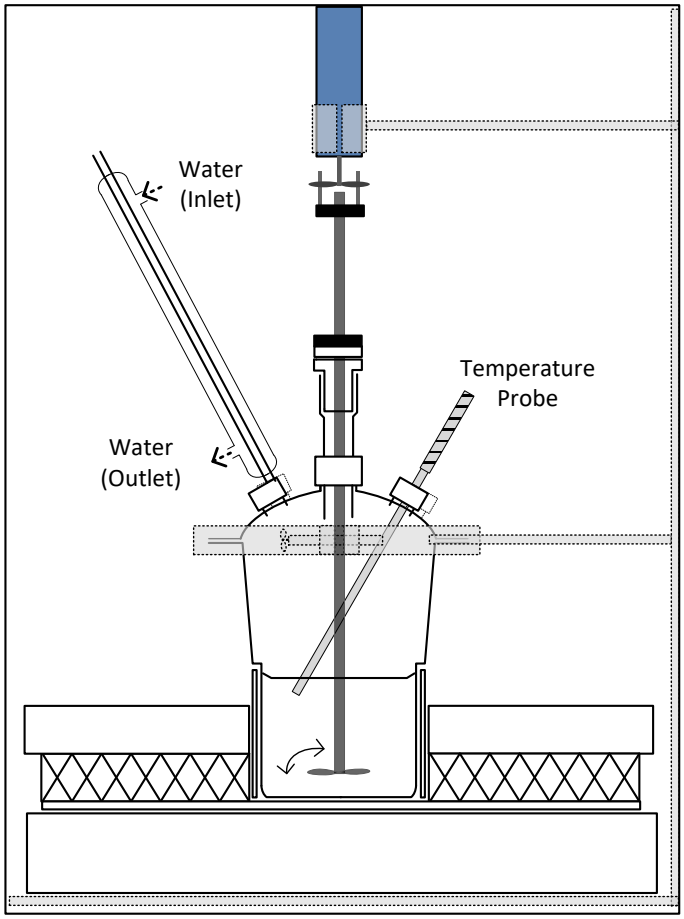

Figure 23 The Trallero and Schlee mini reactor scheme.

In order to optimize the process, stirring rate, retention time, temperature and pulp density were investigated. Each parameter was studied separately, keeping the others constant, and choosing the combination that gave the best results. In each case, Ca and Si in leachates were below the detection limit and Ce, Nd, Y and La recovery was lower than 1 %.

6.3.1 Stirring rate

Initially, experiments were carried out by examining four different stirring rates, 100, 200, 400 and 600 revolutions per minute (rpm), while keeping constant all the other parameters at 150 °C, 5 % w/v pulp density and 24 hours. Results are given in Figure 24. At these conditions, it is possible to observe an increase of Fe, Ti and Sc extraction when the stirring rate increases from 100 to 200 rpm (from 55 % of Sc, 57 % of Fe and 65 % of Ti at 100 rpm to 67 % of Sc, 75 % of Fe and 72 % of Ti at 200 rpm). On the other hand, as the stirring rate increases from 200 to 600 rpm, Fe, Ti and Sc extraction is observed to linearly decrease (from 67 % of Sc, 75 % of Fe and 72 % of Ti at 200 rpm to 37 % of Sc, 46 % of Ti and only 9 % for Fe at 600 rpm). Na and Al recovery are slightly affected by the stirring rate as they remain almost stable in a range of 17-32 % of the recovery. This effect of stirring rate on metal

recovery is typical in hydrometallurgy. Under low stirring rates, a thick boundary layer is developed on the surface of the solid particles, making the diffusion of chemical species from and to the solid particles surface inefficient. Therefore, at stirring rates lower than 200 rpm, the leaching process is slowed down and the metal recovery decreases, as it is seen in Figure 24. At stirring rates higher than 200 rpm, the thickness of the boundary layer is substantially decreased, but the high convective mass transfer of reactants from the surface of the particles, makes the surface reactions again inefficient and thus the recovery yields are diminishing, as it is seen in Figure 24. Therefore, a compromise is always found under intermediate stirring rates which, for this system, is around 200 rpm. At this stirring rate, Fe, Ti and Sc have the highest recovery yields (75, 72 and 67 % respectively).

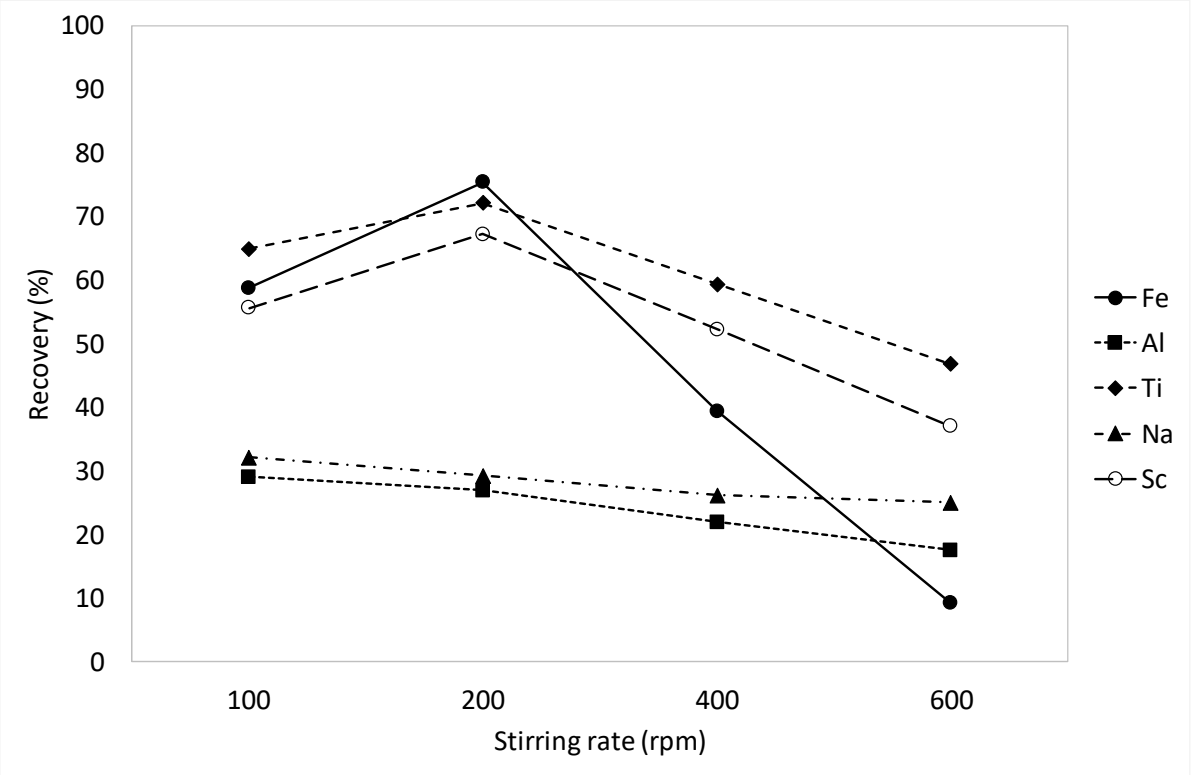

Figure 24 Investigation of the stirring rate effect on metals dissolution by leaching BR with [Emim][HSO4] at 150 °C, 5 % w/v pulp density for 24 hours.

6.3.2 Kinetic studies

Several sets of kinetic experiments have been performed at 200 rpm stirring rate, 5 % w/v pulp density, analyzing the behavior of the system at three different temperatures: 150, 175 and 200 °C. In Figure 25 it is observed that at low temperature (150 °C), all metals show the same trend in the first twelve hours; an initial metal dissolution occurred in the first six hours, whilst in the following six hours, metals dissolution is decreased, reaching their lowest concentration at 12 hours retention time. This unusual behavior can be attributed to the precipitation of Ca as $CaSO_4$ that massively

occurs within the first 6 hours (Figure 26), while Fe dissolution is low. In the latter 6 hours, adsorption phenomena are more important and faster than dissolution and, being in contact with anhydrite, metals are removed from the leachates, attaining the minimum at 12 hours. Then, metals continue their dissolution and as the anhydrite precipitation has been completed, they are gradually desorbed, increasing their concentration in solution and reaching the equilibrium at 24 hours retention time, with the exception of iron that continues to be dissolved but at a substantially lower rate.

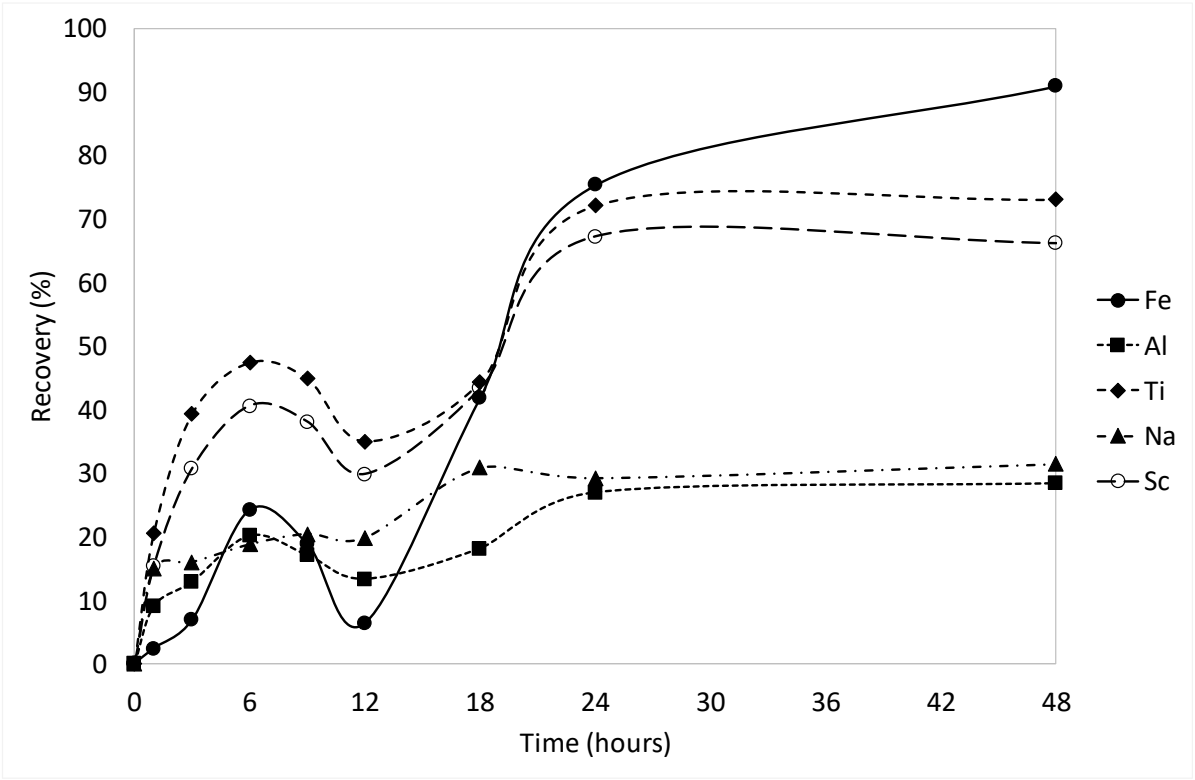

Figure 25 Kinetic curves for metals dissolution by leaching BR with [Emim][HSO_4] at 1, 3, 6, 12, 18, 24 and 48 hours, 200 rpm, 150 °C and 5 % w/v pulp density.

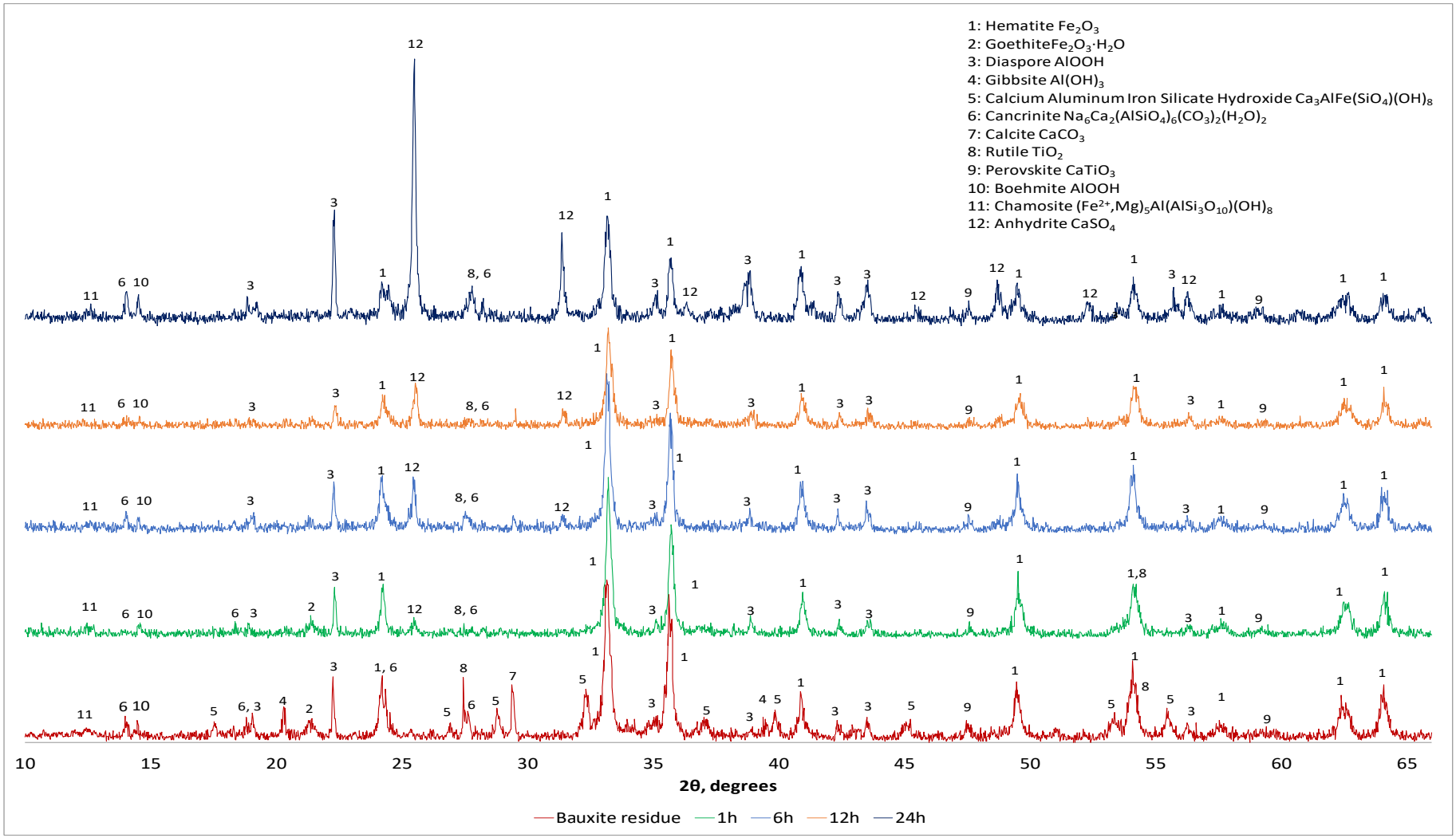

Figure 26 Comparison between XRD of bauxite residue and solid residue after leaching bauxite residue at 150 °C, 200 rpm, 5 % w/v pulp density for 1, 6, 12 and 24 hours

Kinetic studies have been carried out at 175 °C (Figure 27), in this case, the unusual dissolution phenomenon observed at 150 °C is not seen and the plateau has been reached faster, after 12 hours, achieving 90 % of Fe, 70 % of Ti and Sc dissolution and again moderate Al and Na recovery (30 %).

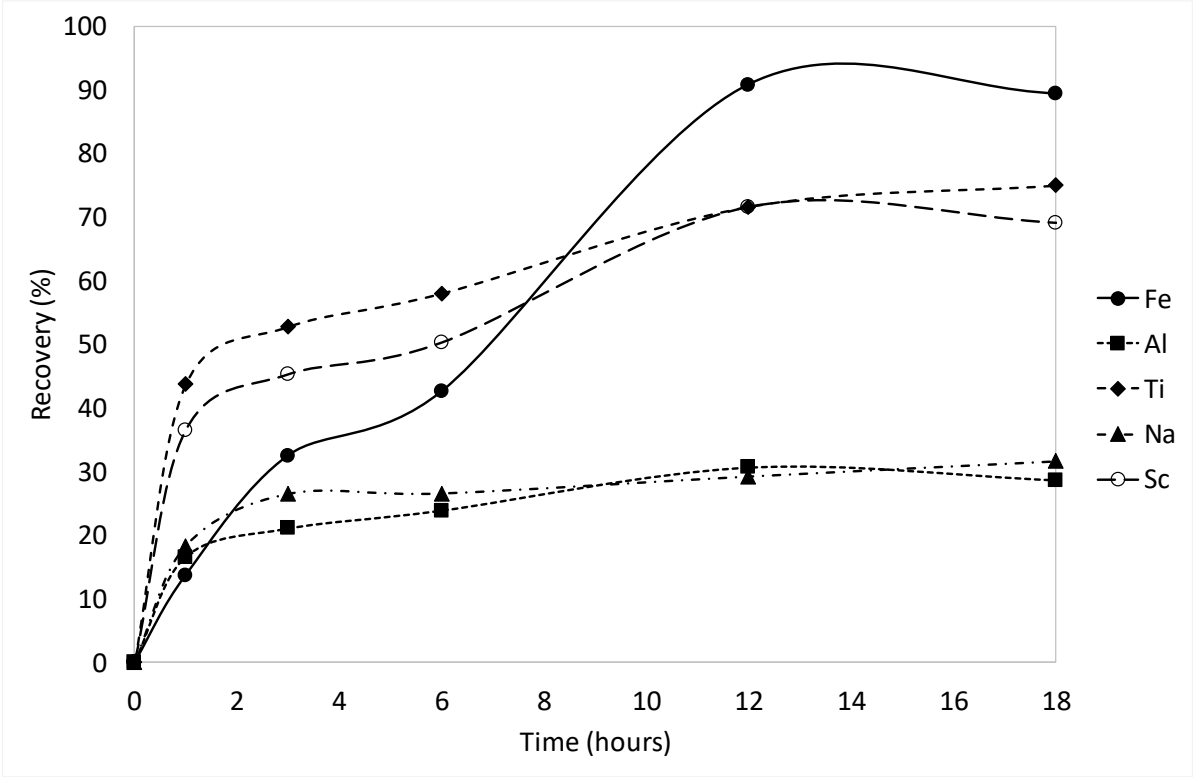

Figure 27 Kinetic curves for metals dissolution by leaching BR with [Emim][HSO_4] at 1, 3, 6, 12 and 18 hours, 200 rpm, 175 °C and 5 % w/v pulp density.

After 1 hour, more than 35 % of Sc has been dissolved, this, as mentioned above, is due to the fact that goethite is totally dissolved and hematite starts to be leached as well. The equilibrium has been reached at 70 % of Sc and 90 % of Fe recovery, which is in agreement with Vind et al. studies, as the main mineralogical Sc containing phases in bauxite residue are hematite and goethite (55 and 25 % on average respectively) [13].

At 200 °C (Figure 28), Fe, Ti and Sc are considerably leached even after 1 hour (60-74 %). The maximum extraction of these metals has been reached after 12 hours, where Fe is almost totally dissolved, Ti recovery is over 90 % and Sc reaches nearly 80 %. Al and Na dissolution remains stable along the kinetic curve in a range of 30-40 %.

Extraction of Sc at these high recovery yields (nearly 80 %), when Fe is also almost totally dissolved, again confirms that Sc was found to be hosted mainly in hematite and goethite mineralogical phases in bauxite residue [13], as already mentioned. It was hypothesized before, that in the same experimental setup as given here, the unrecovered proportion of Sc (about 20 %) may be associated

mainly with the chemically durable zirconium orthosilicate ($ZrSiO_4$), that contains around 10 % of the total Sc in bauxite residue, but also with other undissolved (or partially dissolved) phases as boehmite, diaspore and titanium-containing phases, that have been determined to be carriers of Sc in Greek BR [13].

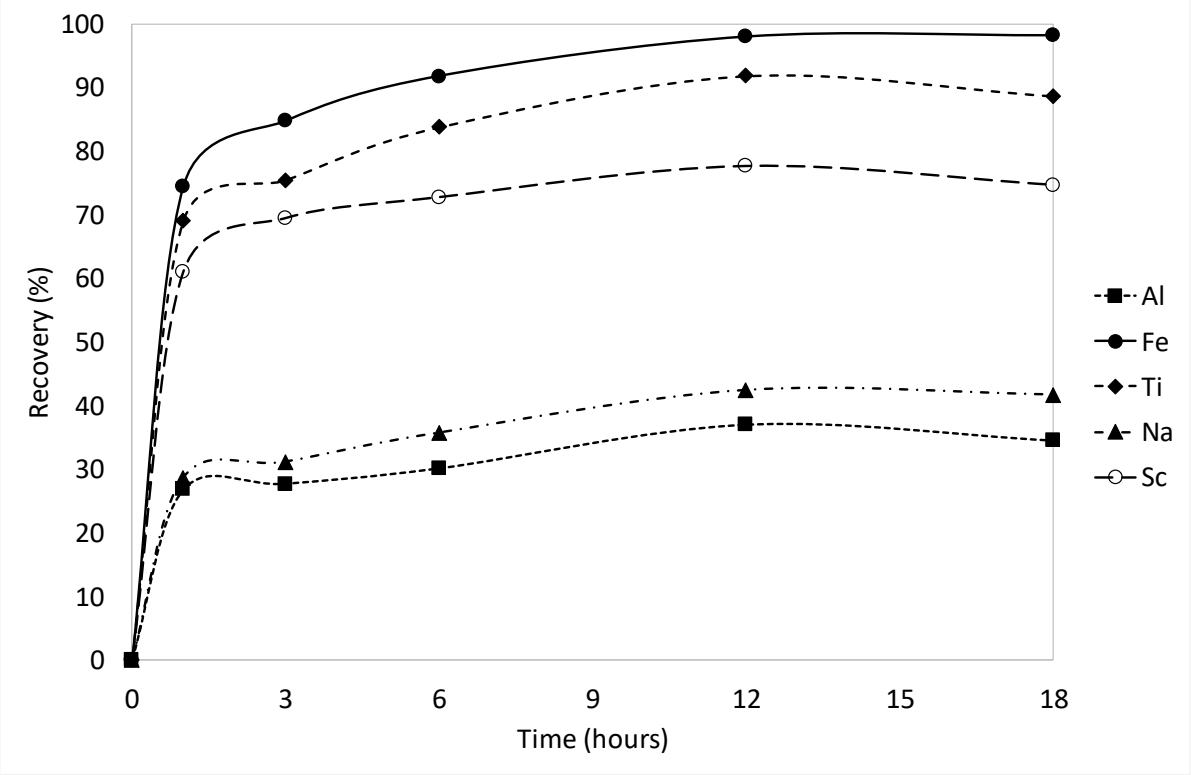

Figure 28 Kinetic curves for metals dissolution by leaching BR with [Emim][HSO_4] at 1, 3, 6, 12 and 18 hours, 200 rpm, 200 °C and 5 % w/v pulp density.

6.3.3 Pulp density

Four experiments have been conducted to investigate the effect of pulp density on the system, at 2.5, 5, 10 and 14.3 % w/v pulp density, under constant temperature, time and stirring rate (200 °C, 12 hours and 200 rpm). Results are shown in Figure 29. Fe, Ti and Sc present constant recovery in the area of 2.5-5 % w/v pulp density (almost total dissolution for Fe, 88 % for Ti and 78 % for Sc). This behavior can be explained by the extremely high ionic liquid excess and the relatively low viscosity of the system due to the low concentration of dissolved metals. By increasing pulp density, the ionic liquid excess decreases and viscosity rises substantially, due to the increase of the number of suspended BR particles as well as the dissolved metal concentrations affecting the ions mobility phenomena and the thickness of the boundary layer. This results in a sharp and linear decreasing recovery, reaching the minimum at 14.3 % w/v (60 % of Fe, 70 % Ti and 14 % of Sc). Experiments at

pulp density higher than 14.3 % w/v were not carried out due to the high viscosity, which prevented filtration and caused serious problems during the leaching process.

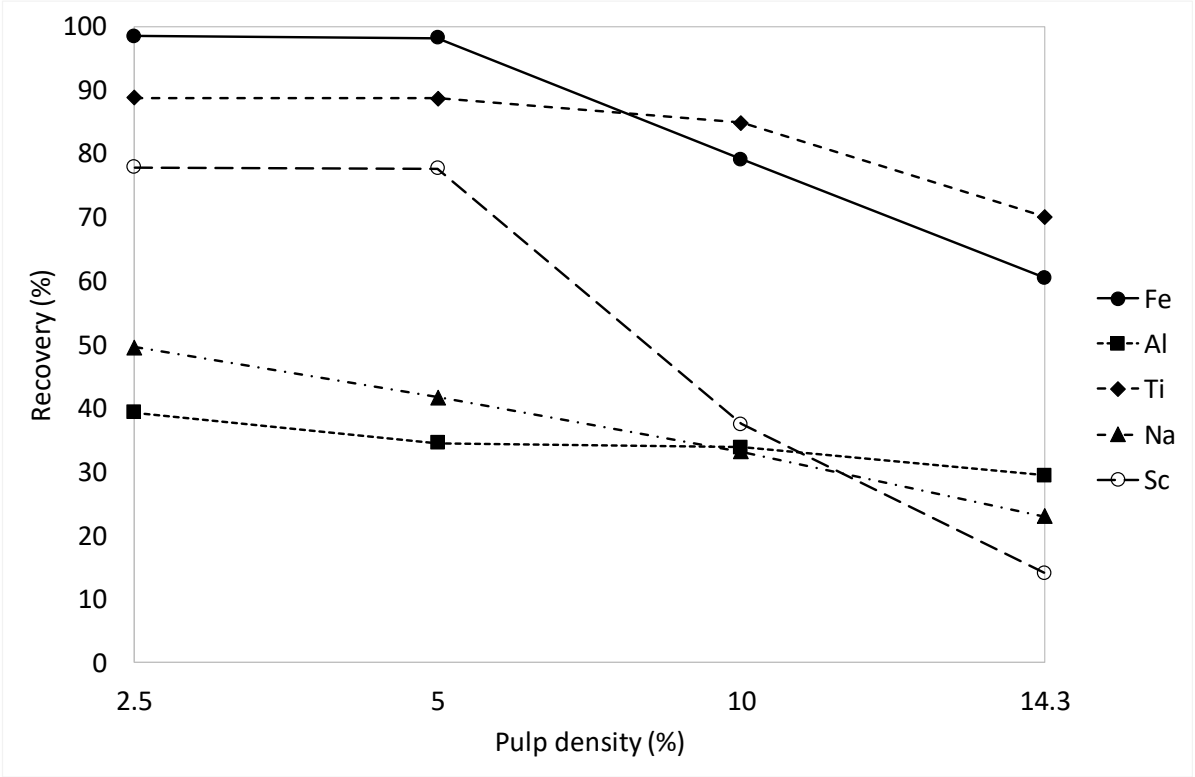

Figure 29 Study on the system behavior for metals dissolution by changing pulp density when leaching BR with [Emim][HSO_4] at 12 hours, 200 rpm, 200 °C.

6.3.4 Leaching bauxite residue at optimum conditions

It can be concluded that 200 rpm, 200 °C, 12 hours and 5 % w/v pulp density are the optimum conditions for leaching BR and obtaining obtain the best results, in terms of Ti and Sc recovery, when bauxite residue is directly leached with [Emim][HSO_4] (Figure 30).

At the optimum conditions, Fe was almost totally dissolved and Sc recovery yield was nearly 80 %. As already mentioned before, this outcome is in accordance with Vind et al. as Sc is mainly hosted in hematite and goethite mineralogical phases (55% and 25%, respectively) in bauxite residue [13]. The undissolved Sc content might be attributed to $ZrSiO_4$, containing around 10 % of the total Sc in bauxite residue, but also to other phases, such as boehmite, diaspore, and titanium-containing phases that host Sc in Greek bauxite residue [13].

At these conditions, 90 % of Ti was dissolved, while Al and Na were partially extracted (in a range of 30 – 40%). Si and REEs dissolutions were found to be negligible, whereas Ca was partially dissolved and precipitated as $CaSO_4$ consuming about 2 wt.% of the ionic liquid.

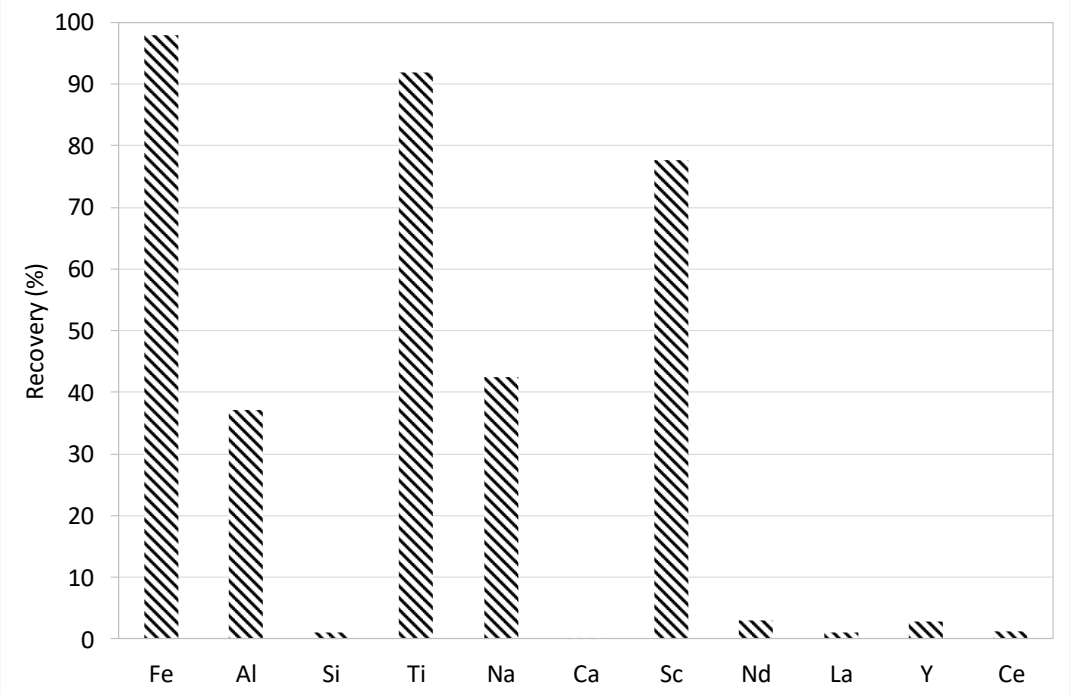

Figure 30 Metal recoveries at optimum conditions: 200 rpm, 200 °C, 12 hours and 5 % w/v pulp density.

7. Characterization of the solid residues after leaching

Solid residues were characterized via fusion method (already described in chapter 5) and XRD. Microstructural characterization was carried out by a JEOL 6380 LV Scanning Electron Microscope coupled with Energy Dispersive System (SEM-EDS) and a JEOL 2100 HR 200kV Transmission Electron Microscope (TEM) in order to detect and locate REEs.

With this purpose, two kinds of samples were taken into consideration, one rich in Fe (reddish), from the bauxite residue dissolution at mild conditions (150 °C, at 200 rpm, 24 h, 5 % w/v pulp density), hereafter referred a S1, and another Fe – depleted (greyish) after complete dissolution at optimum conditions (200 rpm, 200 °C, 12 h, 5 % w/v pulp density), from now on named S2 (Figure 31).

Sample S1 Sample S2

Figure 31 Solid residues after leaching. The reddish one (Sample S1) is from the dissolution of BR at 150 °C, 200 rpm, 5% w/v pulp density for 24 h and the greyish one (Sample S2) is from the dissolution of BR at optimum conditions.

7.1 Characterization of the left-over residues S1 and S2

The left-over residue S1 was found to be the 61 wt.% of the weight of the initial BR mass; its composition is given in Figure 32; this sample is rich in iron and aluminum, which are the main components of the sample, followed by calcium and silicon. REEs remain in the solid residue (except for scandium that has been leached for 67 %).

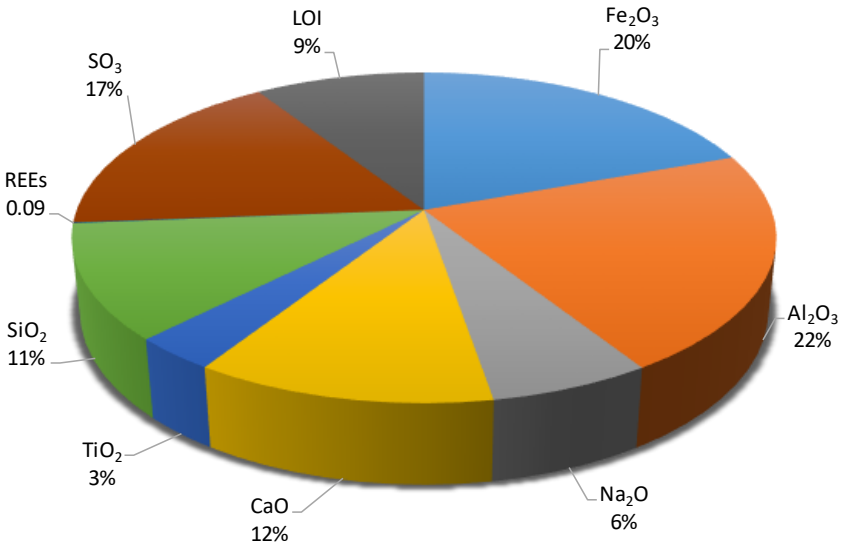

Figure 32 Chemical composition of the solid residue (S1) after leaching bauxite residue at 150 °C, 200 rpm and 5% w/v pulp density for 24h.

This behavior has been confirmed by SEM-EDS analysis as the matrix is mainly composed of aluminum oxides and Ca-Al Silicates; Fe oxides particles persist to leaching and remain enclosed in the matrix (Figure 33).

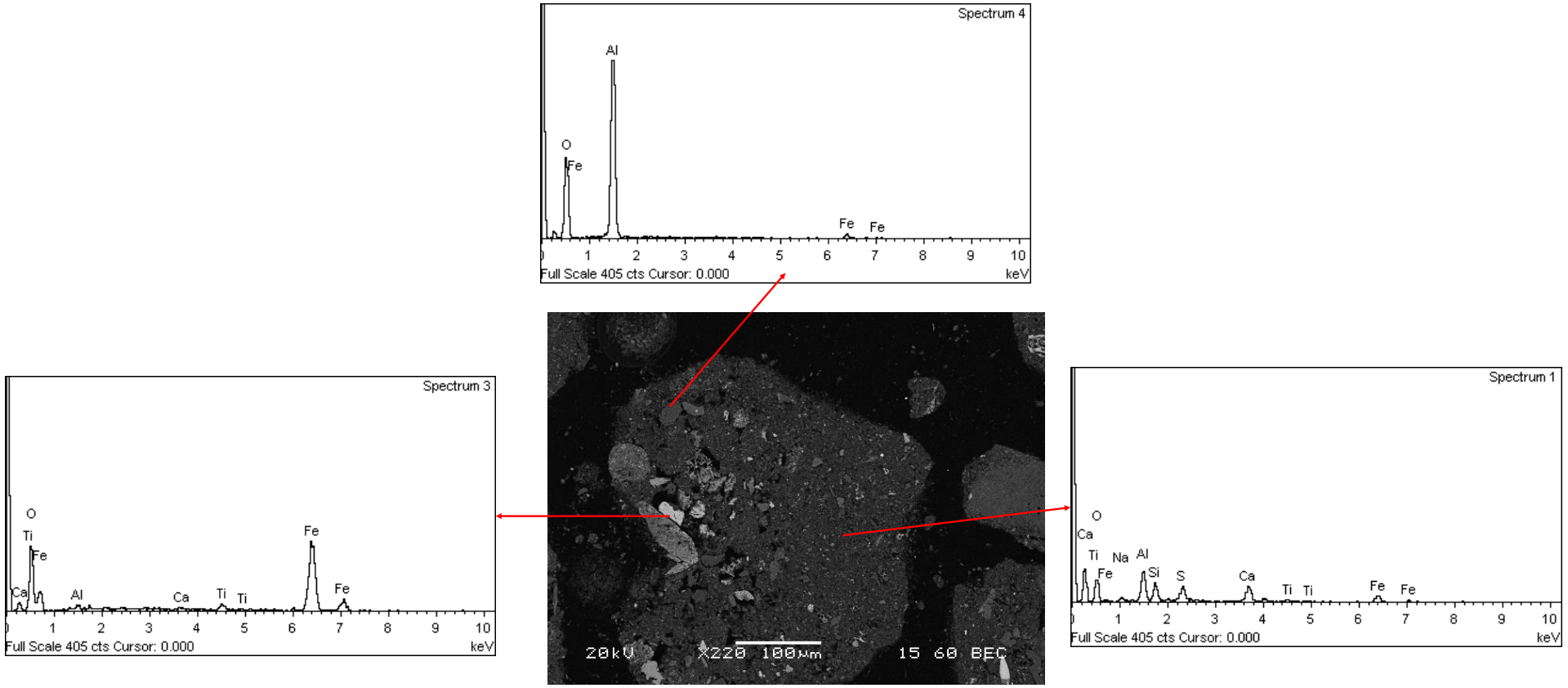

Figure 33 S1 matrix SEM-EDS image.

The left-over residue S2 was the 48 wt.% of the initial BR mass. As it can be seen from the chemical analysis shown in Figure 34, S2 is high in aluminum, calcium and silicon, while it is depleted in iron and titanium. This was also confirmed by SEM-EDS analysis (Figure 35) as the matrix, mainly composed of Al, Ca, Na silicates, surrounds phases transitioning from $CaCO_3$ to $CaSO_4$. Also in this case, REEs remain in the solid residue (with the exception of scandium) and can be leached afterward.

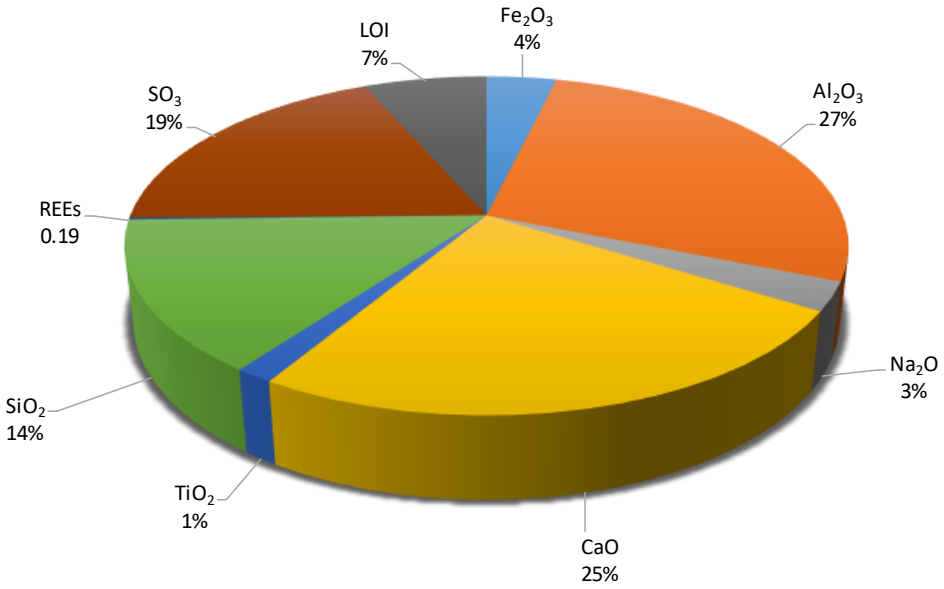

Figure 34 Chemical composition of the solid residue (S2) after leaching bauxite residue at optimum conditions, 200 °C, 200 rpm and 5% w/v pulp density for 12 h.

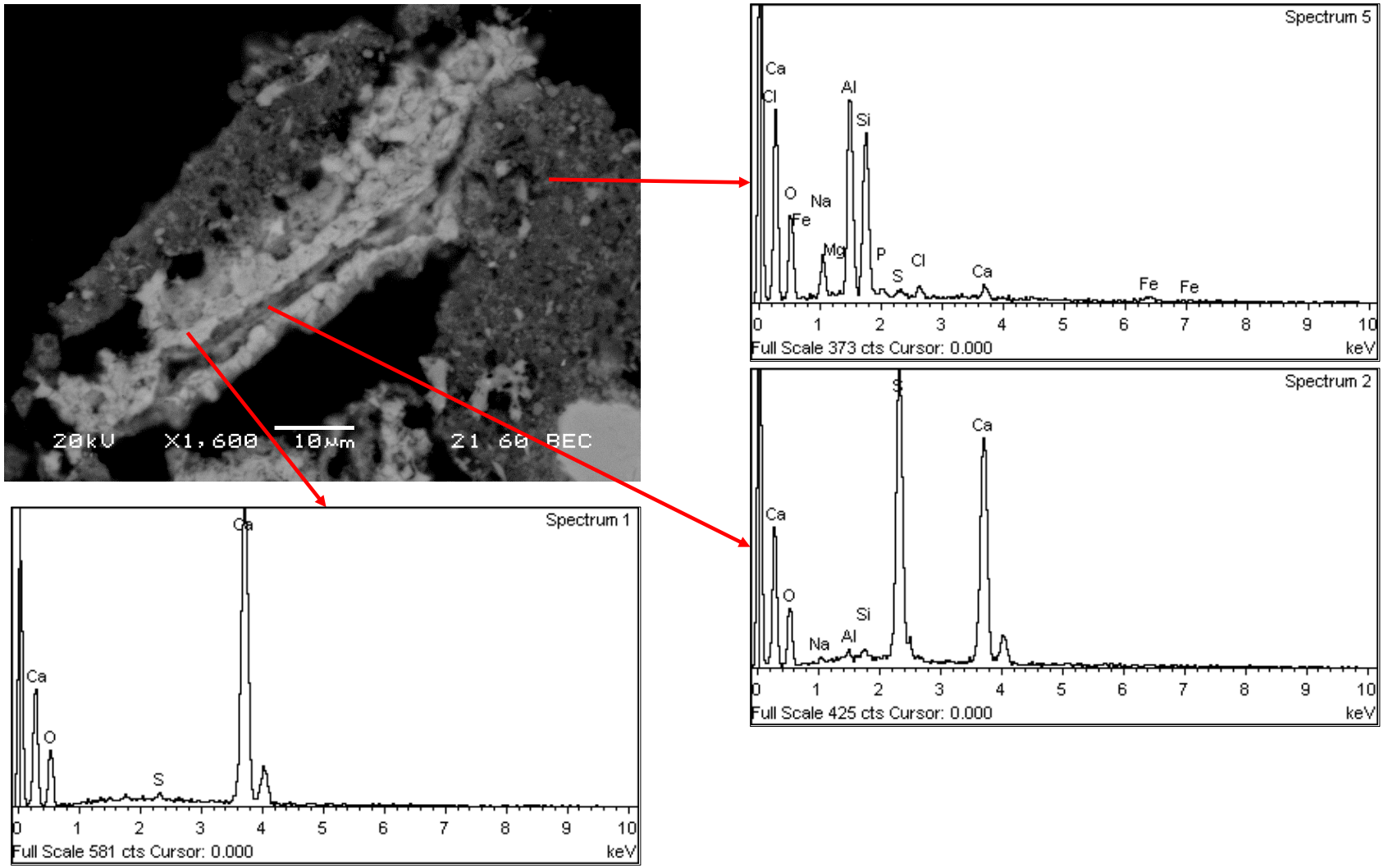

Figure 35 SEM image of the matrix of the residue after leaching S2.

Both samples were analyzed via XRD and a comparison between bauxite residue, S1 and S2 is given in Figure 36. There are three differences between the two samples, (I) one is due to the presence of hematite, (II) one to the massive formation of $CaSO_4$ and the (III) last is due to the peaks attributed to the other mineralogical phases that gradually disappear after leaching.

(I) The difference in color between the two samples, is due to the fact that when BR was leached at mild condition, hematite still existed, giving the red color to the left-over residue (S1); on the other hand, at more severe conditions, hematite was totally dissolved and the solid residue remained grey (S2).

(II) In addition, a new mineralogical phase is created during leaching, the calcium sulfate anhydrite ($CaSO_4$), which was formed due to the interaction between calcium and the anion of the ionic liquid. This mineralogical phase caused the consumption of about 2 wt.% of the IL when BR was leached at optimum conditions. Making a comparison between the two XRD's profiles, when BR was leached at severe conditions, Ca was completely dissolved and massively precipitated as $CaSO_4$ (S2), while at milder conditions $CaSO_4$ mineralogical phase formation was not complete, as it is possible to observe by the number and intensity of the peaks in Figure 36.

(III) Moreover, it is possible to observe that peaks attributed to hematite, goethite, calcium aluminum iron silicate hydroxide, gibbsite and perovskite, which are present in bauxite residue, gradually disappear after leaching. In both samples, aluminum phases like diaspore and boehmite remain relatively intact after leaching as well as cancrinite, chamosite and calcite. The above observations explain well the behavior of Al and Na during leaching as their main minerals in BR such as diaspore, boehmite and cancrinite remain insoluble, leading to low to moderate recoveries.

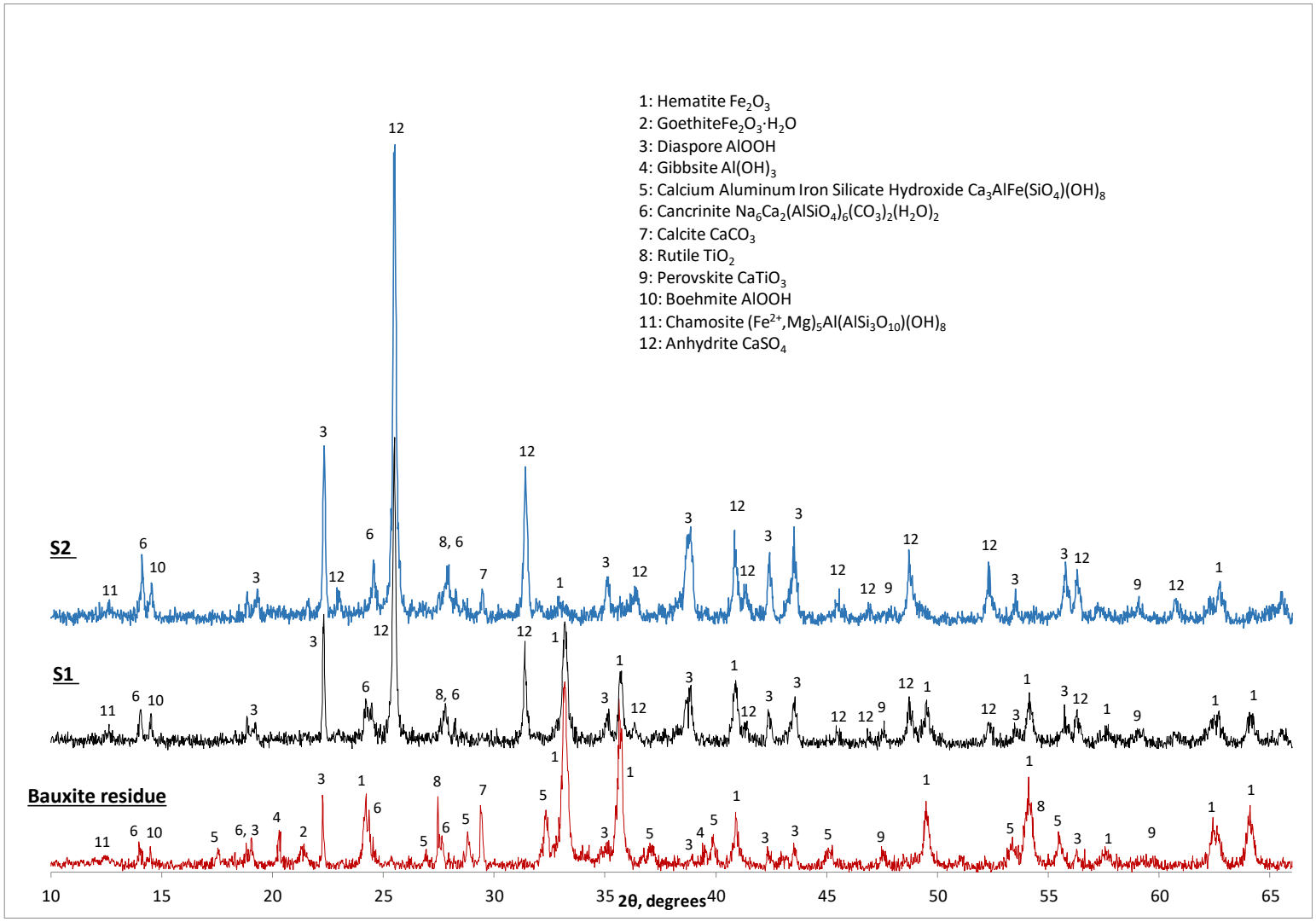

Figure 36 XRD comparison between bauxite residue, Fe-rich solid residue after leaching (S1) and Fe-depleted solid residue after leaching (S2).

7.2 REEs in the solid residues S1 and S2

The main purpose of the left-over residues' characterization was to locate REEs particles and find a reason why they were not dissolved even at severe conditions.

S1 was analyzed with SEM-EDS and heavy rare earth (HREE) phosphate particles were found in the matrix, surrounded by Fe oxides particles and TiO_2, with the major constituent being yttrium (YPO_4) and presence of erbium, gadolinium, europium, dysprosium, ytterbium and samarium (Figure 37). As Vind et al. explain, heavy rare hearth phosphate particles are small (few µm) and endure the Bayer process digestion, as they are present in the same form in bauxite ores [14]. Therefore, we can conclude that this kind of phases remains intact also during the ionic liquid dissolution of BR.

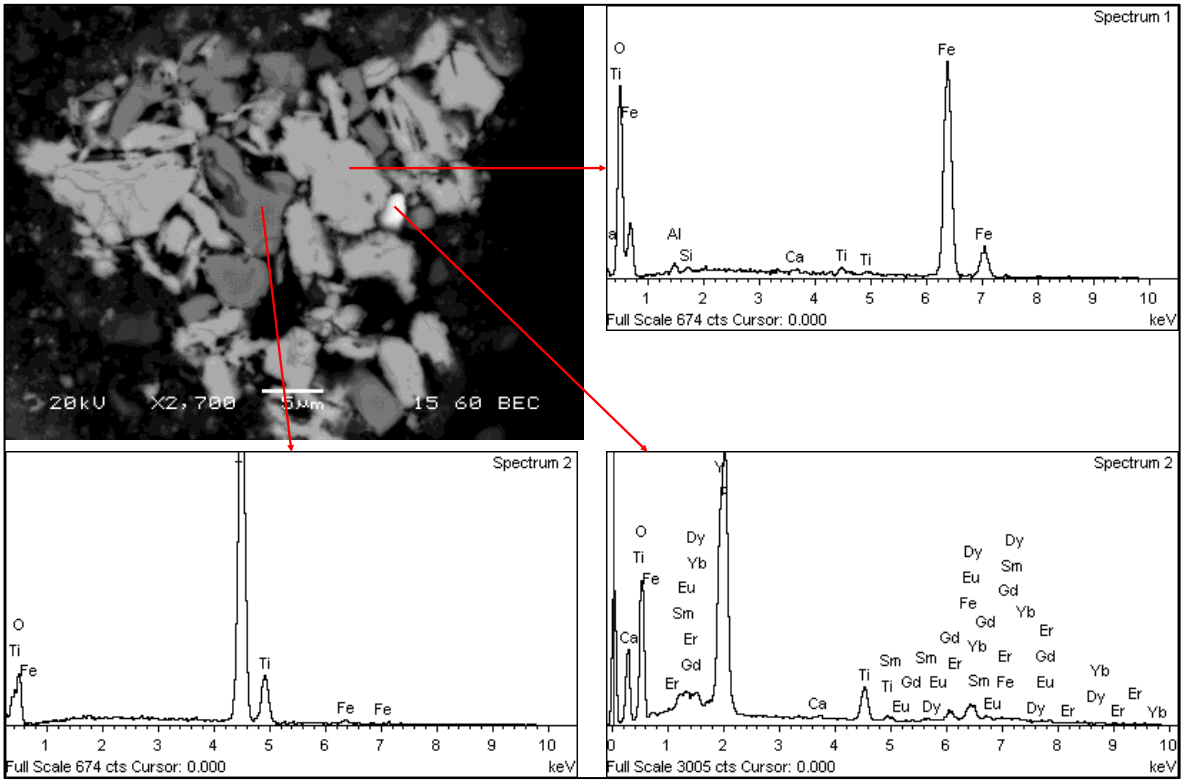

Figure 37 S1 SEM-EDS image: TiO_2 and Fe oxides particles enclose a small (2x3µm) YPO_4 particle that contains also other heavy rare earths.

Light rare earth (LREE) particles were also found in the form of calcium sodium titanate [(REEs, Ca, Na)(Ti, Fe)O_3] (Figure 38). This kind of particles are relatively big (particle in Figure 38 is 15x17 µm) and are formed during the Bayer process [14]. (REEs, Ca, Na)(Ti, Fe)O_3 particles endure the ionic liquid leaching, as their shape is the same as in bauxite residue.

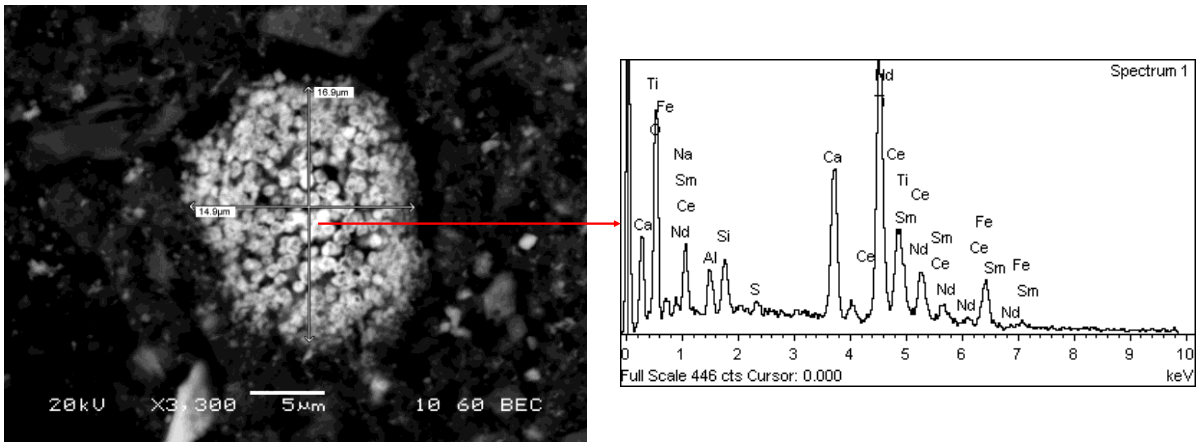

Figure 38 SEM-EDS image of a (REEs, Ca, Na)(Ti, Fe)O_3 particle present in the solid residue (S1) after ionic liquid leaching at 150 °C, 200 rpm, 5 % w/v pulp density for 24 hours.

As mapping confirms, Ce and Nd are the main LREEs in the particle (Figure 39) and Sm is also present. LREEs distribution in the particle is homogeneous, they are rich in Ti which is predominant on the edges, together with Ca as well as with Na. Al is absent and Fe and Si are slightly present, while sulfur surrounds the particle in the form of $CaSO_4$.

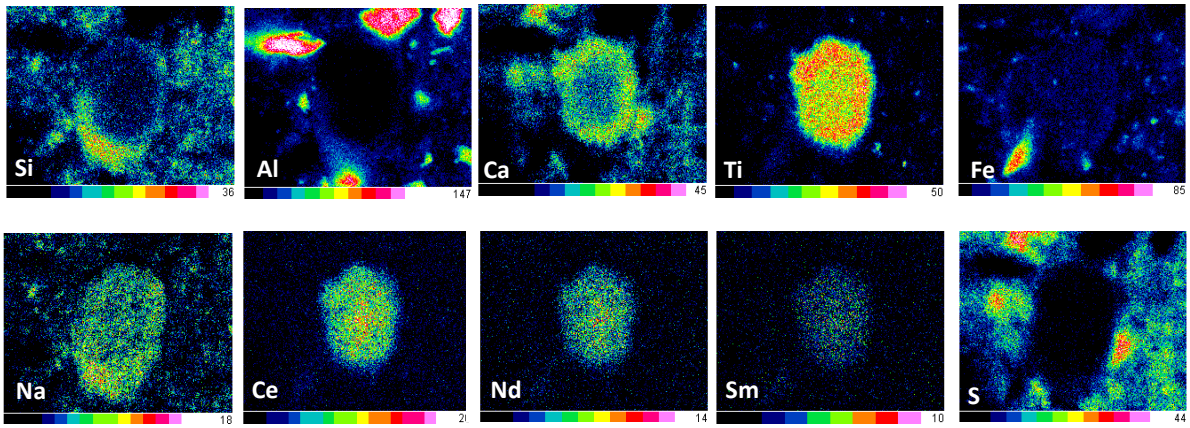

Figure 39 SEM-EDS elemental mapping of a (REEs, Ca, Na)(Ti, Fe)O_3 particle present in the solid residue (S1) after ionic liquid leaching at 150 °C, 200 rpm, 5 % w/v pulp density for 24 hours.

From the above observations, we can conclude that in S1, the solid residue obtained by leaching BR at milder conditions, both heavy and light REEs endure the ionic liquid dissolution, remaining intact as they were in BR.

In S2, small REEs containing particles (about 10 µm) were detected in SEM-EDS, in particular, YPO_4 particles including heavy rare earths like gadolinium and dysprosium (Figure 40).

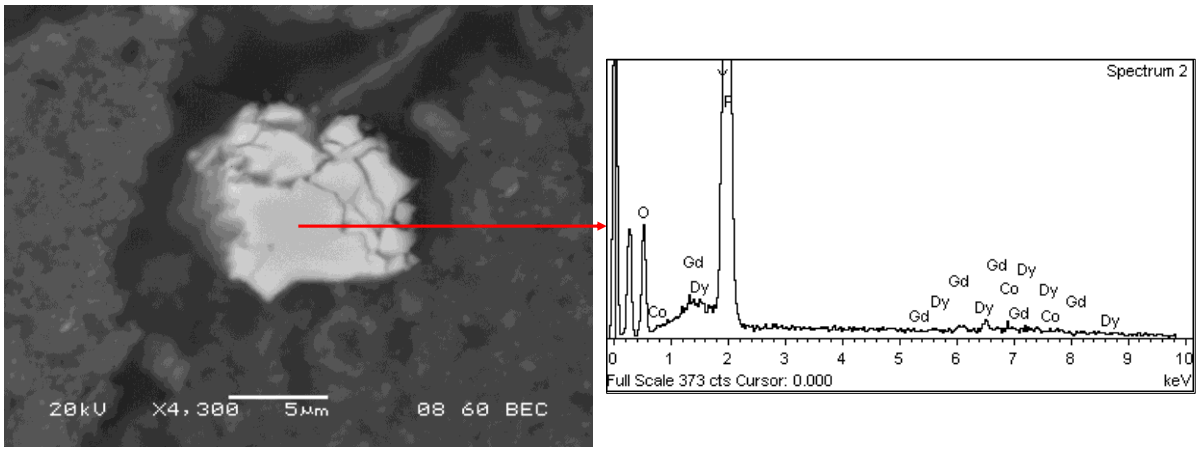

Figure 40 SEM-EDS image of a YPO_4 particle present in the solid residue (S2) after ionic liquid leaching at 200 °C, 200 rpm, 5 % w/v pulp density for 12 hours.

This is consistent with Vind et al. studies of raw bauxite residue [14] where the presence of heavy rare earth phosphates with the major constituent being yttrium and containing other heavy REEs like gadolinium, dysprosium and erbium is reported. This is an indication that these grains endure the [Emim][HSO_4] leaching process, without being subjected to any dissolution and thus explaining the negligible heavy REEs recoveries.

Small mixed calcium-cerium phosphate particles were also identified, in this case, grains included light rare earths like neodymium, lanthanum and samarium (Figure 41).

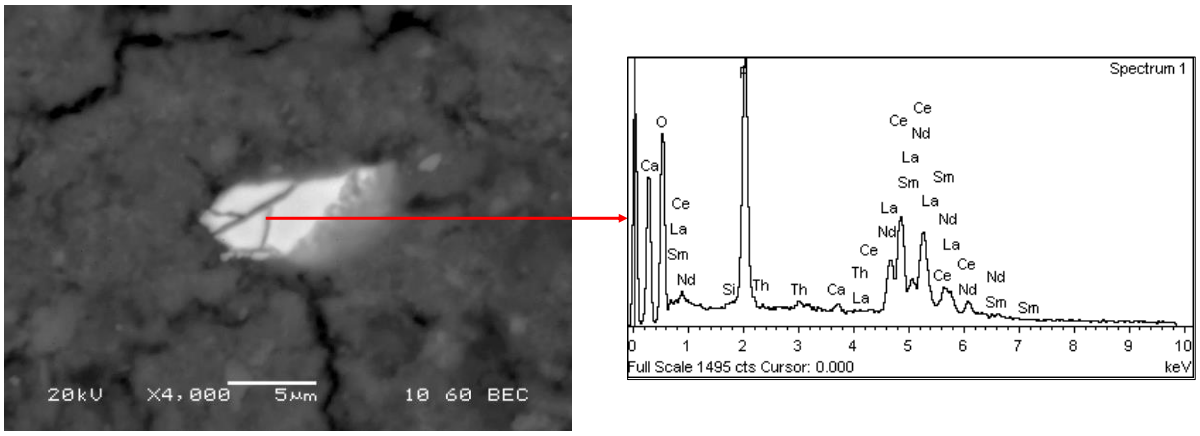

Figure 41 SEM-EDS image of a $CePO_4$ particle present in S2.

Vind et al. reported the presence of light rare earths as calcium-containing phosphate phases in bauxite residue [14]. In the case of the solid residue after leaching (S2), grains containing light REEs (LREEs) phosphates are also present. This may indicate a partial dissolution of calcium from the mixed Ca-LREEs phases, leaving behind smaller phosphate particles which are beneficiated in LREEs. This

was also implied by TEM analysis, detecting very fine (<500 nm) particles of Al-containing $CePO_4$ (Figure 42).

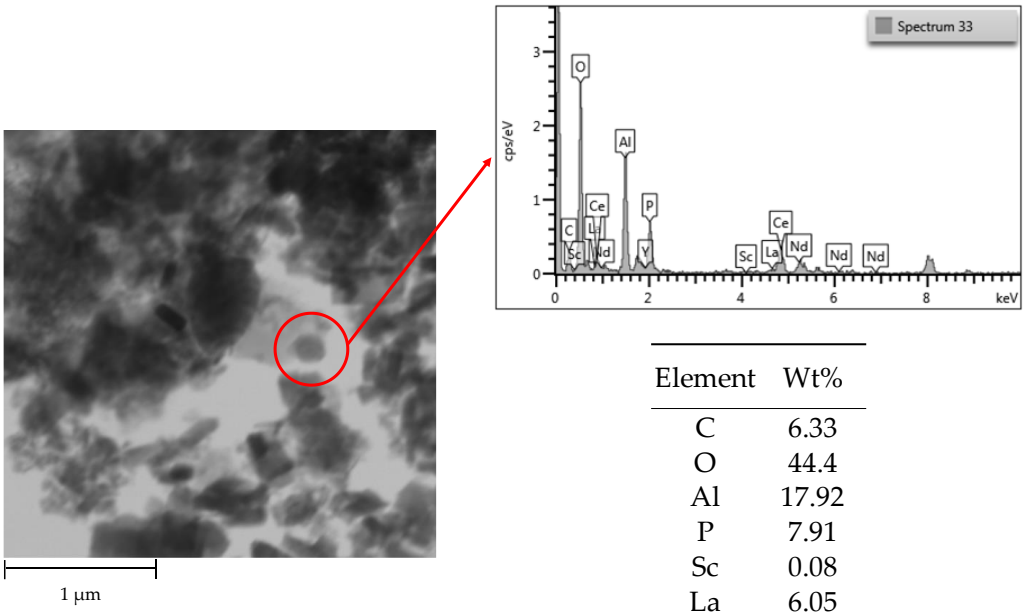

Element	Wt%
C	6.33
O	44.4
Al	17.92
P	7.91
Sc	0.08
La	6.05
Ce	17.17
Nd	0.13
Total:	100

Figure 42 TEM image of a $CePO_4$, Al containing, particle present in S2.

Also in the case of S2, the residue obtained by leaching BR at heavy conditions, REEs remained unchanged in mineralogy with the respect of the initial BR. Solid residue after leaching could be treated for selectively leaching REEs afterwards.

8. Metals extraction from the leachate

As already described in chapter 4, the term solvent extraction (SX) refers to a preferential distribution of a solute between two immiscible liquid phases in contact with each other [110]. Usually SX systems involve an aqueous phase and an organic phase, but it can also consist of two immiscible molten salts phases, a molten salt and an organic solvent or two immiscible organic solvents [83,111]. Generally, a pregnant liquid solution (PLS) that contains the dissolved solute, is put into contact with another immiscible phase. The two phases need to have different polarities and be immiscible with each other, in order to create two distinct phases. Moreover, they need to show a short phase disengagement time after mixing and the extractant has to be soluble in the less-polar phase and insoluble in the more-polar phase [83].

Many extractants can be used for recovering metals from leachates [83,111,113–117,121]. Extractants containing sulfur donor atoms are expected to be strong extractants for metal ions as the donor atoms of common bases have electronegativities increasing in the order: S<Br<N<Cl<O<F [133].

The most commonly used acidic organophosphorus extractants are divided into phosphoric, phosphonic and phosphinic acids (Figure 43) and extract metals by cation exchange mechanism [121].

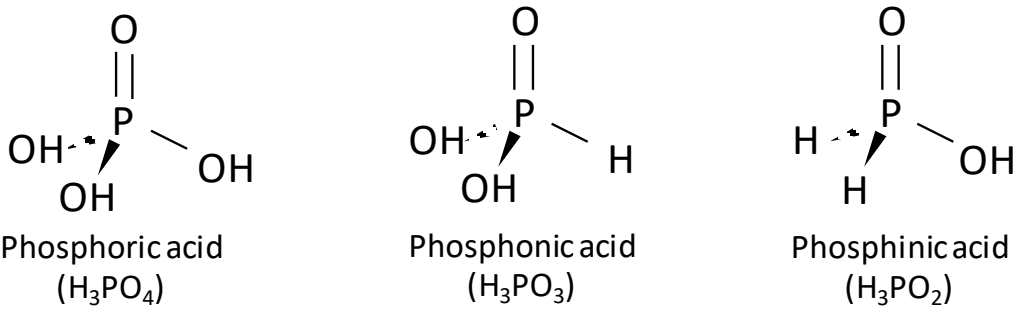

Figure 43 Structures of the commonly used acidic phosphorus-based extractants.

Generally, the neutral organo-phosphorus extractants are divided into four types: trialkyl phosphate, dialkyl-alkyl phosphonate, dialkyl-alkyl phosphinate and trialkyl phosphine oxide with the structures shown in Figure 44 Structures of the phosphorous-based solvating extractants. and are based on solvating extraction mechanism [121].

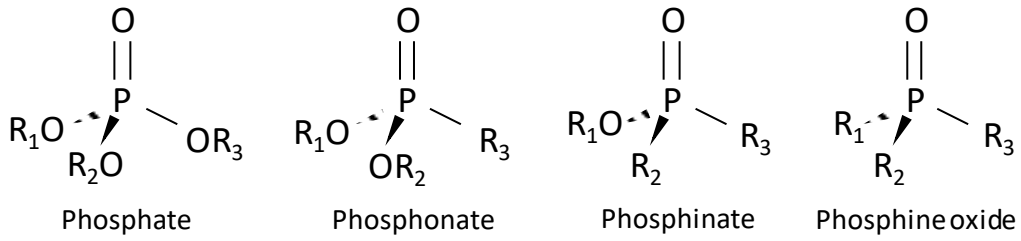

Figure 44 Structures of the phosphorous-based solvating extractants.

Flett explains that the mechanism of metal extraction by acidic extractants from aqueous solutions is governed by a cation exchange mechanism as in equation (14):

$$\mathrm{M_a^{n+}} + (\mathrm{n}+\mathrm{x})(\mathrm{RH})_\mathrm{o} = (\mathrm{MR_n}\cdot \mathrm{xRH})_\mathrm{o} + \mathrm{nH_a^+} \tag{14}$$

where $\mathrm{M_a^{n+}}$ is an n-valent metal cation in the IL phase, RH is the organic acid, the subscript “a” and “o” stand for the aqueous and the organic phases respectively [134]. In case of this work, where the ion is complexed by the anion of the IL, the proposed reaction for the SX with acidic extractants is the following:

$$[\mathrm{M_2(SO_4)_n}]_\mathrm{IL} + (\mathrm{n}+\mathrm{x})(\mathrm{RH})_\mathrm{O} = (\mathrm{M_2R_n}\cdot \mathrm{xRH})_\mathrm{O} + (\mathrm{nHSO_4})_\mathrm{IL} \tag{15}$$

where M is the n-valent metal, RH is the organic acid and the subscript “IL” and “o” stand for the IL leachates and the organic phases, respectively.

On the other hand, metal extraction mechanism by neutral reagents is based on the solvation of metal complexes by electron-donor-containing extractants [120,121,134]. General reaction is presented as following:

$$(MX_n)_a + \mathrm{y(P)_O} = (MX_nP_y)_\mathrm{O} \tag{16}$$

where M is the n-valent metal, X is a mono-valent anion P is the neutral phosphine oxides and the subscript “a” and “o” stand for the aqueous and the organic phases respectively [134].

In case of this work, the reaction that takes places by extracting metals from IL leachates with a neutral extractant is presented in equation (17):

$$[\mathrm{M_2(SO_4)_n}]_\mathrm{IL} + \mathrm{y(P)_O} = \left[\mathrm{M_2(SO_4)_n \cdot P_y}\right]_\mathrm{O} \tag{17}$$

Where the subscript “IL” and “o” stand for the IL leachates and the organic phases, respectively.

For the abovementioned reasons, three acidic organophosphorus extractants and a mixture of four trialkylphosphine oxides have been chosen in this work for extracting metals from the PLS obtained by leaching BR with the IL [Emim][HSO_4].

Table 6 Extractants used for recovering metals from the PLS obtained by leaching BR with [Emim][HSO_4].

Extractant	**Commercial name**	**Kind**
di-(2-ethylhexyl)phosphoric acid	D2EHPA	acidic
di-(2-ethylexhyl)phosphonic acid	Ionquest 801	
bis(2,4,4-trimethylpentyl)phosphinic acid	Cyanex 272	
trioctylphosphine oxide, dioctyl(hexyl)phosphine oxide, dihexyl(octyl)phosphine oxide, trihexylphosphine oxide	Cyanex 923	neutral

As presented in Table 6, D2EHPA, Ionquest 801 and Cyanex 272 were tested as acidic extractants and molecular structures are shown in Figure 45.

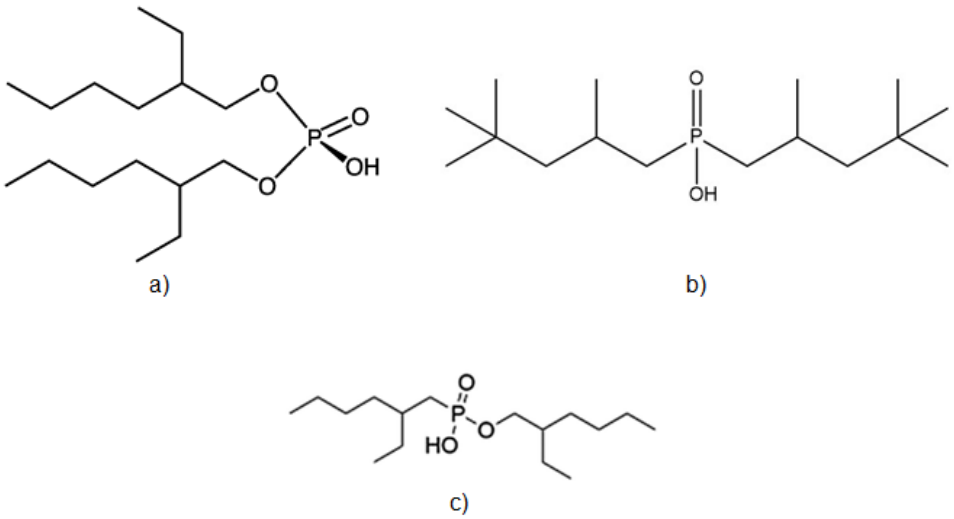

Figure 45 Molecular structures of di-(2-ethylhexyl)phosphoric acid (D2HEPA) (a), bis(2,4,4-trimethylpentyl)phosphinic acid (Cyanex 272) (b) and di-(2-ethylexhyl)phosphonic acid (IONQUEST 801) (c).

On the other hand, the neutral solvating extractant chosen was Cyanex 923, a mixture of four phosphine oxides whose molecular structures are shown in Figure 46.

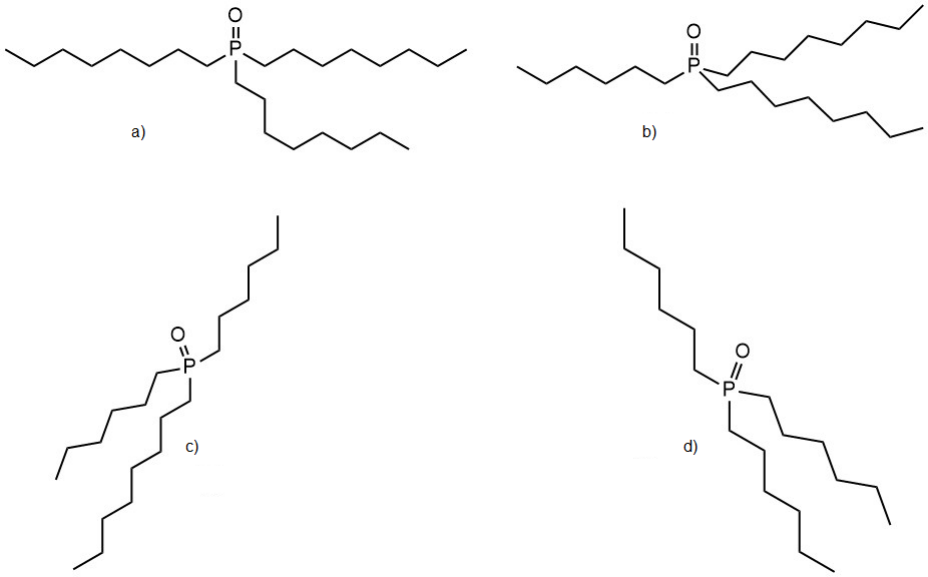

Figure 46 Cyanex 923 is a mixture of phosphine oxides: trioctylphosphine oxide (a), dioctyl(hexyl)phosphine oxide (b), dihexyl(octyl)phosphine oxide (c), trihexylphosphine oxide (d).

Parameters like phase disengagement, temperature, organic to IL ratio and extractant concentration were investigated aiming to find a suitable method to extract all the metals contained in a PLS obtained by leaching BR with the IL [Emim][HSO_4] for reusing the IL for subsequent uses.

8.1 Preliminary studies

For these experiments, the PLS from leaching BR with [Emim][HSO_4] at optimum conditions (12 hours, at 200 °C and 200 rpm) was employed. After leaching, the pulp was filtrated by adding dimethyl sulfoxide (DMSO) as non-volatile/viscous solvent in order to decrease the viscosity of the PLS and ease the filtration step [39]. A synthetic leach solution was also prepared considering the composition of the real one. The required amount of Fe_2O_3, TiO_2, Al_2O_3 and Sc_2O_3 were dissolved in [Emim][HSO_4] for 12 hours, at 200 °C and 200 rpm. In this case, DMSO was not added to the leach solution to observe the behavior of the solvent extraction process with a high viscous solution. Like in the case of real PLS, the synthetic leach solution was prepared by leaching oxides with [Emim][HSO_4] in a Trallero and Schlee mini reactor combined with a mechanical stirrer, a vapor condenser and a temperature controller. Samples were then digested through acidic treatment (HNO_3 65 % v/v and aqua regia) and analyzed. Fe and Al were detected with AAS, Ti and Sc with an ICP-OES.

The real PLS composition is shown in Table 7. As it is possible to observe, the main metal is Fe which accounts to 3.9 g/L, followed by Ti (384 mg/L) and Al (370 mg/L); Sc contributes with 1.3 mg/L.

Table 7 Composition of the solution obtained by leaching bauxite residue with [Emim][HSO_4].

Metal	Composition
Fe	3.9 g L^{-1}
Al	369 mg L^{-1}
Ti	378 mg L^{-1}
Sc	1.3 mg L^{-1}

The synthetic PLS composition simulates the real PLS composition, but it contains a significant amount of Sc (91 mg/L), as it is shown in Table 8, to clearly observe the behavior of this element in comparison with the others.

Table 8 Synthetic pregnant liquid solution (PLS) composition.

Metal	Composition
Fe	4.8 g L^{-1}
Al	340 mg L^{-1}
Ti	184 mg L^{-1}
Sc	91 mg L^{-1}

Solvent extraction preliminary experiments were conducted by using D2EHPA, Ionquest 801, Cyanex 272 and Cyanex 923. Parameters of these experiments are shown in Table 9.

Table 9 Preliminary SX experiments parameters.

Kind of PLS	Extractant concentration (% v/v)	Organic to IL ratio (O:IL)	Temperature (°C)
Synthetic	10	1:1 2:1	55
Real	20	1:1	room

Extractants were diluted in kerosene D85 at 10 % v/v, 1:1 and 2:1 organic to IL ratio (hereinafter referred as O:IL) were applied for synthetic PLS. Tests with real PLS were carried out at 20 % v/v and 1:1 O:IL. The correct immiscibility and phase disengagement between the different organic extractant phases and the IL one were verified by putting in contact the PLS (both synthetic and real) with the diluted extractants. Experiments with synthetic PLS were done at 55 °C to have a viscosity closer to the organic reagent, whereas experiments with real PLS were executed at room temperature since the viscosity, in this case, is much lower than the case in synthetic solution. Agitation improves the distribution of the solute between the two phases as the phase boundary area between them increases, until the equilibrium is reached [117]. For this reason, in both cases,

magnetic stirrers have been used to assure the correct agitation between the two phases. Kinetic tests were performed by sampling 5 mL of both phases at 15, 30, 60 and 120 minutes.

Samples were centrifuged and PLS phases were subjected to acidic digestion and analyzed. Extraction efficiency was calculated in percentages as the equation (18):

$$E\% = \frac{[A]_{ORG}}{[A]_{ORG} + [A]_{PLS}} \cdot 100 \quad (18)$$

where $[A]_{ORG}$ and $[A]_{PLS}$ are the metal concentrations at equilibrium in the extraction phase and PLS, respectively.

8.1.1 Cyanex 272

In the case of Cyanex 272, the separation between the extractant and the synthetic PLS phases took less than a minute due to the synthetic PLS high viscosity, while it was almost immediate with the real PLS. Tests performed with synthetic PLS at 10 % v/v extractant concentration 1:1 (Figure 47a) and 2:1 O:IL (Figure 47b) show a moderate Ti extraction (30 – 40 %). In both cases, the extraction of both Al and Fe are moderate, while Sc recovery is observed as 70 % at 1:1 O:IL and almost 90 % at 2:1 O:IL after 120 minutes.

Kinetic tests with real PLS at 1:1 O:IL and 20 % v/v Cyanex 272 concentration show a remarkable increase in metal loading, in fact, all metals are removed after 60 minutes (Figure 47c). Lowering viscosity and increasing extractant Cyanex 272 concentration affect positively on metals recovery. As the major aim is to transfer loaded ions into the extractant and reuse the IL, Cyanex 272 could be one of the promising organic extractants in this aspect.

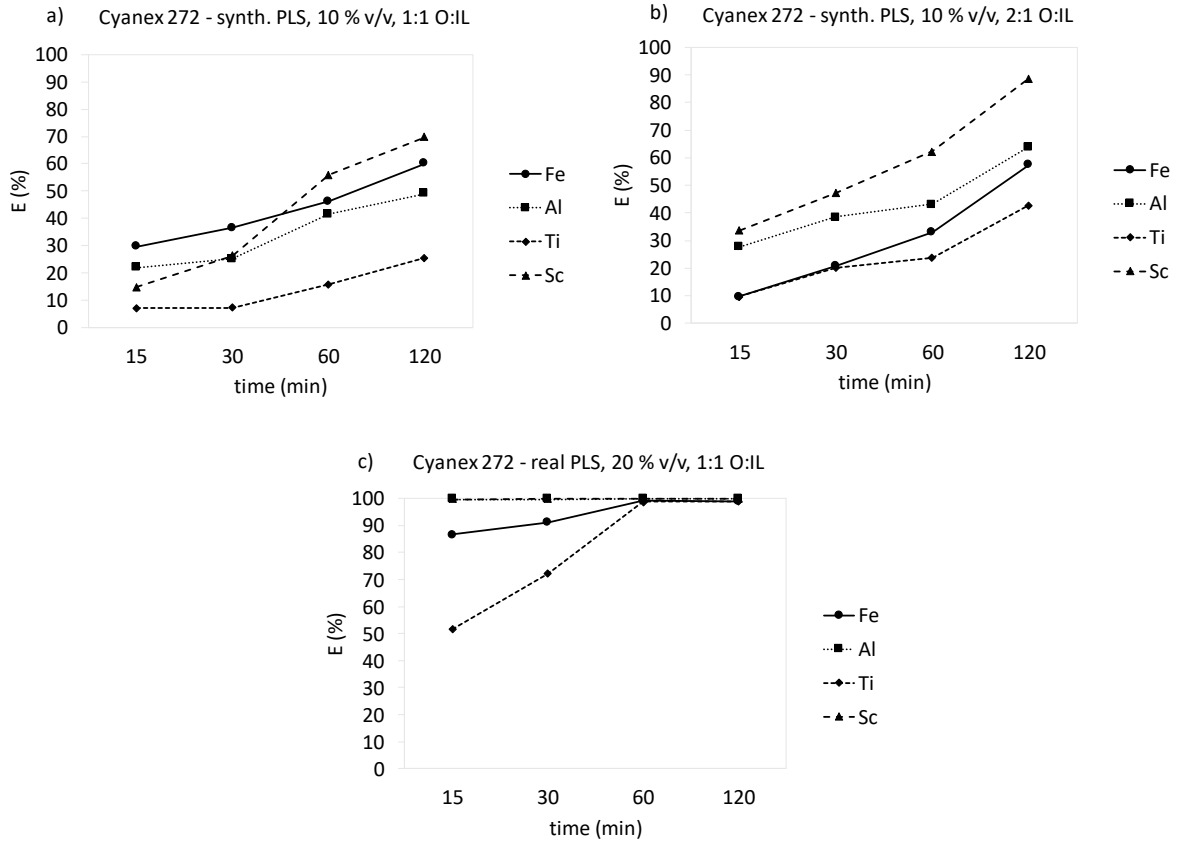

Figure 47 Metals extraction with Cyanex 272: from synthetic PLS at 10 % v/v in Kerosene D85, 1:1 O:IL (a) and 2:1 O:IL (b); from real PLS at 1:1 O:IL and 20 % v/v in Kerosene D85 (c).

8.1.2 Ionquest 801

Phase disengagement tests showed a very slow separation between the extractant and the synthetic PLS phases that took more than 3 minutes. On the contrary, phase disengagement resulted to be almost immediate with real PLS samples like the Cyanex 272 case. Experiments performed by using Ionquest 801 as extractant show similar behavior as the other extractants. In fact, also in this case, results are slightly different when O:IL changes from 1:1 to 2:1 (Figure 48a and b), showing a limited Ti extraction (less than 30 %), a moderate removal of Al (50 %) and a considerable amount of Fe (70 %). Sc is the only metal that benefits of increasing O:IL to 2:1, in fact after 15 minutes it is 10 % extracted at 1:1 O:IL (Figure 48a), while it is 40 % removed at 2:1 O:IL (Figure 48b).

Performing experiments with the real PLS, all metals are almost totally extracted after 15 minutes, with the exception of Ti that is totally removed after 60 minutes (Figure 48c).

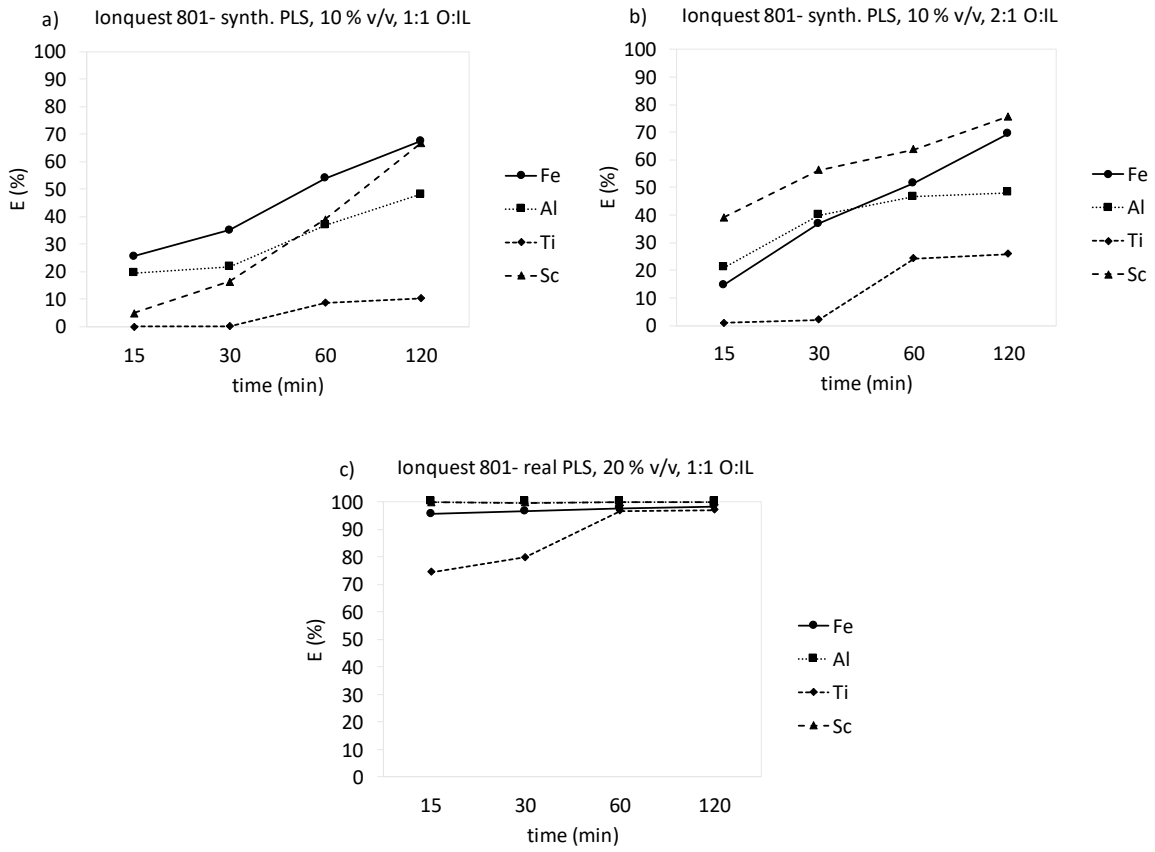

Figure 48 Metals extraction with IONQUEST 801: from synthetic PLS at 10 % v/v in Kerosene D85, 1:1 O:IL (a) and 2:1 O:IL (b); from real PLS at 1:1 O:IL and 20 % v/v in Kerosene D85 (c).

8.1.3 Cyanex 923

The separation between the extractant and the synthetic PLS phases for Cyanex 923 was as fast as in the case of Cyanex 272, in fact, it took less than a minute and was instantaneous for the real PLS samples. Experiments carried out with 10 % v/v Cyanex 923 showed a limited Fe and Ti extraction at 1:1 and 2:1 O:IL. Al was slightly affected by the increase of O:IL, reaching 60 % at 2:1 O:IL and about 85 % of Sc was extracted in both cases (Figure 49a and b). When increasing Cyanex 923 concentration to 20 % v/v results from experiments performed with real PLS showed a complete extraction of Al, high recovery of Fe and Sc (about 80 %) and moderate recovery of Ti (almost 70 %) after 15 minutes (Figure 49c). Results do not change much over time. This extractant resulted to be not so effective for metals removal from [Emim][HSO_4] solutions.

Although incomplete extraction of the metal ions is observed in all cases, this organic extractant also proposes some advantages over the other extractants. In Figure 49a and b enhanced selectivity for Sc and Al than the others is shown. While Fe and Ti, two of the problematic elements for Sc recovery during SX operations as these elements are generally co-extracted with Sc, stayed 10 % extraction

levels, almost 90 % of Sc was extracted from the IL PLS. Therefore, this organic phase could be used to selectively recover Sc from IL PLS first before loading other metal ions in a dual-stage SX circuit.

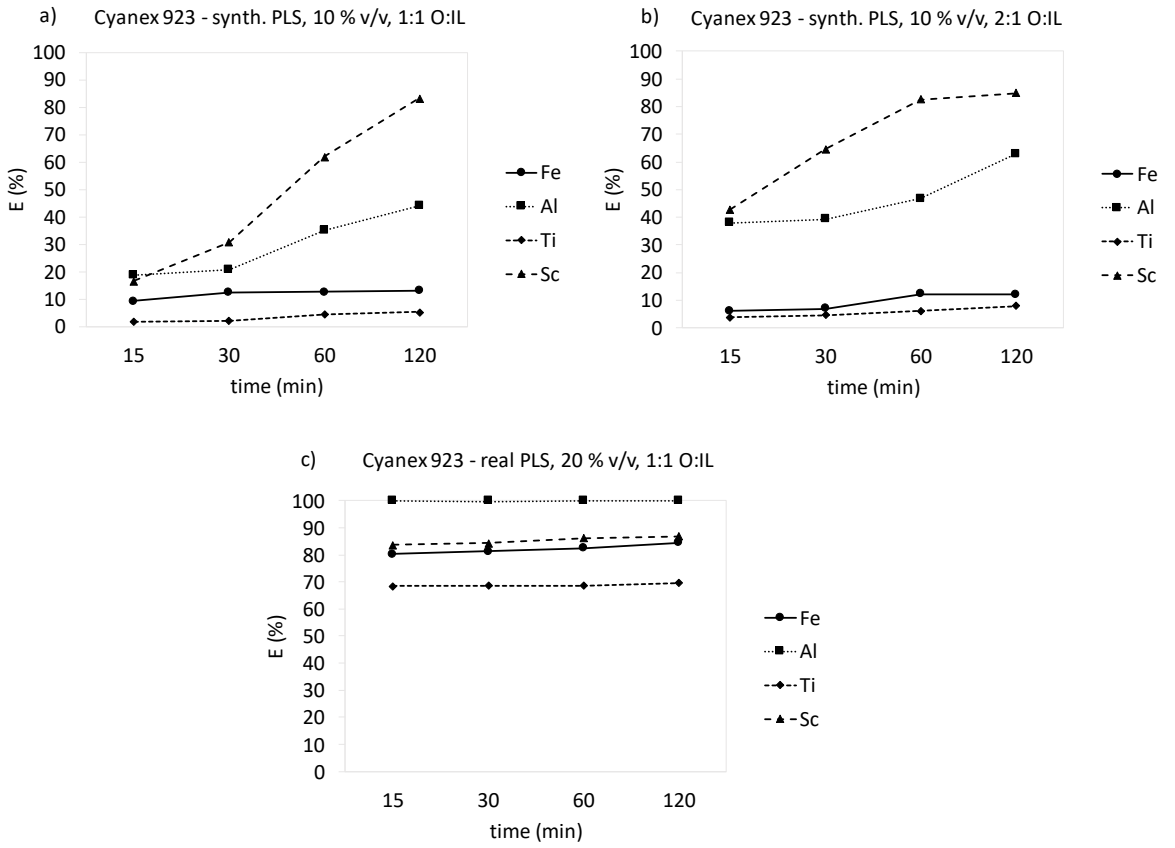

Figure 49 Metals extraction with Cyanex 923: from synthetic PLS at 10 % v/v in Kerosene D85, 1:1 O:IL (a) and 2:1 O:IL (b); from real PLS at 1:1 O:IL and 20 % v/v in Kerosene D85 (c).

8.1.4 D2EHPA

Phase disengagement between synthetic PLS and D2EHPA extractant phases was quite slow, in fact, necessitated of about 2 minutes for separating, whereas it was immediate for the real PLS samples as in the other reagents. The metals extraction trends with D2EHPA are shown in Figure 50. In case of synthetic PLS, experiments carried out at 1:1 O:IL (Figure 50a) show a moderate extraction of Ti even after 120 minutes (<20 %); all the other metals present a moderate extraction (60 – 70 %) after 120 minutes. When O:IL increases to 2:1 (Figure 50b), there is a substantial increase in Ti extraction that reaches 50 % after 120 minutes. All the other metals extraction slightly increases reaching a range of 70 – 80 % after 120 minutes. By varying O:IL from 1:1 to 2:1 does not significantly improve efficiency in metals extraction.

Experiments with the real PLS were conducted at 20 % v/v of D2EHPA in Kerosene D85 (Figure 50c), results show a total extraction of metals after 15 minutes. This behavior can be accounted not only to the increase of extractant concentration, but also to the fact that experiments were carried out at a lower viscosity comparing to the synthetic PLS. D2EHPA is able to extract metals form viscous and non-viscous [Emim][HSO_4] solutions. In case of non-viscous solutions, the optimum conditions are 20 % v/v extractant concentration, 1:1 O:IL and 15 minutes, whilst with viscous solutions more time is needed to extract metals.

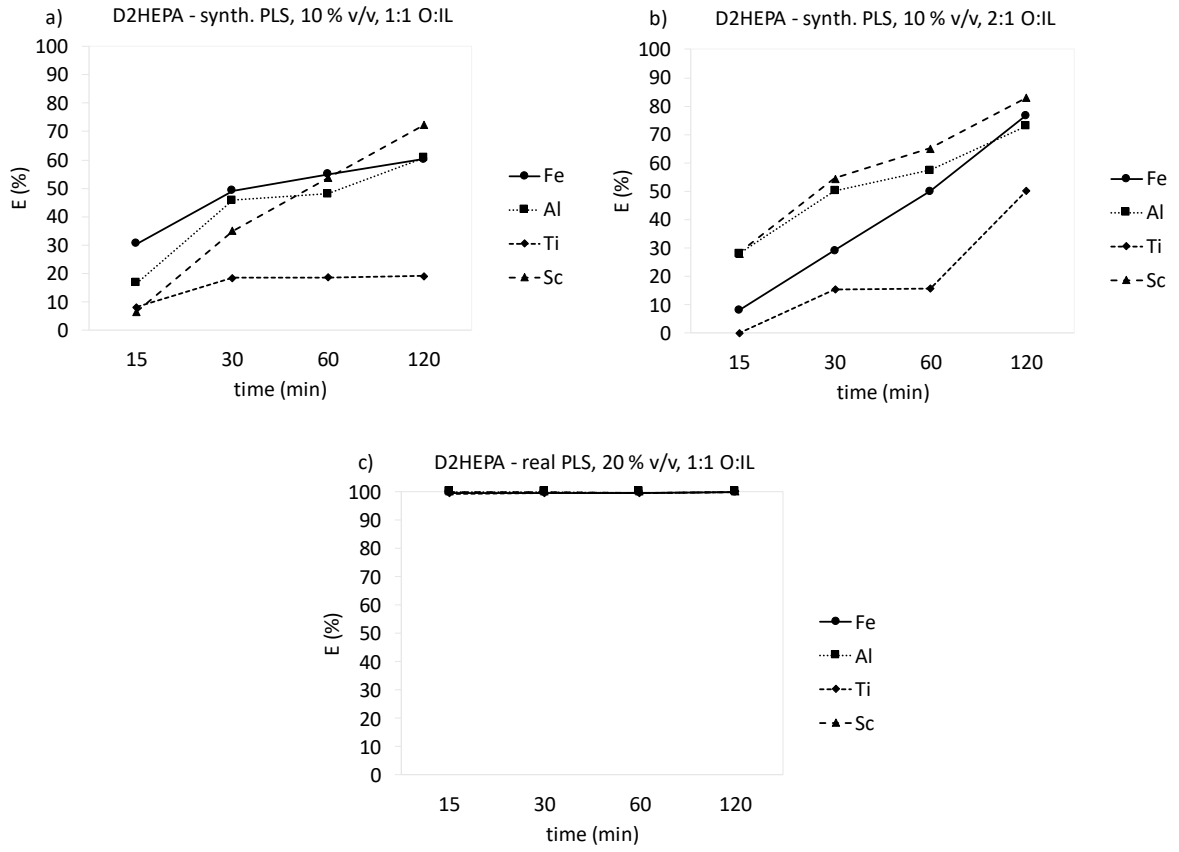

Figure 50 Metals extraction with D2EHPA: from synthetic PLS at 10 % v/v in Kerosene D85, 1:1 O:IL (a) and 2:1 O:IL (b); from real PLS at 1:1 O:IL and 20 % v/v (c) in Kerosene D85.

Even though D2EHPA was previously shown one of the best reagents for Sc extraction with high selectivity in aqueous solutions [115], when SX is performed with ILs, this selectivity is decreased significantly with high co-extraction levels of the metal ions. However, as D2EHPA showed immediate extraction of the all ions in real PLS (Figure 50c), this reagent could be the best option for stripping ions from IL PLS among the other tested extracted when the price, efficiency and kinetics are considered.

8.2 Multi-stage solvent extraction process

For these experiments, a synthetic pregnant leaching solution (PLS) was obtained by simulating the concentration of metals from leaching BR with [Emim][HSO_4] at optimum conditions. Batch experiments were performed in a Trallero and Schlee mini reactor combined with a mechanical stirrer, a vapor condenser and a temperature controller. The required amount of Fe_2O_3, TiO_2, Al_2O_3, Na_2O and Sc_2O_3 were dissolved in [Emim][HSO_4] for 12 hours, at 200 °C and 200 rpm. Filtration was performed by avoiding the addition of DMSO which would prevent the regeneration of the IL. Samples were then digested through acidic treatment (HNO_3 65% v/v and aqua regia) and analyzed. Fe and Al and Na were detected with AAS, Ti and Sc with ICP-OES.

The PLS composition is shown in Table 10. As it is possible to observe, the main metal is Fe which accounts to 13.93 g/L, followed by Al (1.53 g/L), Ti (1.13 g/L) and Na (580 mg/L); Sc contributes with 4.9 mg/L.

Table 10 Composition of the PLS obtained by leaching bauxite residue with [Emim][HSO_4] at optimum conditions.

Metal	Composition (g/L)
Fe	13.93
Al	1.53
Ti	1.13
Na	0.58
Sc	0.0049

Solvent extraction experiments were done at 55 °C to have a viscosity closer to the organic reagent; magnetic stirrers have been used to assure the correct agitation between the two phases. Based on results already discussed in chapter 8.1, a multi-stage process was executed, as it is shown in Figure 51.

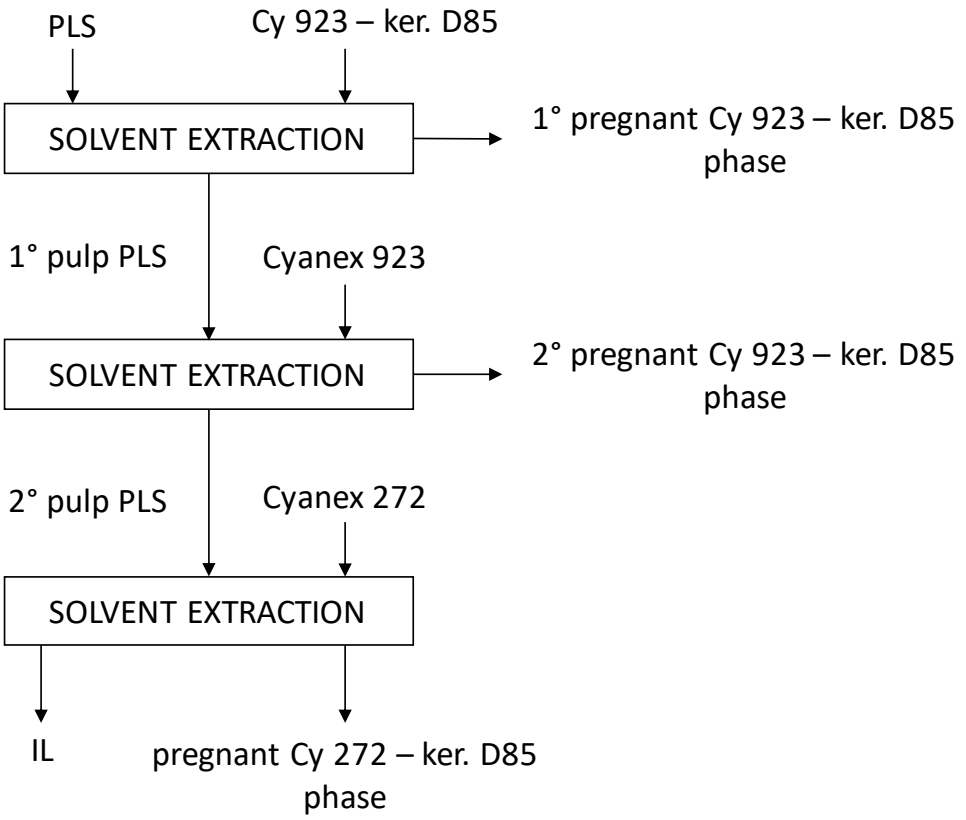

Figure 51 The multi-stage solvent extraction process.

Firstly, a dual-stage extraction process with a neutral mixture of phosphine oxides was applied to selectively extract Sc and Al. Both stages were conducted for 120 minutes, by using Cyanex 923 diluted in kerosene D85 (Cy 923 – ker. D85) at 10 % v/v and 2:1 O:IL. Subsequently, the acidic organophosphorus extractant Cyanex 272 diluted in kerosene D85 (Cy 272 – ker. D85) at 20 % v/v and 1:1 O:IL was employed, by stirring the sample for 60 minutes. The separation between the extractant and the synthetic PLS phases for both extractants, Cyanex 923 and Cyanex 272, took less than a minute. Samples were then centrifuged and pulp PLS phases were subjected to acidic digestion (HNO_3 65 % v/v and aqua regia) and analyzed with AAS and ICP-OES.

As it is possible to observe in Figure 52, in the dual-stage SX with Cyanex 923 at at 10 % v/v and 2:1 O:IL, more than 95 % of Al and Sc, about 60 % of Na and nearly 20 % of Fe and Ti have been extracted. In particular, the first stage is responsible for the extraction of 87 % of Al and 93 % of Sc. Metals can be further purified and used in Al-Sc alloys industry [58].

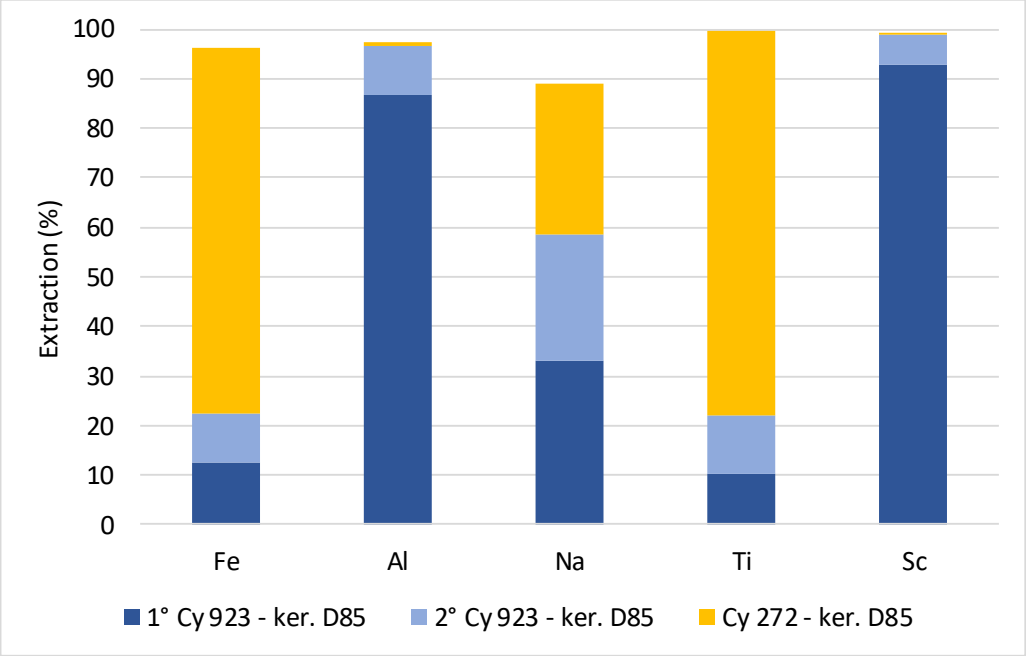

Figure 52 The multi-stage SX process results.

In the third stage, the acidic extractant Cyanex 272 at 20 % v/v and 1:1 O:IL was employed. About 74 % of Fe and 78 % of Ti were extracted. These metals can be recovered and purified afterward. Sc and Al extraction, in this case, was negligible, being less than 1%. Na extraction is limited in all the three stages, as about 30 % has been extracted in the first stage and 25 % in the second stage with Cyanex 923, while about 30 % was extracted in the third stage with Cyanex 972.

In conclusion, this multi-stage extraction process resulted to be efficient for recovering metals from IL leachates as most metals are extracted. Indeed, about 10 % of Na and less than 5 % of Ti, Fe, Al and Sc were left behind in the IL phase and therefore, they can be considered as impurities. IL could be regenerated for further uses as leaching agent, making the process more sustainable.

9. Conclusions

Bauxite residue is currently being managed via stockpiling, storage within settling pond and landfilling. However, these approaches are disadvantageous in terms of potential risk for the environment and storage issues associated with its management. Moreover, BR contains valuable metals (i.e. REEs, Sc, Fe, Ti), therefore it can be considered a valuable secondary raw material resource. In this perspective, a process for recovering valuable metals from BR has been studied within the framework of this PhD thesis. As said previously, ionic liquids can be considered an eco-friendly replacement for mineral acid metals dissolution, providing more economical and sustainable processes for secondary resources. In particular, this research study was focused on the recovery of Sc and Ti from bauxite residue by (1) directly leach it with the Brønsted acidic ionic liquid [Emim][HSO_4]; (2) the resulting pregnant solution was then subjected to solvent extraction to recover metals from the IL and regenerate it for subsequent use.

The bauxite residue was provided by Aluminum of Greece (Mytilineos S.A.) and fully characterized. From the granulometric analysis resulted that 90 wt.% of the material had a particle size smaller than 43 µm. The main minerals were hematite, calcium aluminum iron silicate hydroxide, cancrinite, diaspore, goethite and perovskite. Iron oxide was the major constituent in the bauxite residue accounting for about 42 wt.%. It was followed by aluminum oxide with 16 wt.%, while titanium oxide was 4 wt.% and total rare earth oxides (REO) assessed to 0.2 wt.%. In particular, Sc was 134 ± 4 mg/kg (134 ppm).

The Brønsted acidic ionic liquid 1-ethyl-3-methylimidazolium hydrogen sulfate ([Emim][HSO_4]) has been chosen to directly leach bauxite residue. Its decomposition starts at 250 °C, therefore it has a remarkably high thermal stability. Viscosity measurements have revealed that, even though [Emim][HSO_4] is very viscous at room temperature (1642 mPa·s), by increasing temperature its viscosity dramatically decreases, reaching 15 mPa·s at 200 °C. Moreover, reaction mechanism that takes place has been investigated by analyzing two monometallic solutions of Sc and Al dissolved in [Emim][HSO_4] with ^{1}H and ^{13}C NMR. The results obtained have led to the following proposed reaction:

$$Me_2O_n + n[Emim][HSO_4] \leftrightarrow Me_2(SO_4)_n + nOH^- + n[Emim]^+ \quad (13)$$

Subsequently, bauxite residue was directly leached with [Emim][HSO_4] and process was optimized by evaluating parameters like stirring rate, temperature, time and pulp density.

Each parameter was assessed separately, keeping the others constant, and choosing the combination that gave the best results. The first parameters taken into consideration was the stirring rate; it was possible to observe that under low (100 rpm) and high (600 rpm) stirring rates, metals recoveries were low. This is due to the fact that under low stirring rates a thick boundary layer is developed on the surface of the solid particles, making the diffusion of chemical species from and to the solid particles surface inefficient. On the other hand, at high stirring rates, the thickness of the boundary layer substantially decreases, but the high convective mass transfer of reactants from the surface of the particles, makes the surface reactions again inefficient and thus the recovery yields are diminishing. Therefore 200 rpm was found to give the best results, in terms of Sc and Ti recoveries. At this stirring rate, Fe, Ti and Sc have the highest recovery yields (75, 72 and 67 % respectively). Metals like Na and Al were slightly affected by the stirring rate as they remained almost stable in a range of 17-32 % recovery yields.

The behavior of the system was analyzed by performing kinetic tests at 150, 175 and 200 °C. Leaching temperature and time greatly affected the system, as it was found that at mild conditions (150 °C), Sc and Ti dissolution could not exceed about 70 %, while Fe can be leached at about 80 % after 24 hours. By raising temperature, also metals recovery yields increased in less time; in fact, at 175 °C, 90 % of Fe and 70 % of Ti and Sc dissolution was reached after 12 hours. At harsher conditions (200 °C), metals like Fe, Ti and Sc have been considerably leached even after 1 hour (60 – 74 %). However, the maximum extraction of these metals has been reached after 12 hours, where Fe was almost totally dissolved, Ti recovery was over 90 % and Sc reached nearly 80 %. At each temperature chosen, Al and Na dissolution remained stable along the kinetic curves in a range of 30 – 40 %.

The effect of pulp density on the leaching system was also investigated. At low pulp densities (2.5 – 5 % w/v), there is a consistent excess of the IL, therefore it was possible to obtain the best results in terms of Ti and Sc dissolution (88 % of Ti and 78 % of Sc; Fe was almost totally leached). When increasing pulp density (10 – 14.3 % w/v), also viscosity increased as the IL excess was lower. This fact had led to a lower recovery of all metals taken into consideration.

In conclusion, the optimum conditions, in terms of Ti and Sc recovery, were 200 rpm, 200 °C, 12 hours and 5 % w/v pulp density. At these conditions, Fe was almost totally dissolved and Sc recovery yield was nearly 80 %. It was not possible to have high recovery yields of Sc without having co-dissolution of iron. This is because Sc is mainly hosted in hematite and goethite mineralogical phases (55 % and 25 %, respectively) in bauxite residue [13]. Moreover, 90 % of Ti was dissolved and Al and Na were partially extracted (in a range of 30 – 40 %). Si and REEs dissolutions were found to be negligible, whereas Ca was partially dissolved and precipitated as $CaSO_4$ consuming about 2 wt.% of the ionic liquid.

After solid/liquid separation, the solid residue after leaching has been characterized. The matrix was mainly composed of Al, Ca, Na silicates and surrounded phases transitioning from calcite ($CaCO_3$) to calcium sulfate anhydrite ($CaSO_4$). $CaSO_4$ is a new mineralogical phase formed due to the interaction between calcium and the anion of the ionic liquid.

An attempt to locate REES in the solid residue after leaching was made, as they were not dissolved during the leaching process. With this purpose two samples were analyzed with SEM-EDS and TEM, one Fe-depleted derived from leaching BR at optimum conditions and one rich in Fe, derived from leaching BR at milder conditions.

The Fe – depleted sample was proved to contain small REEs particles of about 10 µm. In particular, heavy rare earths like gadolinium and dysprosium were located in YPO_4 particles. These grains endure the [Emim][HSO_4] leaching process, as this kind of particles were previously located in bauxite residue [14]. In view of this fact, it is possible to explain the negligible recoveries of heavy REEs since they are not subjected to any dissolution. Light REEs, including neodymium, lanthanum and samarium, were identified in small mixed calcium-cerium phosphate particles. This may indicate a partial dissolution of calcium from the mixed Ca – light REEs phases, leaving behind smaller phosphate particles which are beneficiated in light REEs. Since REEs remain in the solid residue, this could be further treated for subsequently extracting REEs. Moreover, being rich in calcium, aluminum and silicon, the Fe – depleted solid residue could be employed in building material applications.

The Fe – rich sample was also analyzed, where both heavy and light REEs endure the ionic liquid dissolution, remaining intact as the same kind of particles were located in BR [14]. More in detail, heavy REE phosphate particles were found in the matrix, surrounded by iron oxides particles and titanium oxide, with the major constituent being yttrium (YPO_4) and presence of erbium, gadolinium, europium, dysprosium, ytterbium and samarium. Moreover, relatively big light REE particles were also found in the form of calcium sodium titanate [(REEs, Ca, Na)(Ti, Fe)O_3], which endure the ionic liquid leaching, as their shape is the same as in bauxite residue.

Among the technologies for scandium separation and purification, solvent extraction has the advantages of high extraction capacity and ease of operating at large scales, and therefore the next stage involved the metals recovery from the pregnant liquid solution (PLS). Preliminary studies on solvent extraction (SX) have been carried out on synthetic solutions. Cyanex 272, D2EHPA, Ionquest 801 and Cyanex 923 diluted in kerosene D85 were examined as possible extractants for metals contained in the PLS. Parameters like phase disengagement, extractant concentration and organic to IL ratio were investigated to produce kinetic curves at 15, 30, 60 and 120 minutes retention time. Although retention time was affected by the presence of DMSO in some cases, this does not affect solvent extraction process in terms of loading efficiency and it is possible to perform tests with viscous solutions at about 60 °C. This would allow to avoid the use of DMSO during the filtration step after leaching, simplifying the whole process. O:IL ratio has a minor effect on the efficiency of the process, while by changing extractant concentration, all the recoveries enhanced significantly. From the results obtained, it can be concluded that the neutral extractant, Cyanex 923, was the best for selective Sc extraction from IL PLSs and could be used for its recovery as a pretreatment before loading all the ions in the PLS. Moreover, D2EHPA at 20 % v/v and 1:1 O:IL resulted to be the best parameters combination to extract metals, in fact after 15 minutes almost 100 % of Fe, Al, Ti and Sc were recovered from PLS. Therefore, both selective Sc extraction, as well as reuse of IL, could be carried out with a multi-stage SX process. Firstly, a dual-stage extraction process with a neutral mixture of phosphine oxides was applied to selectively extract Sc and Al, succeeding to extract more than 95 % of Al and Sc, about 60 % of Na and nearly 20 % of Fe and Ti. Al and Sc could be further purified and used in Al-Sc alloys industry [58]. In the third stage, the acidic extractant Cyanex was employed for extracting 74 % of Fe and 78 % of Ti. It can be concluded that about 10 % of Na, and less than 5 % of Ti, Fe, Al and Sc remained in the IL phase and could be considered as impurities for a subsequent use of the IL as leaching agent.

In summary, the only way to have high recovery yields of Sc by directly leaching bauxite residue with [Emim][HSO_4] was to have also an almost complete co-dissolution of iron. The presence of iron in the PLS may be an issue for a subsequent recovery of this metal, which could be overcome by subjecting the PLS to a multi-stage SX process. Therefore, the neutral phosphine extractant Cyanex 923 has been employed to selectively extract Sc from PLS, which was treated with an acidic extractant afterwards for extracting all the other metals. In this way, the ionic liquid could be regenerated for further uses, making the process economically and environmentally viable.

9.1 Outlook

In this PhD thesis a conceptual flowsheet for recovering metals from bauxite residue was proposed. Bauxite residue was directly leached with the ionic liquid [Emim][HSO_4] and metals were subsequentially recovered through a multi-stage solvent extraction process. However, some aspects of this work need to be studied more in details. Furthermore, energy and cost calculations need to be performed for evaluating the economic feasibility at higher scale. This paragraph describes the proposals for future work.

Bauxite residue was leached with [Emim][HSO_4] and solid/liquid separation was performed by cooling the system at 120 °C and adding a non-viscous/volatile solvent to decrease viscosity of the system. Too high viscosity would prevent the room temperature filtration stage. Furthermore, a synthetic pregnant leaching solution simulating the concentration of metals from leaching bauxite residue with [Emim][HSO_4] at optimum conditions was produced. In this case, filtration was performed by avoiding the addition of the non-viscous/volatile solvent which would hamper the regeneration of the ionic liquid. However, high temperature filtration needs to be tested on the system obtained by directly leaching bauxite residue with [Emim][HSO_4] at optimum conditions.

Moreover, previous studies have focused on metals extraction from the pregnant liquid solution. However, further work required on solvent extraction process unit is the stripping of metals from the organic extractant phases. Metals could be subsequentially purified, hence resulting in a stream that can be economically processed with available refining technologies.

In addition, regeneration and subsequent use of the ionic liquid need to be studied more in detail, to verify the eventual feasibility of a continuous metal recovery process. In that way a complete utilization of bauxite residue would be proposed.

References

1. Zhang, R.; Zheng, S.; Ma, S.; Zhang, Y. Recovery of Alumina and Alkali in Bayer Red Mud by the Formation of Andradite-Grossular Hydrogarnet in Hydrothermal Process. *J. Hazard. Mater.* **2011**, *189* (3), 827–835.
2. Evans, K. The History, Challenges, and New Developments in the Management and Use of Bauxite Residue. *J. Sustain. Metall.* **2016**, *2* (4), 316–331.
3. Kumar, S.; Kumar, R.; Bandopadhyay, A. Innovative Methodologies for the Utilisation of Wastes from Metallurgical and Allied Industries. *Resour. Conserv. Recycl.* **2006**, *48* (4), 301–314.
4. Klauber, C.; Gräfe, M.; Power, G. Bauxite Residue Issues: II. Options for Residue Utilization. *Hydrometallurgy* **2011**, *108* (1–2), 11–32.
5. Power, G.; Gräfe, M.; Klauber, C. Bauxite Residue Issues: I. Current Management, Disposal and Storage Practices. *Hydrometallurgy* **2011**, *108* (1–2), 33–45.
6. Adamson, A. N.; Bloore, E. J.; Carr, A. R. Basic Principles of Bayer Process Design. In *Essential Readings in Light Metals*; Springer International Publishing: Cham, 2016; pp 100–117.
7. Vind, J.; Alexandri, A.; Vassiliadou, V.; Panias, D. Distribution of Selected Trace Elements in the Bayer Process. *Metals (Basel).* **2018**, *8* (5), 327.
8. Balomenos, E.; Panias, D.; Paspaliaris, I. Energy and Exergy Analysis of the Primary Aluminum Production Processes: A Review on Current and Future Sustainability. *Miner. Process. Extr. Metall. Rev.* **2011**, *32* (2), 69–89.
9. International Aluminium Institute (IAI) and European Aluminium (EA). *Bauxite Residue Management: Best Practice*; 2015.
10. Balomenos, E.; Kastritis, D.; Panias, D.; Paspaliaris, I.; Boufounos, D. The Enexal Bauxite Residue Treatment Process: Industrial Scale Pilot Plant Results. In *Light Metals 2014*; John Wiley & Sons, Inc.: Hoboken, NJ, USA, 2014; Vol. 9781118889, pp 141–147.
11. European Aluminium Association (EAA). *Environmental Profile Report for the European Aluminium Industry April 2013-Data for the Year 2010 Life Cycle Inventory Data for Aluminium Production and Transformation Processes in Europe*; 2013.
12. Gräfe, M.; Power, G.; Klauber, C. Bauxite Residue Issues: III. Alkalinity and Associated Chemistry. *Hydrometallurgy* **2011**, *108* (1–2), 60–79.
13. Vind, J.; Malfliet, A.; Bonomi, C.; Paiste, P.; Sajó, I. E.; Blanpain, B.; Tkaczyk, A. H.; Vassiliadou, V.; Panias, D. Modes of Occurrences of Scandium in Greek Bauxite and Bauxite Residue. *Miner. Eng.* **2018**, *123*, 35–48.
14. Vind, J.; Malfliet, A.; Blanpain, B.; Tsakiridis, P.; Tkaczyk, A.; Vassiliadou, V.; Panias, D. Rare Earth Element Phases in Bauxite Residue. *Minerals* **2018**, *8* (2), 77.
15. The Bayer Process http://bauxite.world-aluminium.org/index.php?id=208&L=0 (accessed Mar 14, 2019).
16. Kaußen, F. M.; Friedrich, B. Methods for Alkaline Recovery of Aluminum from Bauxite Residue. *J. Sustain. Metall.* **2016**, *2* (4), 353–364.
17. Authier-Martin, M.; Forte, G.; Ostap, S.; See, J. The Mineralogy of Bauxite for Producing

Smelter-Grade Alumina. *JOM* **2001**, *53* (12), 36–40.

18. Paramguru, R. K.; Rath, P. C.; Misra, V. N. Trends in Red Mud Utilization - A Review. *Miner. Process. Extr. Metall. Rev.* **2004**, *26* (1), 1–29.
19. Hudson, L. K.; Misra, C.; Perrotta, A. J.; Wefers, K.; Williams, F. S. Aluminum Oxide. In *Ullmann's Encyclopedia of Industrial Chemistry*; Wiley-VCH Verlag GmbH & Co. KGaA: Weinheim, Germany, 2000.
20. Chin, L. A. D. The State-of-the-Art in Bayer Process Technology. In *Light Metals 1988*; 1988; pp 49–53.
21. Bánvölgyi, G. Scale Formation in Alumina Refineries. In *Proceedings of the 34th International Conference and Exhibition ICSOBA*; Quebec, QC, Canada; pp 1–14.
22. Balomenos, E.; Gianopoulou, I.; Panias, D.; Paspaliaris, I. *ENEXAL: Novel Technologies for Enhanced Energy and Exergy Efficiencies in Primary Aluminium Production Industry*.
23. Liu, Z.; Li, H. Metallurgical Process for Valuable Elements Recovery from Red Mud—A Review. *Hydrometallurgy* **2015**, *155*, 29–43.
24. Ochsenkühn-Petropulu, M.; Lyberopulu, T.; Ochsenkühn, K. M.; Parissakis, G. Recovery of Lanthanides and Yttrium from Red Mud by Selective Leaching. *Anal. Chim. Acta* **1996**, *319* (1–2), 249–254.
25. Liu, Y.; Naidu, R. Hidden Values in Bauxite Residue (Red Mud): Recovery of Metals. *Waste Manag.* **2014**, *34* (12), 2662–2673.
26. World Aluminium — Alumina Production http://www.world-aluminium.org/statistics/alumina-production/#histogram (accessed Jun 19, 2019).
27. Balomenos, E. *EU MSCA-ETN REDMUD Policy Brief*; 2018.
28. Evans, K.; Nordheim, E.; Tsesmelis, K. Bauxite Residue Management. In *Light Metals 2012*; Springer International Publishing: Cham, 2012; pp 63–66.
29. Ruyters, S.; Mertens, J.; Vassilieva, E.; Dehandschutter, B.; Poffijn, A.; Smolders, E. The Red Mud Accident in Ajka (Hungary): Plant Toxicity and Trace Metal Bioavailability in Red Mud Contaminated Soil. *Environ. Sci. Technol.* **2011**, *45* (4), 1616–1622.
30. Bánvölgyi, G. The Red Mud Pond Dam Failure at Ajka (Hungary) and Subsequent Developments György (George) Bánvölgyi. In *Bauxite residue seminar, ICSOBA 2011*; Goa, India, 2011.
31. Tsakiridis, P. E.; Agatzini-Leonardou, S.; Oustadakis, P. Red Mud Addition in the Raw Meal for the Production of Portland Cement Clinker. *J. Hazard. Mater.* **2004**, *116* (1–2), 103–110.
32. Vangelatos, I.; Angelopoulos, G. N.; Boufounos, D. Utilization of Ferroalumina as Raw Material in the Production of Ordinary Portland Cement. *J. Hazard. Mater.* **2009**, *168* (1), 473–478.
33. Pontikes, Y.; Angelopoulos, G. N. Bauxite Residue in Cement and Cementitious Applications: Current Status and a Possible Way Forward. *Resour. Conserv. Recycl.* **2013**, *73*, 53–63.
34. Singh, M.; Upadhayay, S. N.; Prasad, P. M. Preparation of Special Cements from Red Mud. *Waste Manag.* **1996**, *16* (8), 665–670.
35. Cardenia, C.; Balomenos, E.; Panias, D. Iron Recovery from Bauxite Residue Through Reductive Roasting and Wet Magnetic Separation. *J. Sustain. Metall.* **2019**, *5* (1), 9–19.
36. Yagmurlu, B.; Alkan, G.; Xakalashe, B. S.; Friedrich, B. *Combined SAF Smelting and*

Hydrometallurgical Treatment of Bauxite Residue for Enhanced Valuable Metal Recovery Electronic Scrap Recycling View Project Circular Economy (Recycling Processes) for Batteries View Project; 2017.

37. Erçağ, E.; Apak, R. Furnace Smelting and Extractive Metallurgy of Red Mud: Recovery of TiO2, Al2O3 and Pig Iron. *J. Chem. Technol. Biotechnol.* **1997**, *70* (3), 241–246.

38. Alkan, G.; Schier, C.; Gronen, L.; Stopic, S.; Friedrich, B.; Alkan, G.; Schier, C.; Gronen, L.; Stopic, S.; Friedrich, B. A Mineralogical Assessment on Residues after Acidic Leaching of Bauxite Residue (Red Mud) for Titanium Recovery. *Metals (Basel).* **2017**, *7* (11), 458.

39. Bonomi, C.; Alexandri, A.; Vind, J.; Panagiotopoulou, A.; Tsakiridis, P.; Panias, D. Scandium and Titanium Recovery from Bauxite Residue by Direct Leaching with a Brønsted Acidic Ionic Liquid. *Metals (Basel).* **2018**, 8 (10), 834.

40. Agatzini-Leonardou, S.; Oustadakis, P.; Tsakiridis, P. E.; Markopoulos, C. Titanium Leaching from Red Mud by Diluted Sulfuric Acid at Atmospheric Pressure. *J. Hazard. Mater.* **2008**, *157* (2–3), 579–586.

41. Bruckard, W. J.; Calle, C. M.; Davidson, R. H.; Glenn, A. M.; Jahanshahi, S.; Somerville, M. A.; Sparrow, G. J.; Zhang, L. Smelting of Bauxite Residue to Form a Soluble Sodium Aluminium Silicate Phase to Recover Alumina and Soda. *Miner. Process. Extr. Metall.* **2010**, *119* (1), 18–26.

42. Alkan, G.; Yagmurlu, B.; Cakmakoglu, S.; Hertel, T.; Kaya, Ş.; Gronen, L.; Stopic, S.; Friedrich, B. Novel Approach for Enhanced Scandium and Titanium Leaching Efficiency from Bauxite Residue with Suppressed Silica Gel Formation. *Sci. Rep.* **2018**, *8* (1), 5676.

43. Ochsenkühn-Petropoulou, M. T.; Hatzilyberis, K. S.; Mendrinos, L. N.; Salmas, C. E. Pilot-Plant Investigation of the Leaching Process for the Recovery of Scandium from Red Mud. *Ind. Eng. Chem. Res.* **2002**, *41* (23), 5794–5801.

44. Hertel, T.; Blanpain, B.; Pontikes, Y. A Proposal for a 100 % Use of Bauxite Residue Towards Inorganic Polymer Mortar. *J. Sustain. Metall.* **2016**, *2* (4), 394–404.

45. McConchie, D. .; Clark, M. .; Hanahan, C. .; Davies-McConchie, F. The Use of Seawater-Neutralised Bauxite Refinery Residues in the Management of Acid Sulphate Soils, Sulphidic Mine Tailings and Acid Mine Drainage. In *3rd Queensland Environmental Conference: Sustainable Solutions or Industry and Government*; Environmental Engineering Society, 2000; pp 201–208.

46. Biswas, W. K.; Cooling, D. Sustainability Assessment of Red Sand as a Substitute for Virgin Sand and Crushed Limestone. *J. Ind. Ecol.* **2013**, *17* (5), n/a-n/a.

47. Klauber, C.; Gräfe, M.; Power, G. Bauxite Residue Utilization and the Lack Thereof. In *The Bauxite Residue Seminar, ICSOBA 2011*; Goa, India, 2011; pp 188–195.

48. Bonomi, C.; Cardenia, C.; Yin, P. T. W.; Panias, D. Review of Technologies in the Recovery of Iron, Aluminium, Titanium and Rare Earth Elements from Bauxite Residue (Red Mud). In *3rd InternationalSymposium on Enhanced Landfill Mining | Lisbon – Portugal | 8th – 10th February 2016*; Lisboa, 2016; pp 259–276.

49. Borra, C. R.; Blanpain, B.; Pontikes, Y.; Binnemans, K.; Van Gerven, T. Recovery of Rare Earths and Other Valuable Metals From Bauxite Residue (Red Mud): A Review. *J. Sustain. Metall.* **2016**, *2* (4), 365–386.

50. Yagmurlu, B.; Dittrich, C.; Friedrich, B. Precipitation Trends of Scandium in Synthetic Red Mud Solutions with Different Precipitation Agents. *J. Sustain. Metall.* **2017**, *3* (1), 90–98.

51. Yagmurlu, B.; Dittrich, C.; Friedrich, B.; Yagmurlu, B.; Dittrich, C.; Friedrich, B. Effect of Aqueous Media on the Recovery of Scandium by Selective Precipitation. *Metals (Basel).* **2018**, *8* (5), 314.

52. Avdibegović, D.; Yagmurlu, B.; Dittrich, C.; Regadío, M.; Friedrich, B.; Binnemans, K. Combined Multi-Step Precipitation and Supported Ionic Liquid Phase Chromatography for the Recovery of Rare Earths from Leach Solutions of Bauxite Residues. *Hydrometallurgy* **2018**, *180*, 229–235.

53. Avdibegović, D.; Regadío, M.; Binnemans, K. Recovery of Scandium(Iii) from Diluted Aqueous Solutions by a Supported Ionic Liquid Phase (SILP). *RSC Adv.* **2017**, *7* (78), 49664–49674.

54. Zhang, W.; Koivula, R.; Wiikinkoski, E.; Xu, J.; Hietala, S.; Lehto, J.; Harjula, R. Efficient and Selective Recovery of Trace Scandium by Inorganic Titanium Phosphate Ion-Exchangers from Leachates of Waste Bauxite Residue. *ACS Sustain. Chem. Eng.* **2017**, *5* (4), 3103–3114.

55. Binnemans, K.; Jones, P. T.; Blanpain, B.; Van Gerven, T.; Pontikes, Y. Towards Zero-Waste Valorisation of Rare-Earth-Containing Industrial Process Residues: A Critical Review. *J. Clean. Prod.* **2015**, *99*, 17–38.

56. Borra, C. R.; Blanpain, B.; Pontikes, Y.; Binnemans, K.; Van Gerven, T. Smelting of Bauxite Residue (Red Mud) in View of Iron and Selective Rare Earths Recovery. *J. Sustain. Metall.* **2016**, *2* (1), 28–37.

57. Borra, C. R.; Pontikes, Y.; Binnemans, K.; Van Gerven, T. Leaching of Rare Earths from Bauxite Residue (Red Mud). *Miner. Eng.* **2015**, *76*, 20–27.

58. Balomenos, E.; Davris, P.; Pontikes, Y.; Panias, D. Mud2Metal: Lessons Learned on the Path for Complete Utilization of Bauxite Residue Through Industrial Symbiosis. *J. Sustain. Metall.* **2017**, *3* (3), 551–560.

59. Kasliwal, P.; Sai, P. S. T. Enrichment of Titanium Dioxide in Red Mud: A Kinetic Study. *Hydrometallurgy* **1999**, *53* (1), 73–87.

60. Ghorbani, A.; Fakhariyan, A. Recovery of Al2O3, Fe2O3 and TiO2 from Bauxite Processing Waste (Red Mud) by Using Combination of Different Acids. *J. Basic Appl. Sci. Res.* **2013**, *3*, 187–191.

61. Singh, R. K.; Dhadke, P. M. *Extraction and Separation of Titanium(IV) with D2EHPA and PC-88A from Aqueous Perchloric Acid Solutions*; 2002; Vol. 67.

62. European Commission. *Study on the Review of the List of Critical Raw Materials, Executive Summary*; 2017.

63. European Commission. *Critical Raw Materials for the EU: Report of the Ad-Hoc Working Group on Defining Critical Raw Materials*; 2010.

64. European Commission. *Methodology for Establishing the EU List of Critical Raw Materials*; 2017.

65. European Commission. *Study on the Review of the List of the Critical Raw Materials - Critical Raw Materials Factsheets*; 2017.

66. European Commission; Deloitte Sustainability; British Geological Survey; Bureau de Recherches Géologiques et Minières; Netherlands Organisation for Applied Scientific Research. *Study on the Review of the List of the Critical Raw Materials - Critical Raw Materials Factsheets*; 2017.

67. Gambogi, J. Mineral Commodity Summaries, Scandium. *U.S. Geol. Surv.* **2017**, 146–147.

68. Borra, C. R.; Blanpain, B.; Pontikes, Y.; Binnemans, K.; Van Gerven, T. Recovery of Rare Earths and Major Metals from Bauxite Residue (Red Mud) by Alkali Roasting, Smelting, and Leaching. *J. Sustain. Metall.* **2017**, *3* (2), 393–404.

69. Duyvesteyn, W. P. C.; Putnam, G. F. *White Paper - Scandium - A Review of the Element, Its Characteristics, and Current and Emerging Commercial Applications*; 2014; Vol. 2.

70. Ochsenkühn-Petropulu, M.; Lyberopulu, T.; Parissakis, G. Direct Determination of Landthanides, Yttrium and Scandium in Bauxites and Red Mud from Alumina Production. *Anal. Chim. Acta* **1994**, *296* (3), 305–313.

71. Rudnick, R. L.; Gao, S. Composition of the Continental Crust. In *Treatise on Geochemistry*; Elsevier, 2003; pp 1–64.

72. Ochsenkühn-Petropulu, M.; Lyberopulu, T.; Parissakis, G. Selective Separation and Determination of Scandium from Yttrium and Lanthanides in Red Mud by a Combined Ion Exchange/Solvent Extraction Method. *Anal. Chim. Acta* **1995**, *315* (1), 231–237.

73. Alkan, G.; Yagmurlu, B.; Ma, Y.; Xakalashe, B.; Stopic, S. Combining Pyrometallurgical Conditioning and Dry Acid Digestion of Red Mud for Selective Sc Extraction and TiO2 Enrichment in Mineral Phase. In *2nd International Bauxite Residue Valorisation and Best Practices Conference, Athens, Greece*; 2018; pp 215–222.

74. Qu, Y.; Lian, B. Bioleaching of Rare Earth and Radioactive Elements from Red Mud Using Penicillium Tricolor RM-10. *Bioresour. Technol.* **2013**, *136*, 16–23.

75. Davris, P.; Balomenos, E.; Panias, D.; Paspaliaris, I. Selective Leaching of Rare Earth Elements from Bauxite Residue (Red Mud), Using a Functionalized Hydrophobic Ionic Liquid. *Hydrometallurgy* **2016**, *164*, 125–135.

76. MacFarlane, D. R.; Kar, M.; Pringle, J. M. *Fundamentals of Ionic Liquids*; Wiley online library, Ed.; Wiley-VCH Verlag GmbH & Co. KGaA: Weinheim, Germany, 2017.

77. Plechkova, N. V.; Seddon, K. R. Applications of Ionic Liquids in the Chemical Industry. *Chem. Soc. Rev.* **2008**, *37* (1), 123–150.

78. Welton, T. Room-Temperature Ionic Liquids. Solvents for Synthesis and Catalysis. *Chem. Rev.* **1999**, *99* (8), 2071–2083.

79. Park, J.; Jung, Y.; Kusumah, P.; Lee, J.; Kwon, K.; Lee, C. K. Application of Ionic Liquids in Hydrometallurgy. *Int. J. Mol. Sci.* **2014**, *15* (9), 15320–15343.

80. Abbott, A. P.; Frisch, G.; Ryder, K. S. Metal Complexation in Ionic Liquids. *Annu. Reports Prog. Chem. - Sect. A* **2008**, *104* (0), 21–45.

81. Abbott, A. P.; Frisch, G.; Hartley, J.; Ryder, K. S. Processing of Metals and Metal Oxides Using Ionic Liquids. *Green Chem.* **2011**, *13* (3), 471.

82. Tian, G.; Li, J.; Hua, Y. Application of Ionic Liquids in Hydrometallurgy of Nonferrous Metals. *Trans. Nonferrous Met. Soc. China* **2010**, *20* (3), 513–520.

83. Binnemans, K.; Jones, P. T. Solvometallurgy: An Emerging Branch of Extractive Metallurgy. *J. Sustain. Metall.* **2017**, *3* (3), 570–600.

84. Chiappe, C.; Capraro, D.; Conte, V.; Pieraccini, D. Stereoselective Halogenations of Alkenes and Alkynes in Ionic Liquids. *Org. Lett.* **2001**, *3*, 1061–1063.

85. Stark, A.; MacLean, B. L.; Singer, R. D. 1-Ethyl-3-Methylimidazolium Halogenoaluminate Ionic Liquids as Solvents for Friedel–Crafts Acylation Reactions of Ferrocene. *J. Chem. Soc. Dalt.*

Trans. **1999**, *63*, 63–66.

86. Sheldon, R. Catalytic Reactions in Ionic Liquids. *Chem. Commun.* **2001**, *23*, 2399–2407.

87. Kim, H. S.; Kim, Y. J.; Lee, H.; Park, K. Y.; Lee, C.; Chin, C. S. Ionic Liquids Containing Anionic Selenium Species: Applications for the Oxidative Carbonylation of Aniline. *Angew. Chemie Int. Ed.* **2002**, *41* (22), 4300–4303.

88. Lewandowski, A.; Świderska, A. Electrochemical Capacitors with Polymer Electrolytes Based on Ionic Liquids. *Solid State Ionics* **2003**, *161* (3–4), 243–249.

89. Shin, J.-H.; Henderson, W. A.; Passerini, S. Ionic Liquids to the Rescue? Overcoming the Ionic Conductivity Limitations of Polymer Electrolytes. *Electrochem. commun.* **2003**, *5* (12), 1016–1020.

90. Bourbos, E.; Giannopoulou, I.; Karantonis, A.; Paspaliaris, I.; Panias, D. Electrodeposition of Rare Earth Metals from Ionic Liquids. In *Rare Earths Industry*; Elsevier, 2016; pp 199–207.

91. Wellens, S.; Thijs, B.; Möller, C.; Binnemans, K. Separation of Cobalt and Nickel by Solvent Extraction with Two Mutually Immiscible Ionic Liquids. *Phys. Chem. Chem. Phys.* **2013**, *15* (24), 9663.

92. Bonomi, C.; Davris, P.; Balomenos, E.; Giannopoulou, I.; Panias, D. Ionometallurgical Leaching Process of Bauxite Residue: A Comparison between Hydrophilic and Hydrophobic Ionic Liquids. In *Proceedings of 35th International ICSOBA Conference*; Hamburg, Germany, 2017; pp 557–564.

93. Davris, P.; Marinos, D.; Balomenos, E.; Alexandri, A.; Gregou, M.; Panias, D.; Paspaliaris, I. Leaching of Rare Earth Elements from 'Rödberg' Ore of Fen Carbonatite Complex Deposit, Using the Ionic Liquid HbetTf2N. *Hydrometallurgy* **2018**, *175*, 20–27.

94. Dai, S.; Shin, Y. S.; Toth, L. M.; Barnes, C. E. Comparative UV−Vis Studies of Uranyl Chloride Complex in Two Basic Ambient-Temperature Melt Systems: The Observation of Spectral and Thermodynamic Variations Induced via Hydrogen Bonding. *Inorg. Chem.* **1997**, *36* (21), 4900–4902.

95. Nockemann, P.; Thijs, B.; Pittois, S.; Thoen, J.; Glorieux, C.; Van Hecke, K.; Van Meervelt, L.; Kirchner, B.; Binnemans, K. Task-Specific Ionic Liquid for Solubilizing Metal Oxides. *J. Phys. Chem. B* **2006**, *110* (42), 20978–20992.

96. Nockemann, P.; Thijs, B.; Parac-Vogt, T. N.; Van Hecke, K.; Van Meervelt, L.; Tinant, B.; Hartenbach, I.; Schleid, T.; Ngan, V. T.; Nguyen, M. T.; et al. Carboxyl-Functionalized Task-Specific Ionic Liquids for Solubilizing Metal Oxides. *Inorg. Chem.* **2008**, *47* (21), 9987–9999.

97. Abbott, A. P.; Capper, G.; Davies, D. L.; Rasheed, R. K.; Tambyrajah, V. Novel Solvent Properties of Choline Chloride/Urea Mixtures. *Chem. Commun.* **2003**, *0* (1), 70–71.

98. Abbott, A. P.; Boothby, D.; Capper, G.; Davies, D. L.; Rasheed, R. K. Deep Eutectic Solvents Formed between Choline Chloride and Carboxylic Acids: Versatile Alternatives to Ionic Liquids. *J. Am. Chem. Soc.* **2004**, *126* (29), 9142–9147.

99. Abbott, A. P.; Capper, G.; Davies, D. L.; McKenzie, K. J.; Obi, S. U. Solubility of Metal Oxides in Deep Eutectic Solvents Based on Choline Chloride. *J. Chem. Eng. data* **2006**, *51* (4), 1280–1282.

100. Abbott, A. P.; Capper, G.; Davies, D. L.; Shikotra, P. Processing Metal Oxides Using Ionic Liquids. *Miner. Process. Extr. Metall.* **2006**, *115* (1), 15–18.

101. Abbott, A. P.; Capper, G.; Davies, D. L.; Rasheed, R. K.; Pragna, S. Selective Extraction of Metals from Mixed Oxide Matrixes Using Choline-Based Ionic Liquids. *Inorg. Chem.* **2005**, *44* (19),

6497–6499.

102. Whitehead, J. A.; Lawrance, G. A.; McCluskey, A. 'Green' Leaching: Recyclable and Selective Leaching of Gold-Bearing Ore in an Ionic Liquid. *Green Chem.* **2004**, *6* (7), 313–315.

103. Whitehead, J. A.; Zhang, J.; Pereira, N.; McCluskey, A.; Lawrance, G. A. Application of 1-Alkyl-3-Methyl-Imidazolium Ionic Liquids in the Oxidative Leaching of Sulphidic Copper, Gold and Silver Ores. *Hydrometallurgy* **2007**, *88* (1–4), 109–120.

104. Dong, T.; Hua, Y.; Zhang, Q.; Zhou, D. Leaching of Chalcopyrite with Brønsted Acidic Ionic Liquid. *Hydrometallurgy* **2009**, *99* (1–2), 33–38.

105. McCluskey, A.; Lawrance, G. A.; Leitch, S. K.; Owen, M. P.; Hamilton, I. C. Ionic Liquids Industrial Applications for Green Chemistry. *Am. Chem. Soc.* **2002**, *818*, 199–212.

106. Huang, J.; Chen, M.; Chen, H.; Chen, S.; Sun, Q. Leaching Behavior of Copper from Waste Printed Circuit Boards with Brønsted Acidic Ionic Liquid. *Waste Manag.* **2014**, *34* (2), 483–488.

107. Kilicarslan, A.; Saridede, M. N.; Stopic, S.; Friedrich, B. Use of Ionic Liquid in Leaching Process of Brass Wastes for Copper and Zinc Recovery. *Int. J. Miner. Metall. Mater.* **2014**, *21* (2), 138–143.

108. Dupont, D.; Binnemans, K. Recycling of Rare Earths from NdFeB Magnets Using a Combined Leaching/Extraction System Based on the Acidity and Thermomorphism of the Ionic Liquid [Hbet][Tf_2N]. *Green Chem.* **2015**, *17* (4), 2150–2163.

109. Dupont, D.; Binnemans, K. Rare-Earth Recycling Using a Functionalized Ionic Liquid for the Selective Dissolution and Revalorization of Y_2O_3:Eu^{3+} from Lamp Phosphor Waste. *Green Chem.* **2015**, *17* (2), 856–868.

110. Rydberg, J.; Cox, M.; Musikas, C.; Chippin, G. R. *Principles and Practices of Solvent Extraction. Second Edition, Revised and Expanded.*, 2nd ed.; Wiley-Blackwell: New York, 2004.

111. Batchu, N. K.; Hoogerstraete, T. Vander; Banerjee, D.; Binnemans, K. Non-Aqueous Solvent Extraction of Rare-Earth Nitrates from Ethylene Glycol to n-Dodecane by Cyanex 923. *Sep. Purif. Technol.* **2017**, *174*, 544–553.

112. Freiser, H.; Nancollas, G. H. *Compendium of Analytical Nomenclature. Definitive Rules 1987. IUPAC*; Blackwell Scientific Publications, Oxford, 1987.

113. Lee, M. .; Ahn, J. .; Lee, E. . Solvent Extraction Separation of Indium and Gallium from Sulphate Solutions Using D2EHPA. *Hydrometallurgy* **2002**, *63* (3), 269–276.

114. Yoon, S. J.; Lee, J.-Y.; Tajima, H.; Yamasaki, A.; Kiyono, F.; Nakazato, T.; Tao, H. Extraction of Lanthanide Ions from Aqueous Solution by Bis(2-Ethylhexyl)Phosphoric Acid with Room-Temperature Ionic Liquids. *J. Ind. Eng. Chem.* **2010**, *16* (3), 350–354.

115. Wang, W.; Pranolo, Y.; Cheng, C. Y. Recovery of Scandium from Synthetic Red Mud Leach Solutions by Solvent Extraction with D2EHPA. *Sep. Purif. Technol.* **2013**, *108*, 96–102.

116. Anitha, M.; Kotekar, M. K.; Singh, D. K.; Vijayalakshmi, R.; Singh, H. Solvent Extraction Studies on Rare Earths from Chloride Medium with Organophosphorous Extractant Dinonyl Phenyl Phosphoric Acid. *Hydrometallurgy* **2014**, *146*, 128–132.

117. Vander Hoogerstraete, T.; Onghena, B.; Binnemans, K. Homogeneous Liquid–Liquid Extraction of Rare Earths with the Betaine—Betainium Bis(Trifluoromethylsulfonyl)Imide Ionic Liquid System. *Int. J. Mol. Sci.* **2013**, *14* (11), 21353–21377.

118. Onghena, B.; Borra, C. R.; Van Gerven, T.; Binnemans, K. Recovery of Scandium from Sulfation-

Roasted Leachates of Bauxite Residue by Solvent Extraction with the Ionic Liquid Betainium Bis(Trifluoromethylsulfonyl)Imide. *Sep. Purif. Technol.* **2017**, *176*, 208–219.

119. Xie, F.; Zhang, T. A.; Dreisinger, D.; Doyle, F. A Critical Review on Solvent Extraction of Rare Earths from Aqueous Solutions. *Miner. Eng.* **2014**, *56*, 10–28.

120. Li, D.; Wang, C. Solvent Extraction of Scandium(III) by Cyanex 923 and Cyanex 925. *Hydrometallurgy* **1998**, *48* (3), 301–312.

121. Wang, W.; Cheng, C. Y. Separation and Purification of Scandium by Solvent Extraction and Related Technologies: A Review. *J. Chem. Technol. Biotechnol.* **2011**, *86* (10), 1237–1246.

122. Larsen, E. M.; Trevorrow, L. V. E. The Systems Formed by Zirconium and Hafnium Tetrachloride with Acetonitrile and Isoamyl Ether. *J. Inorg. Nucl. Chem.* **1956**, *2* (4), 254–259.

123. Latimer, G. W. Distribution of Ion Pairs between Immiscible Nonaqueous Solvents. *Anal. Chem.* **1963**, *35* (12), 1983–1983.

124. Dean, J. A.; Eskew, J. B. Solvent Extraction with Two Immiscible Organic Solvents Separation of Thallium(III). *Anal. Lett.* **1971**, *4* (11), 737–743.

125. Foreman, M. R. S. Progress towards a Process for the Recycling of Nickel Metal Hydride Electric Cells Using a Deep Eutectic Solvent. *Cogent Chem.* **2016**, *2* (1).

126. Shumacher, B. A.; Shines, K. C.; Burton, J. V.; Papp, M. L. A Comparison of Soil Sample Homogenization Techniques. In *Hazardous waste measurements*; Simmons, M. S., Ed.; Lewis Publishers, 1991; pp 53–68.

127. Földvári, M. *Handbook of Thermogravimetric System of Minerals and Its Use in Geological Practice*; Geological Institute of Hungary: Budapest, Hungary, 2011.

128. Castaldi, P.; Silvetti, M.; Santona, L.; Enzo, S.; Melis, P. XRD, FT-IR, and Thermal Analysis of Bauxite Ore.Processing Waste (Red Mud) Exchanged with Heavy Metals. *Clays Clay Miner.* **2008**, *56* (4), 461–469.

129. Sajò, I. E. XDB Powder Diffraction Phase Analytical System, Version 3.107. Budapest, Hungary 2005.

130. Sajó, I. E. X-Ray Diffraction Quantitative Phase Analysis of Bayer Process Solids. In *Proceedings of the 10th International Conference of ICSOBA 23-30 November 2008*; Bhubaneshwar, India, 2008; pp 71–76.

131. Abhilash; Sinha, S.; Sinha, M. K.; Pandey, B. D. Extraction of Lanthanum and Cerium from Indian Red Mud. *Int. J. Miner. Process.* **2014**, *127*, 70–73.

132. Petrakova, O.; Klimentenok, G.; Panov, A.; Gorbachev, S. Application of Modern Methods for Red Mud Processing to Produce Rare Earth Elements. In *Proceedings of the 1st European Rare Earth Resources Conference (ERES 2014)*; Milos, Greece, 2014; pp 221–229.

133. Sole, K. C.; Hiskey, J. B. Solvent Extraction of Copper by Cyanex 272, Cyanex 302 and Cyanex 301. *Hydrometallurgy* **1995**, *37* (2), 129–147.

134. Flett, D. S. Solvent Extraction in Hydrometallurgy : The Role of Organophosphorus Extractants. *J. Organomet. Chem.* **2005**, *690*, 2426–2438.